Aus der Medizinischen Universitätsklinik und Poliklinik Tübingen
Abteilung für Innere Medizin VIII
Medizinische Onkologie und Pneumologie

Oncolytic Virotherapy of Neuroendocrine Neoplasms with oncolytic measles vaccine virus

Inaugural-Dissertation zur Erlangung des Doktorgrades der Medizin
der Medizinischen Fakultät
der Eberhard Karls Universität
zu Tübingen

vorgelegt von
Scheicher, Nikolai Valentin
2024

Dekan: Professor Dr. B. Pichler

1. Berichterstatter: Professor Dr. U. Lauer

2. Berichterstatter: Professorin Dr. R. Klein

Tag der Disputation: 21.03.2024

Für meine Oma Erika.

Table of contents

1. Introduction

1.1 Neuroendocrine neoplasms

Neuroendocrine neoplasms (NENs) represent a heterogenous group of various malignancies deriving from hormone producing (endocrine) cells that can evolve in almost every part of the human body, with the gastrointestinal-tract (62-67 %) and the lungs (22 %) being the most frequent primary sites [1]. If NENs are no longer a localized disease, metastases are most often found in the liver, followed by the lungs and bones (see figure 1). Neuroendocrine tumors (NETs) from the gastroenteropancreatic system are referred to as “GEP-NETs” and can be further subdivided into pancreatic (pNETs), small intestinal (siNETs) and gastric NETs (gNETS).

Originally described as “carcinoids” in the beginning of the 20th century [2], this term proved to be problematic and multiple classifications were used ever since trying to narrow the heterogenous group of multiple tumors further down. Nowadays neuroendocrine neoplasms can be further subdivided into well-differentiated neuroendocrine tumors (NETs) or poorly-differentiated neuroendocrine carcinomas (NECs). This is done analyzing various specific mutations for NETs/NECs, for example entity-defining mutations in the tumor protein 53 (TP53) gene or retinoblastoma transcriptional corepressor 1 (RB1) for NECs, both famous tumor suppressor genes, or Menin 1 (MEN1) and ATRX Chromatin Remodeler (ATRX) mutations in NETs [3], [4].

Further histological grading of NETs is depending on their histological classification taking into consideration their Ki-67 index (Kiel Protein), an antibody used for immunohistochemical staining strictly correlating with cell proliferation [5]. While a well differentiated NET with a Ki-67 index < 3 % is categorized as G1, G2 NETs have Ki-67 indexes between 3-20 %. Strongly proliferating tumors with Ki-67-indexes over 20 % are classified as G3. The current classification for the most frequent NENs of the gastrointestinal tract and of hepatopancreatobiliary organs according to the World Health Organization (WHO) 2019 classification of tumors of the digestive system is shown in table 1 below [3].

Another, older classification categorizes NENs according to their anatomic site, therefore using their embryonic origin during the division of the digestive tract to relate them to fore-, mid- or hindgut [6]. Their common denominator is the expression of neuroendocrine markers such as chromogranin A (CgA) and synaptophysin (Syn). Only one third of all NENs show hormonal functionality, meaning the majority of NENs is functionally inactive, thus complicating early diagnosis. However, in the minority of cases with hormone secreting NENs, patients can present with the so called “carcinoid syndrome”, a triad consisting of a flush, diarrhea and heart-failure.

NENs are relatively rare, accounting for about 0.5 % of all newly diagnosed malignancies, but a rapidly increasing incidence, for example in the USA, has been reported [7]. Another study in Switzerland showed an increasing incidence for GEP-NETs in the last 40 years, too, while the reasons are not entirely understood and are most likely multifactorial [8].

Around one fifth of the patients are metastatic at first presentation, yet NEN metastatic potential varies considerably by primary site, as NENs with primary tumors in the small intestine or pancreatohepatobiliary sites comprise the highest metastatic risk with the liver being the most common site of metastasis [9]. While the 5-year-survival of patients with localized disease ranges from 78 % to 93 % and thus constitutes a relatively good prognosis, 5-year-survival in metastatic disease with 19 % to 38 % is still poor [9].

As with most localized solid tumors, surgery is the primary therapeutic curative option. If curative treatment choices such as surgery are lacking in metastatic disease, currently available therapeutic options are somatostatin analogs, systemic chemotherapy, the mTOR inhibitor everolimus, peptide receptor radiotherapy, radiation, the multikinase inhibitor Sunitinib, interferon or debulking surgery with limited efficiency and poor prognosis [10].

NECs, which are rapidly growing and early invasive and metastatic tumors, can be subdivided into large and small cell tumors according to their histological presentation. They are most often found in the lung and can, if inoperable, be treated with chemotherapeutic platinum-regimes due to the high cell proliferation rate, but nevertheless constitute a very poor prognosis [11]. Fortunately, there are some studies reporting a decreasing incidence in lung NECs, which is likely due to reduced consumption of tobacco [8].

For the experiments in this dissertation, a broad spectrum of four NET and one NEC cell line deriving from both the lungs and the gastrointestinal tract was used to embrace the heterogenous group of NENs.

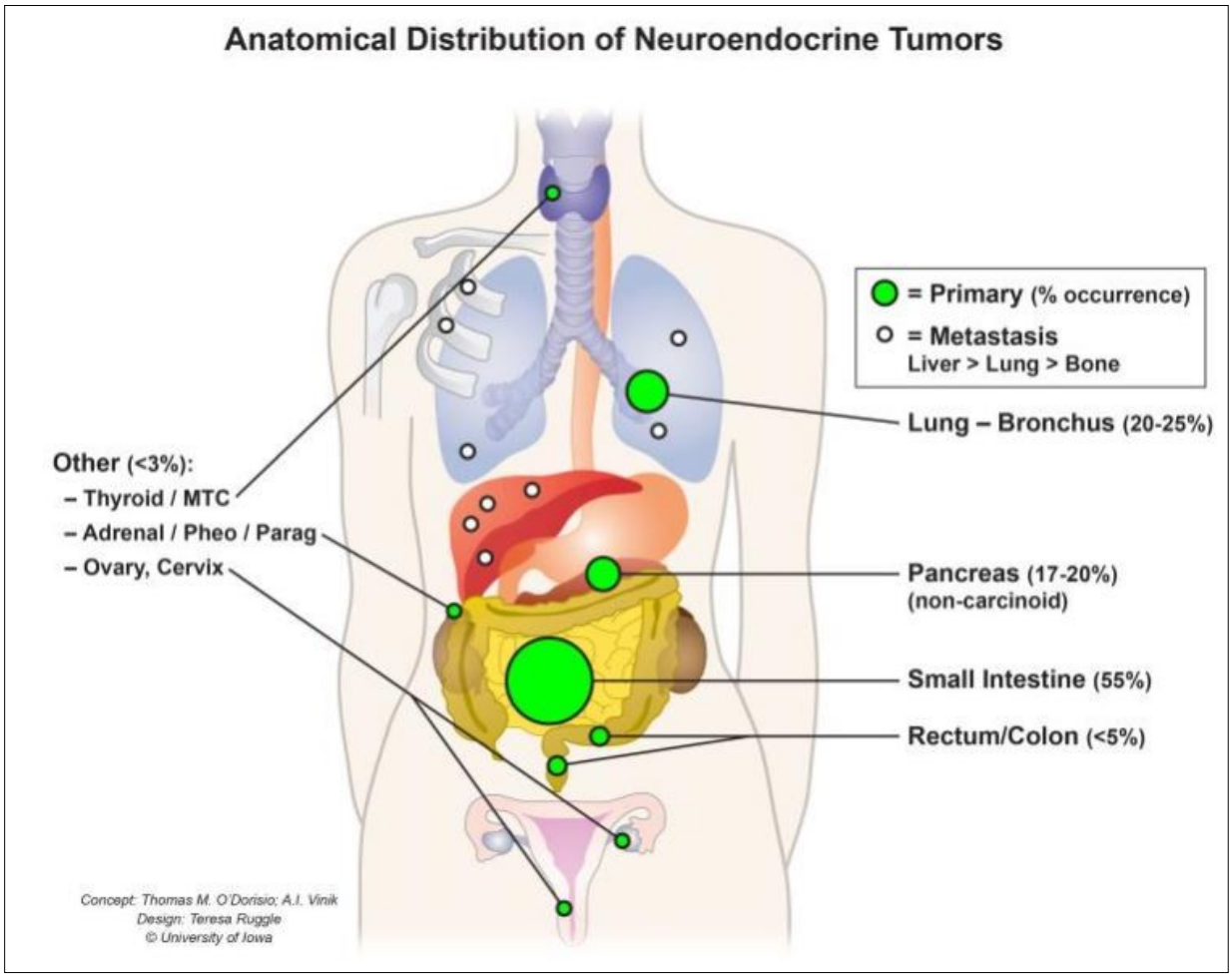

Figure 1: Anatomical distribution of NETs displaying primary and metastatic sites and their frequency. Abbreviations: Paraganglioma (Parag), Pheochromocytoma (Pheo), Medullary thyroid carcinoma (MTC). With permission taken from [X1].

Classification and grading of neuroendocrine neoplasms (NENs) of the GI tract and hepato-pancreatobiliary organs.

Terminology	Differentiation	Grade	Ki-67 index
NET G1	Well differentiated	Low	< 3 %
NET G2	Well differentiated	Intermediate	3-20 %
NET G3	Well differentiated	High	> 20 %
NEC, small cell type	Poorly differentiated	High	> 20 %
NEC, large cell type	Poorly differentiated	High	> 20 %

Table 1: Classification and grading of neuroendocrine neoplasms (NENs) of the gastrointestinal tract (GI tract) and hepatopancreatobiliary organs. Modified from the 2019 WHO classification of tumors of the digestive system.

1.2 Virotherapy

1.2.1 Introduction

Immuno-oncology therapies have revolutionized the treatment for several tumor entities and gained broad scientific interest, climaxing in the Nobel prize for medicine 2018 which was awarded to James P. Allison and Tasuku Honjo “for their discovery of cancer therapy by inhibition of negative immune regulation” [97].

Oncolytic viruses may well be the next breakthrough in cancer-immunotherapies since they are able to both exhibit direct tumor-selective oncolysis and to trigger a virus-antigen enhanced anti-tumoral immune reaction in a virus-induced highly inflammatory tumor micromilieu, resulting in a strong and long-lasting anti-tumoral systemic immune response [12, 13].

It is well known that certain viruses are oncogenic and can eventually lead to cancer, the most famous example being human papillomaviruses, which play a central role in the development of for example cervical carcinoma [14]. The German virologist Harald zur Hausen was awarded the Nobel Prize for the discovery of the underlying mechanisms in 2009.

1.2.2 Brief history and underlying mechanisms

On the contrary, in the 20th century it was observed that simultaneous viral infections interfered and sometimes even led to remission in cancer patients, exemplarily displayed in the regression of Burkitt’s Lymphoma in association with measles virus infection [15].

These “experiments by nature” soon gained scientific interest and various viruses such as Hepatitis B virus for Hodgkin’s disease in the late 1940s or Mumps virus in the 1970s for different terminal cancers were tested for their ability to successfully oncolyse tumor cells [16].

Soon it became clear that viruses despite being able to exhibit strong tumoricidal effects need specific manipulation to selectively infect tumor cells while leaving healthy tissue unharmed.

The underlying mechanisms of oncolytic virotherapy are shown exemplarily for oncolytic measles vaccine viruses that have been used in this thesis in figure 2 below.

The general idea behind virotherapy is that oncolytic viruses selectively infect and oncolyse tumor cells, leaving healthy surrounding tissue unharmed.

This oncolysis triggers two crucial steps for a potentially successful therapy. First, oncolysis itself reduces the tumor mass, and by the release of viral progeny, which can infect neighboring tumor cells, this effect becomes even stronger.

The second mechanism of virotherapy, nowadays thought to be the more important one, is that the infection and lysis of tumor cells trigger a systemic immune response. This is caused

by the release of tumor-specific neo-antigens in a highly inflammatory viral environment. This leads to immunogenic cell death, dendritic cell activation as well as antigen presentation and thereby priming of T cells [17]. To put it in a nutshell, infection and lysis of tumor cells by oncolytic viruses enhances both the innate and adaptive antitumor activity, explaining why the injection of oncolytic viruses in a single tumor lesion results in anti-tumor effects also in distant metastases as observed in patients suffering from cutaneous melanoma [18]. Therefore, oncolytic virotherapy is especially interesting for metastatic tumors which are difficult to treat and cure.

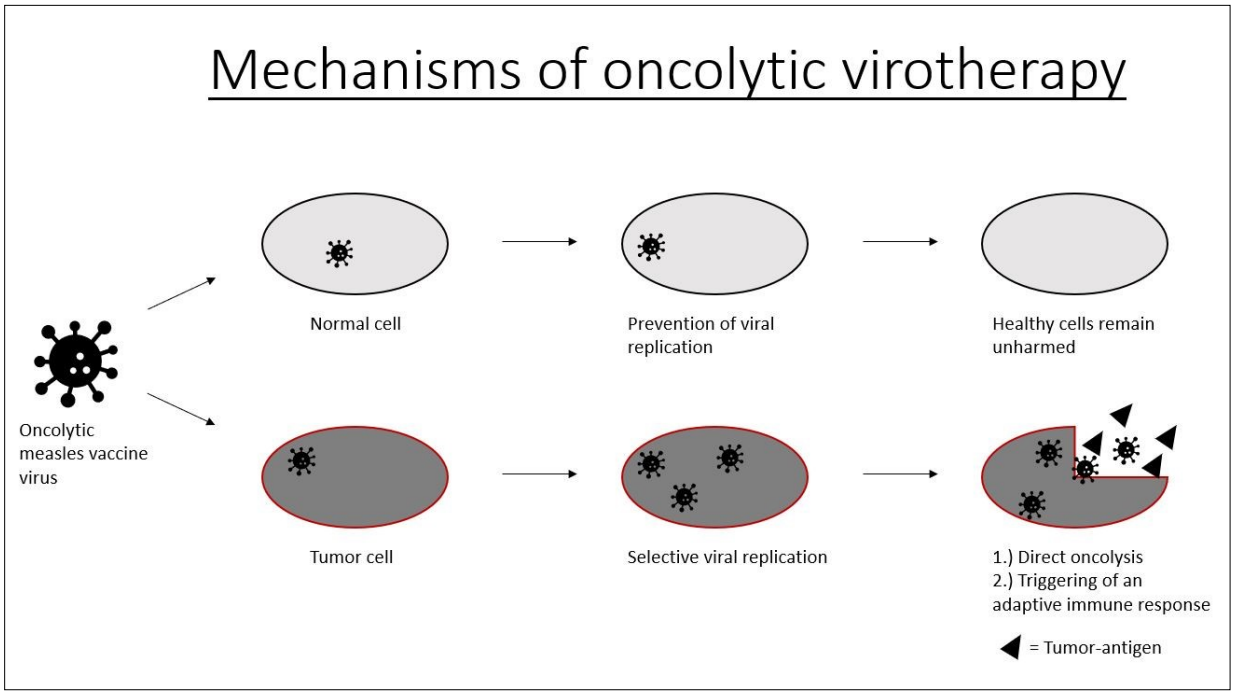

Figure 2: Mechanisms of oncolytic virotherapy with oncolytic measles vaccine virus. The oncolytic measles vaccine virus selectively replicates in tumor cells while replication in normal cells is prevented by an intact innate immune response. Viral infection and replication in tumor cells lead to both direct local tumor destruction and immune activation by the release of tumor-antigens that are recognized by cells of the adaptive immune system, ultimately leading to a systemic tumor-specific immune response.

1.2.3 Genetic modifications of oncolytic viruses

While some viruses have a natural tropism for tumor cells, for example measles virus [19] or herpes virus for highly migratory and invasive carcinomas [20], others have to be safely brought to the respective tumor cells to secure local and selective lysis while sparing healthy tissue.

This brought up the idea of a genetic manipulation of viruses to make them for example suited for selective infection [21].

Genetic manipulation of viruses aims at (i) specifically “targeting” tumor cells, thus ensuring selective infection [22] (ii) improving their oncolytic potential by “arming” [23-25] or (iii) optimizing virus delivery by “shielding”.

Targeted viruses gain their selectivity either by specific entry into tumor cells by retargeting the virus to surface molecules expressed by cancer cells, for example carcinoembryonic antigen (CEA) [22] or post entry by making the expression of essential viral genes dependent on tumor-selective promoters such as the later discussed adenovirus “AdVince” (see 1.4) [26].

Exemplary “armed” viruses are the MeV-SCD virus used in this thesis [25] as described later in 1.3.4.2 or an oncolytic measles virus encoding IL-12 ensuring effector T cell activation and the upregulation of key effector cytokines such as IFN-γ and TNF-α [27].

While the host’s immune system plays an essential role in successful oncolytic virotherapy as described above in 1.2.2, high protective anti-measles antibody titers which have a high prevalence in the population due to vaccination, might interfere with systemically applied MeV, which is essential for a potential treatment of metastatic cancers. Therefore, “shielding” the virus to ensure virus delivery to the various tumor sites is another important step to optimize results of oncolytic virotherapy [28]. Different strategies have been developed to avoid neutralization by pre-existing antibodies: on the one hand infected cellular vehicles such as mesenchymal stem cells are a possible way of transporting for example measles vaccine virus to the effector cells [29]. On the other hand, chemical modifications that coat the oncolytic virus and thereby avoid neutralization by pre-existing antibodies have been developed [30]. Finally, pseudotyping viruses is another strategy to evade neutralizing antibodies. Pseudotyping is a strategy in which viruses are produced with envelope proteins of viruses that do not have a high prevalence in the population. For MeV, this was successfully done pseudotyping it with the canine distemper virus [31].

1.2.4 Clinical usage of oncolytic viruses

A broad spectrum of different potential oncolytic viruses has been assessed on a wide array of various tumor types [13]. The prototype is the viro-immunotherapeutic agent T-VEC/IMLYGIC®, a genetically modified human herpes simplex virus type 1 (HSV-1) expressing granulocyte macrophage colony-stimulating factor (GM-CSF), which was the first virotherapeutic drug being approved by both the Food and Drug Administration (FDA) and European Medicines Agency (EMA) in 2015 for the treatment of advanced melanoma [32, 33]. Meanwhile, T-VEC/IMLYGIC® showed some promising results in ongoing clinical surveillance, too, [34] and is currently assessed in combination with other immunotherapeutic drugs for the treatment of further solid tumors [35].

1.3 Measles virus

1.3.1 Characteristics of measles virus

Measles virus is a highly contagious, enveloped negative strand RNA-virus belonging to the family of Paramyxoviridae and the genus Morbillivirus. Its 16 kb long genome comprises six genes encoding eight proteins, six of them structural (fusion protein F, hemagglutinin H, large protein L, phosphoprotein P, matrix protein M, nucleocapsid protein N) and two non-structural (V protein, C protein) as displayed in figure 3 below. While the two surface glycoproteins hemagglutinin and fusion protein mediate attachment (H) and subsequently membrane fusion and viral entry into the cell (F), the P-, N- and L-proteins initiate replication within the cytoplasm of the cell. Finally, the M protein is considered to be responsible for the assembly and budding of the virion in the end of the replication cycle [36].

Measles virus causes a disease with fever, maculopapular exanthema, respiratory symptoms and conjunctivitis as the typical clinical symptoms. Common complications of measles infection include pneumonia, being the most frequent fatal complication [37] as well as severe complications affecting the central nervous system such as acute postinfectious measles encephalitis or the highly feared subacute sclerosing panencephalitis (SSPE) [38]. Measles disease is especially common among children in developing countries with 869.770 reported total cases with up to 207.500 estimated dead people in 2019, the highest number since 1996 [39] despite the availability of a safe and effective vaccination.

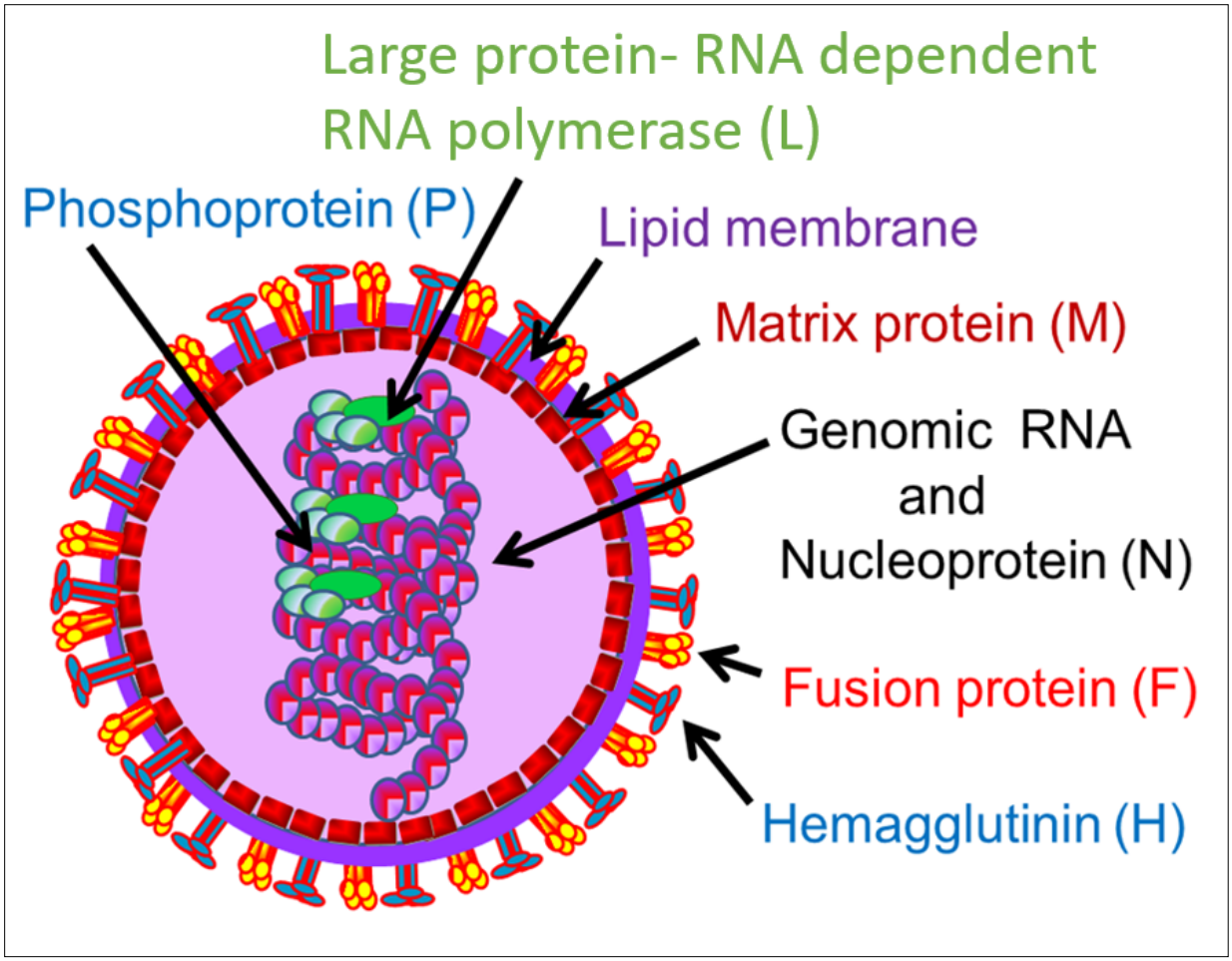

Figure 3: Schematic diagram of a measles virus. Measles virus particles are enveloped with a lipid bilayer membrane and contain six structural proteins: Phosphoprotein P, Large protein-RNA dependent RNA-polymerase L, Matrix protein M, Genomic RNA and Nucleoprotein N, Fusion protein F and Hemagglutinin H. *Modified using Public Domain figures from wikicommons.*

1.3.2 Measles virus receptors

Wild type measles virus can enter cells via two different receptors. First, it can use the so-called signaling lymphocyte activation molecule family member 1 (SLAMF1, also known as CD150), mainly expressed on T and B cells. Moreover, measles virus also uses the so called Nectin cell adhesion molecule 4 for cell entry which was found to be expressed by epithelial cells [40].

Interestingly, measles vaccine strains such as Edmonston B strain have a further option for cell entry, namely CD46, a ubiquitously expressed type 1 transmembrane protein, playing an important role in complement activation [41]. Of note, CD46 was found to be overexpressed on several tumor cells [19], making measles virus an interesting option for oncolytic virotherapy. Lately, CD46 has been targeted in more than 20 clinical trials to treat various types of cancers [42].

1.3.3 Measles virus as an oncolytic virotherapeutic agent

As mentioned in 1.2.2, doctors in the 20th century observed several cases in which simultaneous viral infection in cancer patients led to a reduced tumor burden or even resulted in partial remission. This observation is true for measles virus, too, and most prominently displayed in a case of an eight-year old patient in Uganda [15], whose orbital swelling, which was histologi-

cally diagnosed as a Burkitt lymphoma, began to decrease significantly after the patient developed a typical generalized measles exanthema. Following measles infection, the patient remained in remission for four months without any further anti-tumor therapy.

Since measles is a highly contagious and dangerous infectious disease as described in 1.3.1, wild-type measles virus cannot be used as an oncolytic virotherapeutic agent. However, although the use of a replication-competent virus might cause safety concerns, the measles virus used for oncolytic virotherapy derives from the Edmonston B vaccine lineage [43] which has been used millions of times for vaccinations over the last decades with very few side effects.

Due to their natural tropism to tumor cells oncolytic measles vaccine viruses have been used for a plethora of different cancer cells [44] in both preclinical and clinical studies [45]. Most notably, a study using a measles vaccine virus genetically modified to express the sodium/iodide symporter for the treatment of multiple myeloma [46] showed one case of complete durable remission in a heavily pretreated patient suffering from multiple myeloma. This can be seen as a proof of concept for oncolytic virotherapy using measles vaccine virus. Interestingly, multiple myeloma cells overexpress CD46, too [47]. Moreover, p53 was shown to regulate CD46 expression and thereby potential measles virus infection in myeloma cells [48]: while TP53wt cells inhibit both CD46 expression and consequently measles infection, cells with mutated TP53 overexpressed CD46 and were highly susceptible to measles virus infection.

1.3.4.1 Genetically modified measles viruses

As mentioned above in 1.2.3, there are different ways and goals for the genetic modification of oncolytic viruses. This is true for oncolytic measles viruses as well, which were either targeted, armed or shielded to enhance their therapeutic effect [49].

Genetically engineered viruses have been designed which facilitate tracking of replication behavior by the secretion of soluble marker peptides such as soluble human carcinoembryonic antigen [50] or by the expression of the human thyroidal sodium/iodide symporter (NIS), which allows non-invasive imaging in vivo and can additionally be combined with radiotherapy using ^{131}I [51].

Measles viruses have been retargeted on both entry and post-entry level. On the entry level, oncolytic measles viruses for instance have been retargeted to CD20 on B cells [52] or Epidermal growth factor receptor variant three (EGFRvIII) in glioblastoma cells [53], while retargeting on the post entry level was achieved by the insertion of microRNA-target sequences inhibiting viral spread in healthy tissue [54].

“Armed” oncolytic measles viruses comprise suicide-gene armed viruses such as MeV-SCD described in detail in the section 1.3.4.2 as well as viruses designed to increase immunotherapeutic effects. For this purpose a transgene encoding granulocyte macrophage colony-stimulating factor (GM-CSF) [55] was inserted in order to increase the anti-tumoral effect by recruiting neutrophils to the tumor site or lately IL-12, resulting in strong tumoricidal effects by activating CD3+ cells [27].

1.3.4.2 MeV-SCD

Measles viruses have been armed to enhance their oncolytic potential, one of them being MeV-SCD, which has also been used in this dissertation. It is encoding the suicide gene Super Cytosine Deaminase (SCD), a fusion protein of yeast uracil phosphoribosyltransferase (UPRT) and yeast cytosine deaminase (CD). The fusion protein can locally convert the common antifungal drug 5-fluorocytosine (5-FC), a pyrimidine analogue, into the common chemotherapeutic drug 5-fluorouracil (5-FU) as shown in figure 4 below. Furthermore, it facilitates further conversion of 5-fluorouracil into 5-fluorouridine monophosphate (5-FUMP). After that, 5-FUMP is

either further phosphorylated to 5-fluorouridine triphosphate (5-FUTP), which is incorporated into RNA, thereby inhibiting protein synthesis, or further reduced to 5-fluorodeoxyuridine monophosphate (5-FdUMP) which inhibits the thymidylate synthase, ultimately leading to deoxythymidine triphosphate (dTTP) depletion resulting in inhibition of DNA synthesis as displayed in figure 5. Normally, 5-FU is quickly degraded by dihydropyrimidine dehydrogenase (DPD) into 5-fluoro-ß-alanine (5-FßAL) and subsequently renally excreted. The insertion of UPRT serves as a competitive enzyme, reducing the degradation of 5-FU and thereby enhancing the antitumor effect of 5-FU [56], [57]. The chemotherapeutic compound 5-FU was first discovered in 1957 [58] and has been in use for the treatment of various cancers for decades and is still a treatment option for NENs if systemic chemotherapy is required [10]. It is a fluoridized form of uracil and therefore incorporated into DNA/RNA, thereby interfering with replication.

MeV-SCD and the exploitation of its suicide gene function by adding the prodrug 5-fluorocytosine (5-FC) has proven to be effective in preclinical models for the treatment of various cancers, e.g. cholangiocarcinoma [23] or acute myeloid leukemia (AML) [25], enhancing the oncolytic effect in comparison to measles virus alone. Moreover, the suicide gene function can together with increasing MOIs overcome resistance phenomena to oncolytic measles virus monotherapy [59].

The great advantage of using MeV-SCD is that the non-toxic compound 5-FC, which is systemically administered, does not have any negative impact on healthy cells, while the local conversion into 5-FU in infected tumor cells lyses specifically the tumor cells, thus avoiding the negative side effects of a systemic chemotherapy. As 5-FU is highly diffusible, neighboring tumor cells that are not primarily infected by MeV-SCD, are damaged by 5-FU as well, which is referred to as the so-called “bystander effect” [60].

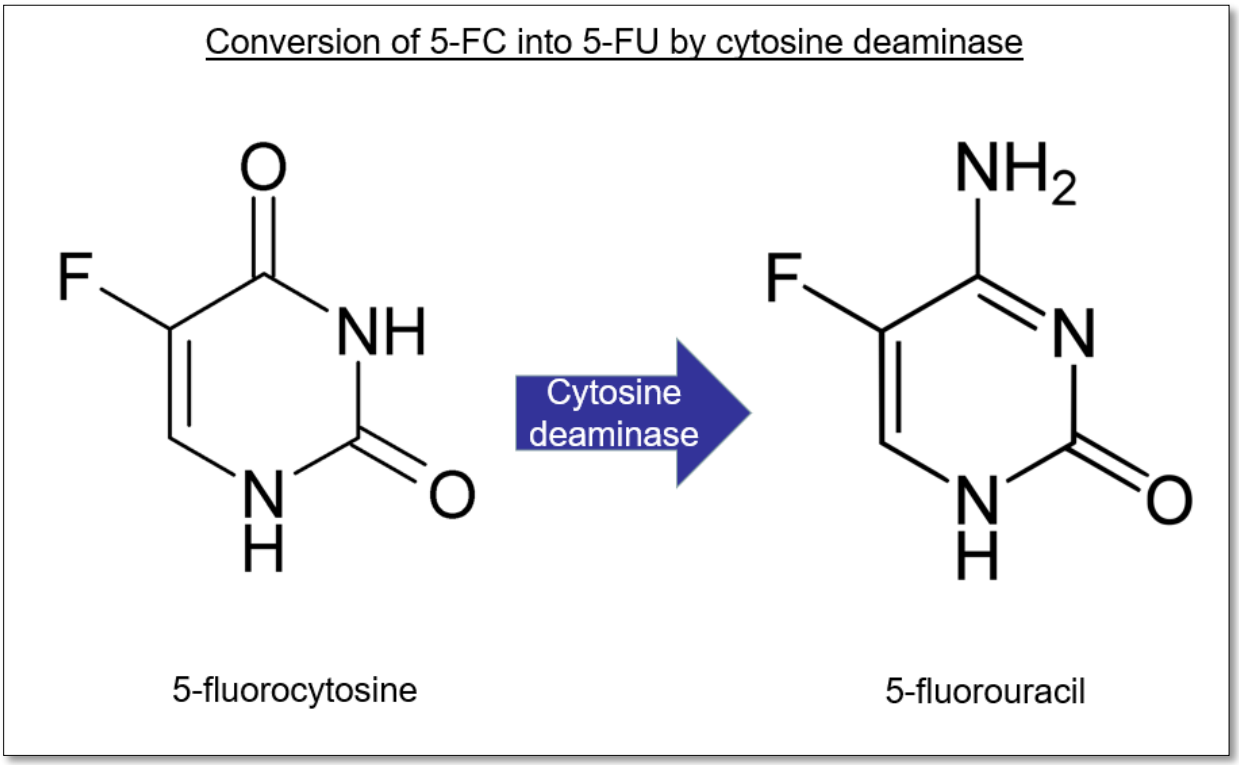

Figure 4: The cytosine deaminase converts the prodrug 5-fluorocytosine (5-FC) locally into the common chemotherapeutic compound 5-fluorouracil (5-FU). 5-FU is further degraded by uracil phosphoribosyltransferase (UPRT) to 5-fluorouridine monophosphate which interferes with DNA/RNA/protein synthesis and DNA-repair. *Modified using Public Domain figures from wikicommons.*

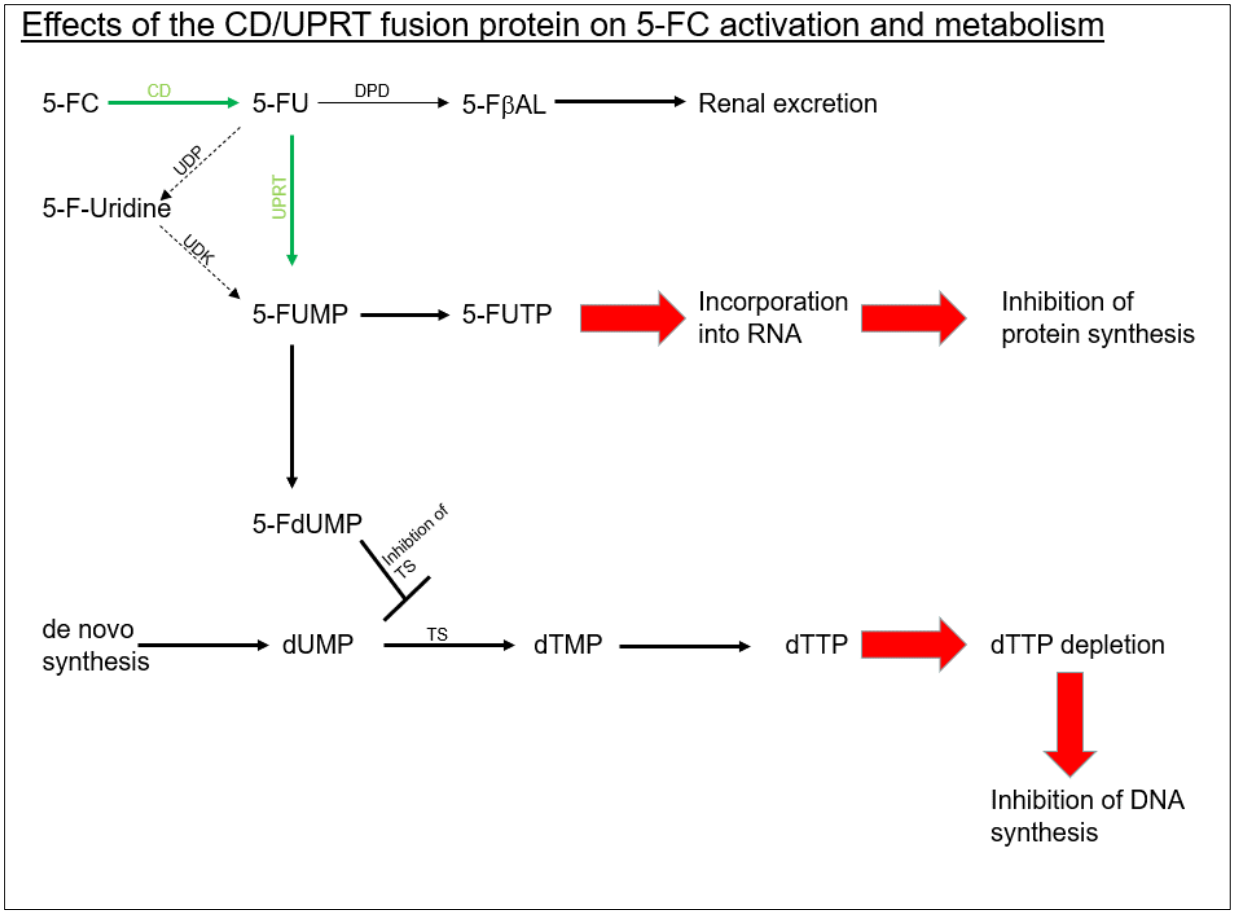

Figure 5: Effects of the CD/UPRT fusion protein on 5-FC activation and metabolism. The uracil phosphoribosyltransferase (UPRT) further converts 5-fluorouracil (5-FU) directly into 5-fluorouridine monophosphate (5-FUMP), thereby accelerating 5-FU activation as well as decreasing 5-FU degradation by dihydropyrimidine dehydrogenase (DPD) into 5-fluoro-ß-alanine (5-FßAL) and subsequently renal excretion. 5-FUMP is on the one hand further metabolized into 5-fluorouridine triphosphate which inhibits protein synthesis as it is incorporated into ribonucleic acid (RNA). On the other hand, it is also converted into 5-fluorodeoxyuridine monophosphate (5-FdUMP) which inhibits thymidylate synthase (TS). Because of that, the conversion of deoxyuridine monophosphate (dUMP) into deoxythymidine monophosphate is reduced, leading to a depletion of deoxythymidine triphosphate (dTTP), ultimately resulting in inhibition of DNA synthesis. *Modified after the original publication from [57].*

1.3.5 Combination therapies

Another possibility to further enhance anti-tumor effects of oncolytic measles vaccine viruses is to combine them with other effective therapeutic modalities, a strategy that is very common in modern oncology for various types of cancer. Therefore, oncolytic measles viruses have been combined in vitro with chemotherapy, for example gemcitabine in pancreatic cancer cell lines [61] in a so called “chemovirotherapy”. Moreover, experimental combination therapy regimes include the other hallmarks of modern cancer therapy such as radiation in in vivo xenograft models [62] and small molecules such as janus-associated kinase (JAK) inhibitors in in vitro models [63]. Moreover, the combination of drugs inducing therapeutic senescence such as doxorubicin or taxol with oncolytic measles vaccine viruses resulted in enhanced killing of tumor cells in cell culture models [64]. This strategy was among others evaluated in this thesis for neuroendocrine neoplasms as well (see 3.4.3).

1.4 Virotherapy for neuroendocrine neoplasms

1.4.1 Overview

Several viruses have been tested for the treatment of neuroendocrine neoplasms both in pre-clinical settings as well as in some clinical trials [65]. A selection of those viruses is displayed in table 2.

Table 2: **Oncolytic viruses used for the treatment of neuroendocrine neoplasms.**

Virus	Status	Modifications	Tumors	References
Seneca Valley Virus (SVV001/ NTX-010)	*Adults*: Phase 2 Clinical trial (prematurely terminated) *Children:* Phase 1 Clinical trial	None	Small cell lung cancer, Neuroblastoma, Rhabdomyosarcoma, other rare tumors with neuroendocrine features	[66] NCT00314925 NCT01017601 NCT01048892
Adenoviruses serotype 5 (Ad5):				
Ad5fkFWKT(CgA-E1A-miR122)	Preclinical	Somatostatin peptide in the fiber knob, E1A gene expression controlled by Chromogranin A promoter, liver-specific degradation of E1A-mRNA by miR122	SI-NETs	[67]
Ad5PTDf35-[Δ24-sNAP]	Preclinical	infection-enhanced, replication-selective (E1AΔ24) armed with soluble HP-NAP	SI-NETs	[24]
Ad5(PTD)(CgA-E1AmiR122)	Phase 1&2 Clinical trial	Protein Transduction Domain as a cell penetrating peptide for enhanced infection, E1A gene expression controlled by Chromogranin A promoter, liver-specific degradation of E1A-mRNA by miR122	Metastatic neuroendocrine Tumors	[26] NCT02749331
Ad-INSM1p-HSV-tk (K5) Ad-INSM1p-Δ24E1A-IRES-HSV-tk	Preclinical	INSM1 promoter, neuron-restrictive silencer elements (NRSEs), expression of a mutated adenovirus E1A and a herpes simplex thymidine-kinase (HSV-tk) gene	Insulinomas	[68]

Adeno-associated viruses and phages (AAVP):				
Oct-AAVPTNF	Preclinical	Presenting biologically active Octreotide on the viral surface; apoptosis promoting tumor necrosis factor	NETs of the pancreas	[69]
Vaccinia virus GLV-1h68	Preclinical	Encodes β-glucuronidase, β-galactosidase and Ruc-GFP marker genes for possible monitoring	NET/NEC cell lines	[70]
Herpes simplex virus type 1				
Talimogene laherparepvec (T-VEC, herpes simplex virus type 1)	Preclinical	Deletion of ICP 34.5 and ICP 47 to ensure tumor-specific replication as well as reduced viral immunogenicity; Insertion of GM-CSF for stimulation of the immune response	NET/NEC cell lines	[71]
T-01 (Herpes simplex virus type 1)	Preclinical		NET cell lines, mouse model	[72]

1.4.2 Seneca valley virus

Seneca valley virus originally has been isolated from cultured cells and the identified cytolytic agent was thus plaque-cloned and designated Seneca Valley Virus 1 (SVV-001). It belongs to the family of Picornaviridae and revealed a potent cytolytic activity and high selectivity for tumor cell lines carrying neuroendocrine features [73].

A first phase I study (NCT00314925: “Safety Study of Seneca Valley Virus in Patients With Solid Tumors With Neuroendocrine Features”) employing a dose escalation scheme of single intravenous (IV) administrations of SVV-001 was initiated in 2006 and proved safety and feasibility of IV delivery to adult patients with heavily pretreated and metastatic neuroendocrine tumors [66]. Of note, all patients cleared virus within the study period and mounted immunity with neutralizing antibodies [74].

Based on the results from this initial trial, a randomized double-blinded phase II study of SVV-001 in patients with extensive-stage small cell lung cancer (SCLC) was initiated in 2010 (NCT01017601: “Seneca Valley Virus-001 After Chemotherapy in Treating Patients with Extensive-Stage Small Cell Lung Cancer”). However, this study was terminated in 2013 due to the results of an interim analysis which declared futility.

In a third pediatric trial (NCT01048892: “Seneca Valley Virus-001 and Cyclophosphamide in Treating Young Patients With Relapsed or Refractory Neuroblastoma, Rhabdomyosarcoma, or Rare Tumors With Neuroendocrine Features”), patients also received SVV-001 IV. However, there were no objective responses (complete or partial) reported [66].

Taken together, SVV-001 achieved great honors in becoming the first oncolytic virus to be tested in both a pediatric and adult phase I trial for recurrent/refractory tumors and the first

oncolytic virus ever to be tested in children worldwide. Despite encouraging preclinical data supporting the use of this virus in tumors expressing neuroendocrine features, objective clinical responses were lacking in both the adult and pediatric phase I studies [66].

1.4.3 Adenoviral (Ad) and Adenovirus-associated virus and phage (AAVP) vectors

Adenovirus serotype 5 has been identified as a potential biological compound for various tumors and now has been tested and optimized on neuroendocrine neoplasms for over a decade, lately leading to a first clinical trial.

First, a replication-selective adenovirus serotype 5 was designed, which has its selectivity due to a chromogranin A (CgA) promoter controlling the expression of the adenoviral E1A gene [75]. As remnant replication in hepatocytes was regarded as a safety issue, especially in scenarios in which NEN metastasis to the liver should be treated, the insertion of a liver-specific miRNA122 was the next consequent step in adenoviral genome modification. This led to a virus whose replication is successfully downregulated in healthy hepatocytes but not in transformed neuroendocrine tumor cells [76].

Moreover, a genetically modified armed adenovirus encoding the soluble Helicobacter pylori-Neutrophil-activating-Protein (HP-NAP) demonstrated successful recruiting of neutrophils and induction of a TH1-type differentiation in the neuroendocrine tumor microenvironment [24].

Finally, a triple modified adenovirus containing three of the above described modifications (CgA promoter, miR122 target sequences, protein transduction domain (PTD)) called Ad5(PTD)(CgA-E1AmiR122)) was generated and denominated after the donor who funded the “AdVince clinical trial" [26]. Importantly, AdVince did not exhibit killing of freshly isolated hepatocytes, but of neuroendocrine tumor cells. Furthermore, AdVince did not activate the complement system or induce considerable amounts of pro-inflammatory cytokines or chemokines. Accordingly, these preclinical data paved the way for a clinical trial, which already has been started.

In March 2016, the first clinical trial treating neuroendocrine tumors with an oncolytic adenovirus started in Uppsala, Sweden. It is an open-labelled, uncontrolled, single-center phase I/IIa clinical study (NCT02749331) to evaluate the safety of repeated infusions of the adenoviral vector AdVince, which is administered into the hepatic artery in patients with metastatic neuroendocrine neoplasms in order to specifically address and treat liver metastases. Patients to be included must show a progressive neuroendocrine carcinoma of gastrointestinal, pancreatic or bronchial origin that is considered impossible to cure with any of the standard treatment options. Study objectives are (i) to determine the maximum tolerated virus dose, (ii) to evaluate the anti-tumoral efficacy of AdVince infusions on metastatic neuroendocrine tumors, (iii) to determine the replication profile of AdVince and (iv) to determine the humoral (antibody) and cytokine-mediated immune response to AdVince. This study is accompanied by tumor mass monitoring using imaging techniques such as (PET)-CT, measuring hormone activity in blood samples as well as detecting changes in the replication profile of AdVince by real time PCR. The estimated primary completion date is August 2023.

1.4.4 GLV-1h68

Vaccinia virus GLV-1h68 is an oncolytic DNA-virus carrying three separate transgenic expression cassettes (β-glucuronidase, β-galactosidase, Ruc-GFP) and was used successfully in both in vitro and in vivo settings for the treatment of various cancers such as human hepatocellular carcinoma or pancreatic adenocarcinoma in a so-called “chemovirotherapy” together with the common chemotherapeutic drugs gemcitabine and nab-Paclitaxel [77, 78]. It also showed promising antitumoral effects in six NET and one NEC cell line in a preclinical cell culture model [70].

1.4.5 T-VEC

Furthermore, T-VEC/IMLYGIC®, a genetically modified human herpes simplex virus type 1 (HSV-1) expressing GM-CSF which was approved by both FDA and EMA, displayed beneficial tumoricidal effects in various NET/NEC cell lines [71].

1.5 Everolimus

Everolimus, sold under the brand name Afinitor, is a medication working as an inhibitor of mammalian target of rapamycin (mTOR). It is part of the World Health Organization's list of Essential Medicines and is used in a variety of clinical settings, especially as an immunosuppressive drug after organ transplantation as well as a possible treatment strategy for various cancers, for example advanced renal cell carcinoma [79].

Everolimus was approved by the FDA for the treatment of metastatic pancreatic neuroendocrine tumors in 2011 and has been studied extensively in four so called "RADIANT" trials [80]. After these trials, the approval expanded on further NETs (nonfunctional, progressive lung and intestinal NETs) in 2016.

Pharmacologically everolimus works as an inhibitor of the protein kinase mTOR, a pathway that plays a crucial role in various diseases, among them the development of malignancies [81].

mTOR is part of the PI3K (phosphatidylinositol-3-kinase)/Akt (protein kinase B)/mTOR pathway, which regulates cell growth, proliferation and metabolism in cells. Growth factors or insulin bind to their respective receptor tyrosine kinase, thereby activating PI3K which then phosphorylates phosphatidylinositol-4,5-bisphosphate (PIP2) into phosphatidylinositol-3,4,5-trisphosphate (PIP3) as displayed in figure 6.

PIP3 can activate the serine/threonine kinase Akt, which ultimately activates mTOR via disinhibition of the tuberous sclerosis proteins 1 and 2 (TSC1/2). Activation of mTOR results in a plethora of downstream functions, among them promotion of cell cycle progression, growth, protein synthesis and metabolism as well as inhibition of autophagy [81]. Everolimus as an inhibitor of mTOR has the reversed effects.

mTOR is the catalytic subunit of two different complexes: mTORC1 and mTORC2. mTORC1 is a complex composed of mTOR, Mammalian lethal with SEC13 protein 8 (mLST8) and the non-core components PRAS40 and DEPTOR. Inhibition of mTORC1 leads to reduced cell growth, proliferation and angiogenesis and is the main target for the mTOR inhibitor everolimus [85].

Furthermore, deregulation of the mTOR-pathway also plays an important role regarding the development of neuroendocrine neoplasms [82].

As everolimus also serves as an immunosuppressive drug for example after organ transplantation, potential interactions when using virotherapeutic drugs might occur. Of note, everolimus did not impair the replication of GLV-1h68, another oncolytic virus, in a combinatorial approach [70].

Moreover, the PI3K/Akt/mTOR pathway has various interactions with different viruses that are reviewed in detail by Le Sage, Cinti, Amorim and Mouland [83] and are displayed in figure 6 below.

Out of the viruses tested in the treatment of NENs, Adenovirus (ADV) is known to activate mTORC1 in the end via a phosphatidylinositol 3-kinase (PI3K) dependent mechanism.

MeV, which was used for this thesis, is known to inhibit Akt kinase, a mechanism which is important for the immunosuppression induced by measles virus [84] and results in mTOR inhibition as well.

Vaccinia virus is known to activate PI3K/Akt through protein integrin β1 (ITGβ1), while herpes simplex virus type 1 (HSV-1) acts via a serine/threonine kinase called Us3 as an Akt mimic and phosphorylates TSC2 directly.

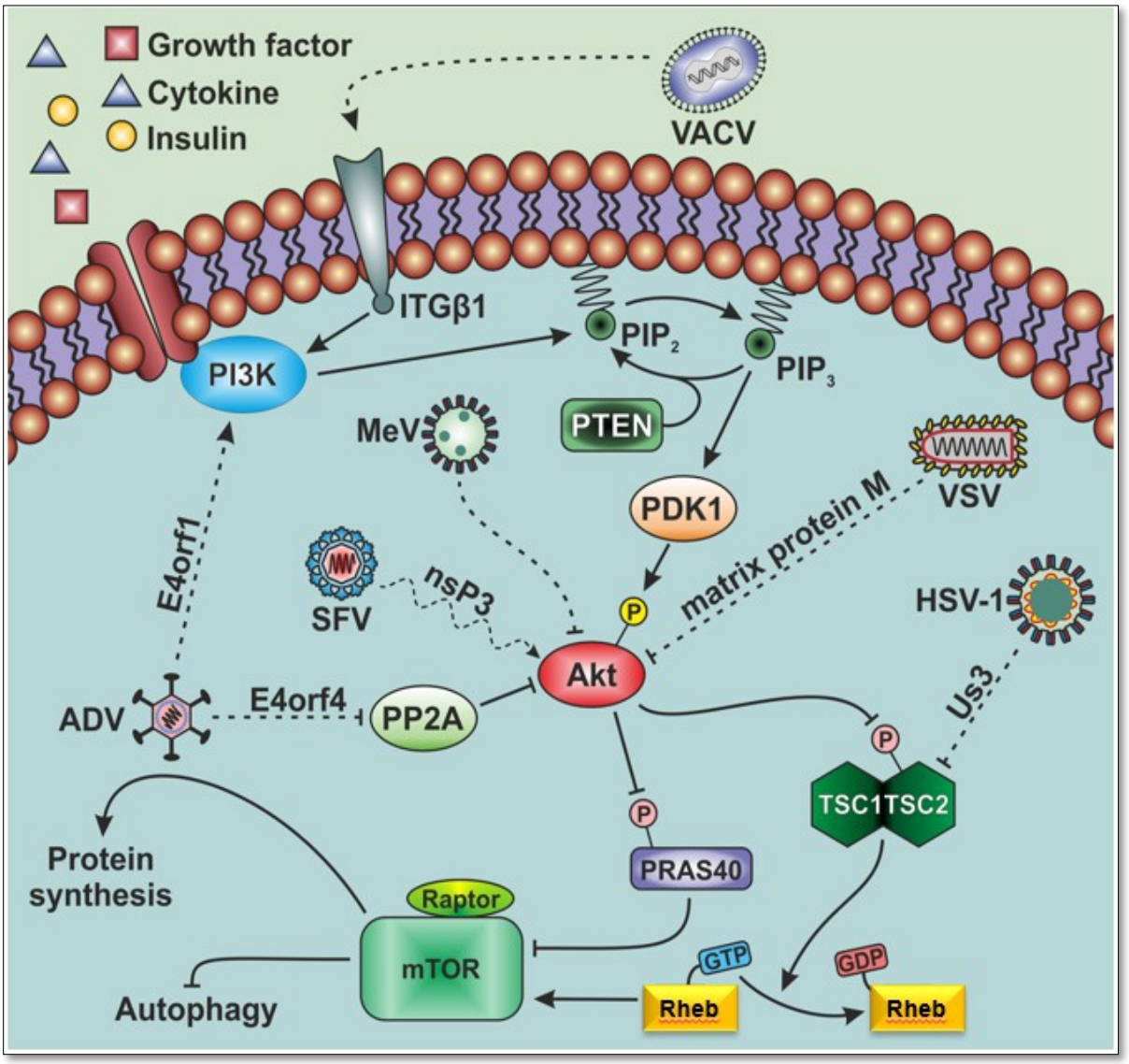

Figure 6: Schematic overview of various viruses interacting with the PI3K/Akt/mTOR pathway. MeV is known to downregulate Akt, leading to a limited immune response of the cell to infections. Out of the other viruses tested for the treatment of NENs, Vaccinia virus (VACV) and Adenovirus (ADV) are known to activate Akt through different mechanisms. Herpes simplex type 1 acts as an "Akt mimic" via the serine/threonine kinase Us3. Abbreviations: phosphatidylinositol 3-kinase (PI3K), Semliki Forest virus (SFV), tuberous sclerosis complex 1/2 (TSC1/2), Vesicular Stomatitis virus (VSV), Herpes Simplex virus type 1 (HSV-1), Ras homolog enriched in brain (Rheb), phosphatidylinositol-4,5-bisphosphate (PIP_2), phosphatidylinositol-3,4,5-trisphosphate (PIP_3), phosphatase and tensin homolog (PTEN), Phosphoinositide-dependent kinase-1 (PDK1), proline-rich Akt substrate of 40 kDa (PRAS40), protein integrin β1 (ITGFβ1). *Modified with permission from [83], figure 1.*

1.6 Aim of the dissertation

The objective of this dissertation was to investigate whether oncolytic virotherapy using oncolytic measles vaccine virus could be a possible treatment option for neuroendocrine neoplasms.

Therefore, it was assessed whether the state-of-the-art suicide-gene (SCD) armed oncolytic measles vaccine virus MeV-SCD can successfully (i) infect, (ii) replicate in and finally (iii) oncolyse tumor cells of neuroendocrine origin in a cell culture model.

Furthermore, it was to be evaluated whether the exploitation of MeV-SCD's suicide function resulted in an enhanced tumoricidal effect.

Moreover, possible interactions with the mTOR-inhibitor everolimus were investigated.

Finally, the combination of senescence inducing compounds and oncolytic measles vaccine virus was analyzed.

To the best of my knowledge, this was the first study using measles vaccine virus as an oncolytic viral agent for the treatment of neuroendocrine neoplasms.

2. Materials and Methods

2.1 Safety

All experiments were performed in a laboratory with Biosafety level 2 (Otfried-Müller-Straße 27, 72076 Tübingen, Germany). Thus, all experiments were carried out under a HERAsafe laminar flow laboratory hood (Heraeus; Hanau, Germany). Disinfection was performed using either 70 % isopropanol (SAV Liquid production; Flintsbach am Inn, Germany) or Descosept (Dr. Schumacher GmbH; Melsungen, Germany). Furthermore, surfaces and consumables in the hood were irradiated for at least 15 minutes with ultraviolet light after working with virus. Waste independent of it being solid or fluid was autoclaved at 2 bar pressure and 121 °C for 20 minutes (Autoclave 3850 EL, Systec; Linden, Germany).

2.2 Cell lines

Cell line	Origin	Source	Medium	Level of differentiation and proliferation rate	Expression of neuroendocrine markers	Expression of mTOR pathway molecules
BON1	Pancreas (foregut)	Dr. Renner MPI Psychiatry, Munich	Medium: DMEM + 10 % FCS	Serotonin positive (rare), peripancreatic lymph node metastasis, proliferation unknown	Synaptophysin: +++ Chromogranin A: +++ CD56: +	pS6: cytoplasm: +++ pmTOR: cytoplasm: + nucleus: +++ pAKT: cytoplasm: + nucleus: +++
QGP-1	Pancreas (foregut)	JCRB	Medium: RPMI-1640 + 10 % FCS	most likely a mixed adenoneuroendocrine carcinoma (MANEC), likely lower than a classical NEC; expresses CEA and secretes mucin Population doubling time 84 h	Synaptophysin: +++ Chromogranin A: ++ CD56: +++	pS6: cytoplasm: +++ pmTOR: cytoplasm: -/+ nucleus: +++ pAKT: cytoplasm: - nucleus: ++
H727	Lung (foregut)	ATCC	Medium: RPMI-1640 + 10 % FCS	-	Synaptophysin: ++ Chromogranin A: ++ CD56: ++	pS6: cytoplasm: +++ pmTOR: cytoplasm: ++ nucleus: ++ pAKT: cytoplasm: + nucleus: ++
UMC-11	Lung (foregut)	ATCC	Medium: RPMI-1640 + 10 % FCS	-	Synaptophysin: +++ Chromogranin A: ++ CD56: +++	pS6: cytoplasm: +++ pmTOR: cytoplasm: - nucleus: + pAKT: cytoplasm: + nucleus: ++
HROC 57	Colon ascendens (midgut)	PD Dr. Michael Linnebacher via Prof. Dr. Bence Sipos	Medium: DMEM/F12 (1:1) + 10 % FCS + 1 % Pen/Strep	Large-cell carcinoma, G3 Population doubling time 35 h	Synaptophysin: ++ Chromogranin A: - CD56: -	pS6: cytoplasm: +++ pmTOR: cytoplasm: +++ nucleus: +++ pAKT: cytoplasm: +++ nucleus: +++

Table 3: Cell lines and their respective culture conditions used for this dissertation. Abbreviations: cluster of differentiation 56 (CD56), phosphorylated-mTOR (pmTOR), phosphorylated-AKT (pAKT), phosphorylated S6 ribosomal protein (pS6). Expression of neuroendocrine markers and mTOR pathway molecules was done before the experiments by a specialized pathologist to ensure neuroendocrine origin.

As can be seen in table 3 above, in this study a panel of four NET and one NEC cell lines deriving from different anatomical origins was used. The H727 and UMC-11 lung NET cell lines were purchased from the American Type Culture Collection (ATCC). The pancreatic cell lines BON1 and QGP-1 were obtained from Dr. Renner (MPI Psychiatry, Munich, Germany) and the Japanese Collection of Research Bioresources Cell Bank (JCRB), respectively. HROC-57 NEC cells deriving from the colon ascendens were obtained from PD Dr. Linnebacher (University Hospital Rostock, Germany) via Prof. Dr. Bence Sipos (University Hospital Tübingen). All five cell lines were described and used for publications previously [86], [87], [88], [89]. To guarantee neuroendocrine origin and differentiation, all cell lines were examined for the expression of neuroendocrine markers by a specialized pathologist before using them in experiments. Furthermore, expression of mTOR pathway molecules was also analyzed beforehand.

Vero cells (African green monkey kidney cells), which were used for titration assays evaluating $TCID_{50}$, were obtained from the German Collection of Microorganisms and Cell Cultures (DSMZ, Braunschweig, Germany).

2.3 Cell Culture

2.3.1 Solutions and media used for cell culture

Material	Source
EDTA-Trypsin	Biochrom, Berlin, Germany
PBS (phosphate-buffered saline)	Sigma Aldrich, Munich, Germany
DMEM (Dulbecco's modified Eagle's medium)	Sigma Aldrich, Munich, Germany
RPMI-1640 (Roswell Park Memorial Institute 1640 medium)	PAA
DMEM/F12	Gibco, Waltham, MA, USA
FCS (fetal calf serum)	PAA
Trypan Blue	Biochrome, Berlin, Germany
Penicillin/Streptomycin	Bio Whittaker, Lonza, Köln, Germany
DMSO (Dimethyl sulfoxide)	AppliChem Darmstadt, Germany

Table 4: Solutions and media and their respective producer used for this dissertation.

2.3.2 Cultivation and passaging of cells

The five cell lines described in the previous section (2.2) were grown as an adherent monolayer in tissue culture flasks with filter caps (75 cm^2 or 150 cm^2, Greiner Bio One; Frickenhausen, Germany) at 37 °C, 95 % humidity and 5 % CO_2 in an incubator. All cultures were tested to be free of mycoplasma.

QGP-1, H727 and UMC-11 cells were cultured in RPMI-1640 medium (Roswell Park Memorial Institute 1640 medium) supplemented with 10 % FCS (fetal calf serum), whereas BON1 and Vero cells (African green monkey kidney cells) were cultured in DMEM (Dulbecco's modified Eagle's medium) plus 10 % FCS. HROC57 cells were grown in DMEM/F12 supplemented with 10 % FCS and 1 % Penicillin/Streptomycin. Cells were analyzed daily using a CK40 contrast light microscope (Olympus, Shinjuku, Tokyo, Japan). Once the cells grew confluent, they were passaged (two to three times per week). For this, the respective medium was prewarmed to 37 °C, then the supernatant was removed, the cells were washed once with PBS before 2 ml of trypsin were added for 2-5 minutes in order to detach the cells. Once the cells were detached, 10 ml of medium were added again to inactivate trypsin. The cell suspension was transferred into a reaction tube and centrifuged at 1000 rpm for 4 minutes at room temperature (RT). The cell pellet was resuspended in fresh medium. Cell lines were split depending on their proliferation rate with one part being cultivated in fresh medium again, the other part being discarded.

2.3.3 Freezing of cells

To create a storage of cells for experiments, all cell lines were expanded and stored at – 80 °C in cryovials. Therefore, cells were first trypsinized and centrifuged as described above in 2.3.2. The remaining cell pellet was resuspended in a medium for cryoconservation containing RPMI-1640 with 20 % FCS and 10 % dimethyl sulfoxide (DMSO).

2.3.4 Thawing of cells

One aliquot of the respective cell line was quickly thawed in a water bath at 37 °C. Then, 10 ml of prewarmed cell culture medium were added and the cells were centrifuged at 1000 rpm for 3 minutes. The supernatant was discarded and the remaining cell pellet resuspended in 14 ml of growth medium. Cells were transferred into a tissue culture flask and stored in in the incubator.

2.3.5 Determining cell count using a Neubauer hemocytometer

To determine the precise cell count for experiments, the respective cells were first trypsinized. After centrifugation 10 µl of the cell suspension were diluted with 90 µl of Trypan Blue (Biochrom). Trypan Blue does not stain vital cells, since an intact cell membrane prevents incorporation of the dye, thus allowing the differentiation between vital colorless and dead blue cells. Next, the counting chamber was prepared by capping the Neubauer hemocytometer with a thin covering glass (figure 7). Following the dilution, a 10 µl sample of the cell suspension was gently pipetted close to the edge of the covering glass, allowing capillary action to draw the sample inside the chamber. Now the cell number was assessed using a CK40 light microscope (Olympus). The hemocytometer is divided into four larger squares, each consisting again of 16 smaller squares (figure 8). Usually, the vital cells in at least two big squares were counted and according to the formula below consequently divided by two, then multiplied by 10^4. Thus, the number of cells was calculated by the following formula:

$$Concentration\left(\frac{cells}{ml}\right) = dilution\ x\ 10^4\ x\ \frac{cells}{square}$$

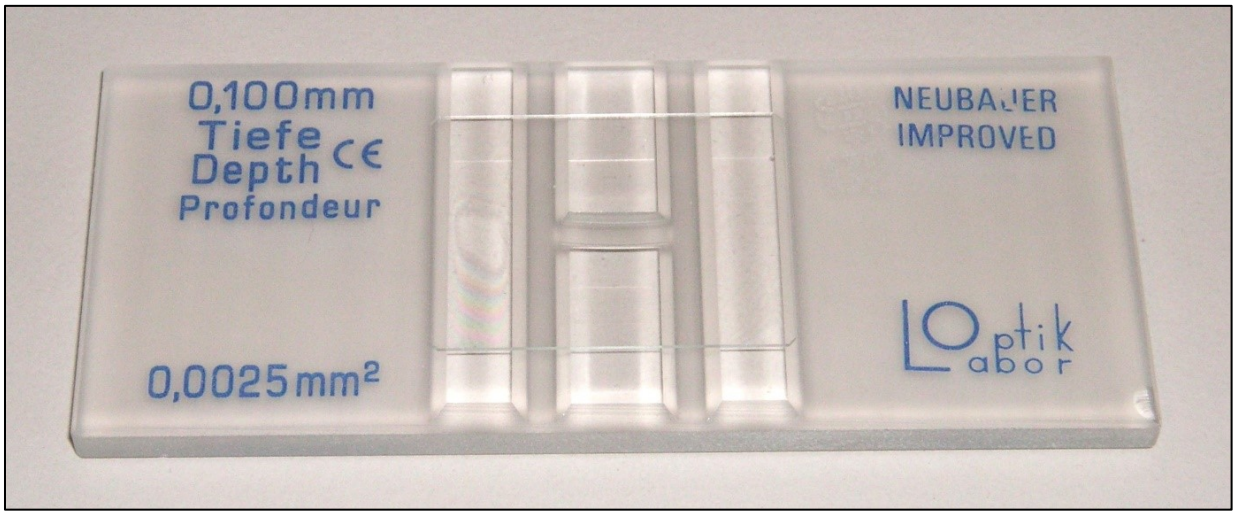

Figure 7: Representative improved Neubauer hemocytometer used for determining cell count.
Picture taken from "https://de.wikipedia.org/wiki/Z%C3%A4hlkammer#/media/Datei:Neubauer_improved_counting_chamber.jpg" (retrieved 18.02.2021).

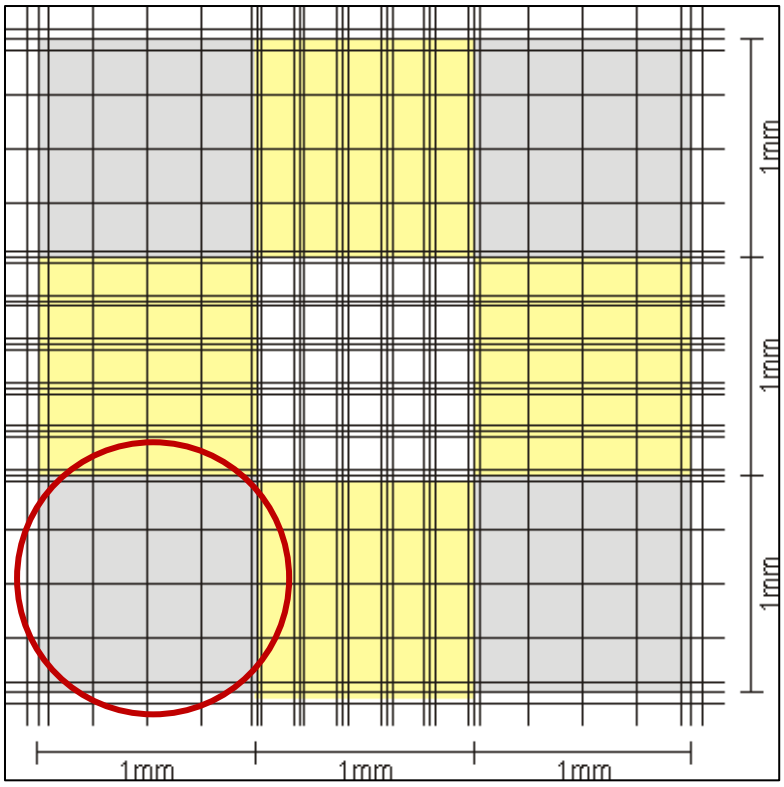

Figure 8: Improved Neubauer chamber grid detail.
Modified after "https://de.wikipedia.org/wiki/Z%C3%A4hlkammer#/media/Datei:Neubauer_improved_schema.gif" (retrieved on 18.02.2021). The hemocytometer is divided into four larger squares, each consisting of 16 smaller squares. One of the large squares is marked with a red circle. Cells were counted in at least two big squares; cell count was calculated by the formula above.

2.3.6 Plating cells for experiments

Due to different growth rates of the respective cell lines, different amounts of cells were seeded for the various experiments as shown in tables 5-7 below.

Table 5: Six-well plate used for different experiments:

A) *Used for growth curves*

Cell line(s)	Number of cells per well in 2 ml medium
BON1	$5*10^5$
QGP-1, UMC-11, H727, HROC57	$4*10^5$

B) *Used for Beta-Galactosidase Assays*

Cell line(s)	Number of cells per well in 2 ml medium
BON1	$1*10^5$
H727	$1*10^5$

Table 6: 24-well plate used for different experiments:

A) *Used for testing of compounds*

Cell line(s)	Number of cells per well in 0.5 ml medium
BON1	$4*10^4$
H727, HROC57	$6*10^4$
QGP-1, UMC-11	$8*10^4$

B) *Used for viral infections*

Cell line(s)	Number of cells per well in 0.5 ml medium
BON1, H727, HROC57	$6*10^4$
QGP-1, UMC-11	$8*10^4$

Table 7: 96-well plate used for titration:

Cell line	Number of cells per well in 0.2 ml medium
Vero cells	10^4

2.4 Measles vaccine viruses

Two different measles vaccine viruses called MeV-GFP and MeV-SCD were employed for the experiments, both deriving from a commercially available original monovalent vaccine batch of measles virus (MeV) strain Mérieux (Sanofi-Pasteur, Leimen, Germany).

MeV-GFP contains a gene encoding green fluorescent protein (GFP), facilitating tracking of the viral infection. The second virus used was armed by the insertion of a gene encoding the prodrug-converting enzyme Super-CD (MeV-SCD).

2.5 Treatment of cells

For the treatment of cells with either 5-FU or everolimus, cells were seeded in 24-well-plates 24 hours prior to treatment (for the number of cells per well of the respective cell line see 2.3.6). One day after plating cells were treated with increasing concentrations of 5-FU/everolimus, each concentration was tested in triplicates.

Concentrations used for 5-FU: 0, 1 nM, 10 nM, 100 nM ,1 µM, 10 µM, 100 µM, 1mM.

Concentrations used for everolimus: 0, 0.01 nM, 0.1 nM, 1 nM, 10 nM, 100 nM, 1 µM, 10 µM.

2.6 Infection of cells

2.6.1 Viral infection of cells with MeV-SCD/MeV-GFP

In general, a defined number of cells varying due to the individual growth rate of the respective cell line (see 2.3.6) was seeded into cell culture multiwell plates 24 hours prior to infection. On the day of infection, medium was removed, and each well was gently washed with prewarmed (37 °C) PBS. In the meantime, one aliquot of the respective virus, which was stored at - 80 °C, was quickly thawed at RT. Cells were then infected at the indicated multiplicity of infection (MOI), which refers to the number of infectious viral particles (PFU) per cell at the time of infection. Therefore, the necessary number of viral particles was calculated, bearing in mind the respective viral titer, for example MeV-SCD 2.1 * 10^7 PFU/ml (plaque forming units/ml). For the infection, viral particles were diluted in Opti-MEM medium (Gibco, Grand Island, NY, USA), using 0.25 ml medium per well. After the infection plates were stored in the incubator at 37 °C and gently turned 90 ° every 15 minutes to secure and facilitate an equal infection. Three hours post infection (hpi) the inoculum was completely removed and replaced by 0.5 ml of normal growth medium.

2.6.2 Viral infection and exploitation of suicide-gene therapy with 5-fluorocytosine (5-FC)

To evaluate a possible enhanced oncolytic effect of MeV-SCD when exploiting its suicide gene function the prodrug was added 3 hpi when the inoculum was removed and replaced with

medium containing 1 mM 5-FC. Remaining cell masses were determined at 72 and 96 hpi with viability assays.

2.7 Sulforhodamine B assay (SRB Assay)

The sulforhodamine B (SRB) cytotoxicity assay is known as the US National Cancer Institute's (NCI) standard assay for measuring the cellular protein content after treatment with cytotoxic substances [90]. In this assay, SRB is used as a dye which binds to basic amino acid residues in an acid environment and can be brought into solution under basic conditions. Using a photometer, the amount of released dye can be measured, which has a linear correlation to the number of remaining cells.

After infecting the cells as described in chapter 2.6, growth medium was removed at 72 hpi or 96 hpi and every well was washed with 0.5 ml ice-cold PBS. Cells were fixed with 0.25 ml/well ice-cold trichloroacetic acid (TCA, 10 % wt/vol) and incubated at 4 °C for at least 30 min. After removing TCA, every well was gently washed 4 times with tap water and dried at 40 °C for at least 12 h.

Each well was stained with 0.25 ml of sulforhodamine B staining solution (0.4 % wt/vol, Sigma, dissolved in 1 % acetic acid) for 10 minutes at RT. In order to remove unbound dye, every well was washed with 1 % acetic acid until the rinse solution was colorless (approximately 4 washes) and dried again at 40 °C for 12 h. Depending on the cell density, 0.5-2 ml of 10 mM Tris base (pH 10.5), were added to each well in order to extract protein-bound dye. The plates were incubated for 10 minutes at RT. Then 80 µl of the solution were transferred to a 96-well flat bottom plate (2 aliquots per 24-well cavity) and optical density was measured with a 96-well microtiter plate reader (Tecan Genios Plus, Tecan) at a wavelength of 550 nm (reference wavelength at 620 nm).

Mean remaining cell mass 96 hours after mock infection without addition of prodrug 5-FC was set as standard value representing 100 % cell mass. Remaining cell masses of infections with different MOIs were related to this mean cell mass.

Sulforhodamine B (SRB) staining solution (0.4% wt/vol):	
SRB	4 g
acidic acid	10 ml
H_2O_{dd}	ad 1 l

Table 8: Sulforhodamine B (SRB) staining solution.

2.8 Viral growth curve

For assessing viral replication within NET/NEC cells and a possible interaction with the mTOR-inhibitor everolimus viral growth curves were performed using titration and the 50 % end point dilution assay ($TCID_{50}$= tissue culture infectious dose 50).

First, NET/NEC cells were seeded in six-well plates (see 2.3.6) and 24 hours later infected with MeV-SCD in 1 ml Opti-MEM at MOIs adjusted to the respective sensitivity to virus infection.

As described in 2.6.1 the inoculum was removed at 3 hpi and cells were washed 3 times with PBS followed by the addition of 1 ml of growth medium. At various points of time (3, 24, 48, 72 and 96 hpi), the supernatant was transferred into an Eppendorf tube. Cells were scraped off in 1 ml of Opti-MEM and stored in another Eppendorf tube. The tubes were directly frozen at - 80 °C.

In order to calculate the $TCID_{50}$, samples were thawed, vortexed and centrifuged for 2 minutes at 3000 rpm in an Eppendorf centrifuge. Supernatants were then used for titration. Next, a dilution series was performed to prepare dilutions ranging from 10^{-1} to 10^{-7}. Therefore, a 96 well plate was used edgewise. 300 µl of each sample were pipetted into the first well. Each of the following wells was prepared with 270 µl of DMEM + 5 % FCS. Now, 30 µl of each well were pipetted into the following one, thereby diluting the solution 1:10. This step was repeated until a dilution of 10^{-7} was reached.

The solutions were carefully aspirated and drained three times and new pipettor tips were used for every single dilution step.

The following titration was performed on Vero cells, which had been seeded in a 96-well plate with each well containing 10^4 Vero cells in 200 µl DMEM supplemented with 5 % FCS the day before titration.

50 µl of each dilution were pipetted in quadruplicates onto the Vero cells for $TCID_{50}$ titration. At 96 hpi, the whole plate was washed with PBS followed by fixation of cells for 10 minutes at RT using 50 µl 4 % PFA. After washing again twice with PBS, cells were blocked for 30 minutes with 100 µl/well of Tris-buffered saline supplemented with Tween 20 (TBS-T: 150 mM NaCl, 50 mM Tris-HCl pH 7.4, 0.02 % Tween-20) and 1 % FCS. Next, cells were incubated for another 30 minutes with anti-MeV-NP diluted 1:1000 in TBS-Tween (50 µl/well) before being washed three times with TBS-T again. Then, the secondary antibody (goat anti-mouse (Molecular Probes, Alexa 546)) diluted 1:1000 in TBS-T) was added using 50 µl per well and plates were incubated for 30 minutes in the dark. Ultimately, cells were washed again three times with TBS-T, before the wells were filled with 50-100 µl of PBS and examined using a fluorescence microscope (IX50, Olympus). A well was declared infected if at least one infected cell was detected by fluorescence microscopy.

Viral titers were then calculated using the following $TCID_{50}$ formula by Spearman (1908) and Kärber (1931):

$$0.7 * 10^{(y-0.5+1.3)} = x\ (\frac{pfu}{ml})$$

Y can be determined counting the infected wells for a certain point of time, for example 72 hpi. For this, columns for each dilution step are analyzed. If all quadruplicates are positive it is counted as (4/4) = 1, if less wells are positive it is counted as a fraction (number of positive wells/4). As displayed in the graph below, for instance *y* can be determined for “72 hpi supernatant” as follows: The first four columns are all positive (4/4)*4 = 4, the fifth column contains 3 infected wells (3/4) = 0.75, while there are only two wells containing infectious particles in the last column (2/4) = 0.5. Taken together, *y* in this example is 4 + 0.75 + 0.5= 5.25. To calculate the virus concentration, *y* now has to be inserted in the formula mentioned above.

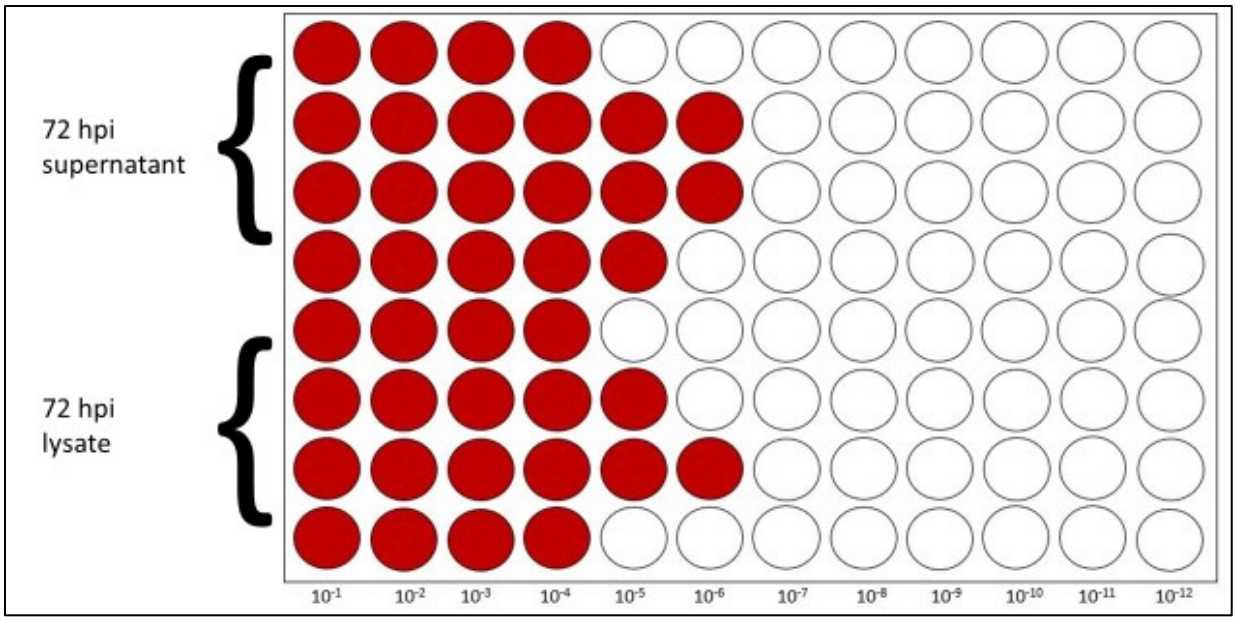

Figure 9: Example of titration of MeV on Vero cells. For each dilution, quadruplicates were pipetted on Vero cells as shown in the graph above. Infected cells were detected using immunofluorescence staining. Red wells indicate at least one infectious particle in the respective well. To calculate the variable *y* mentioned in the formula above, the infectious wells per column are counted and added up.

2.9 Flow Cytometry

2.9.1 Detection of CD46 expression

In order to examine and determine the expression of CD46 on the different NET/NEC cell lines, flow cytometry was performed using an anti-CD46-antibody. The materials used for this experiment are shown in table 9.

Material	Source
Accutase	PAA Laboratories
phycoerythrin (PE)-labeled anti-human CD 46 antibody	eBioscience Inc., San Diego, CA, USA
PE-labeled IgG1 mouse isotype control	eBioscience Inc., San Diego, CA, USA
Gamunex (Fc-blocking solution)	Talecris Biotherapeutics GmbH

Table 9: Materials used for quantification of CD46 receptor expression on cell surfaces by flow cytometry.

First, the respective cells were washed with PBS, then detached using accutase and diluted in FACS buffer (PBS containing 1 % FCS). $5*10^5$ cells were used per stain and diluted again in 3 ml PBS, centrifuged at 4 °C and 1500 rpm.

The cell pellet was dissolved in 50 µl of FACS buffer and 10 µl of Gamunex were added to block Fc receptors. Cells were incubated for five minutes on ice. Afterwards, cells were stained for 30 minutes on ice with either 2.5 µl phycoerythrin (PE) conjugated anti-CD46-antibody or 2.5 µl of the PE-labeled IgG1 mouse isotype control. After staining, 3 ml of PBS were added again followed by another centrifugation step (1200 rpm for 4 minutes). The cell pellet was resuspended in 500 µl of FACS-buffer and stored on ice. Fixation was done by adding 250 µl of 4 % PFA. Measurement of CD46 expression was performed the same day using a FACSCalibur (Becton-Dickinson, Franklin Lakes, NJ, USA) and the software Cell Quest (Becton-Dickinson). Mean fluorescence index (MFI) was calculated by the following formula:

$$\frac{arithmetic\ mean\ of\ CD46}{arithmetic\ mean\ of\ isotype\ control}$$

2.9.2 Quantification of primary infection rates 24 hpi

The various NET/NEC cell lines were seeded in six-well-plates and infected with MeV-GFP at MOIs 0.1, 1 and 10. At 3 hpi, the infection medium was exchanged with 2 ml of standard growth medium. At 24 hpi, the percentage of GFP-expressing cells was determined by flow cytometry. For this experiment, cells were washed with PBS, detached using accutase and resuspended in 1 ml FACS buffer. The cell suspension was transferred into reaction tubes and 3 ml PBS were added. After centrifugation (5 minutes at 302 x g) at RT the pellet was resuspended in FACS buffer. Afterwards cells were fixed with 1.3 % paraformaldehyde (Otto Fischar, Saarbrücken, Germany) and analyzed using the same FACSCalibur and software as mentioned above.

2.10 Fluorescence microscopy of MeV-GFP infected cells

Fluorescence microscopy was used to visualize the viral spread of MeV-GFP in the various NET/NEC cell lines. The respective cells were seeded in 24-well-plates one day before viral infection. Infection was carried out using five different MOIs ranging from 0.001 to 10. The inoculum was removed at 3 hpi and replaced by standard growth medium. Photos were taken 72 and 96 hpi by a camera (F-view, Soft Imaging System) connected to a fluorescence microscope (IX50, Olympus) and the Analysis 3.1 software (Soft Imaging System).

Cell line	Number of cells per well	MOI (MeV-GFP)
NCI-H727	$8*10^4$	0.001, 0.01, 0.1, 1, 10
BON1	$8*10^4$	0.001, 0.01, 0.1, 1, 10
UMC-11	$8*10^4$	0.001, 0.01, 0.1, 1, 10
QGP-1	10^5	0.001, 0.01, 0.1, 1, 10
HROC 57	$6*10^4$	0.001, 0.01, 0.1, 1, 10

Table 10: Characteristics of fluorescence microscopy of MeV-GFP infected NET/NEC cell lines.

2.11 Beta Galactosidase Assay

Cells were seeded 24 hours prior to treatment in six-well plates as described in 2.3.6. Next, the cells were treated with either CX-5461 or Doxorubicin, which served as a positive control.

CX-5461 was used in the following concentrations: 100 nM, 200 nM, 300 nM, 500 nM.

Doxorubicin was used at a concentration of 100 nM.

Medium was replaced 24 hours post treatment. After 96 and 120 hours, respectively, senescence-associated (SA) beta-galactosidase staining was performed as follows.

First, all wells were washed once using neutral PBS. Then cells were fixed using 0.5% glutaraldehyde in neutral PBS for about 10 minutes. Afterwards cells were washed again with neutral PBS, before they were washed twice with PBS pH 6. Finally, 1 ml of the freshly prepared X-Gal staining solution (composition see table 11 below) was added to each well, before incubating the plate sealed and protected from light at 37 °C for a few hours. Plates were checked visually every 30 minutes until the staining in the background control started to become positive. The plates were then washed three times with PBS, afterwards 1 ml of 70 % Glycerin was added to each well and the plate was kept in the fridge at 4 °C until photos were taken using the NIKON eclipse 80i microscope and the NIKON DS-Fi3 camera, the F-View Imaging System and the analysis software.

Reagents	Amount	Source
PBS/MgCl	18.5 ml	
0.2 M $K_3Fe(CN)_6$	0.5 ml	Sigma
0.2 M $K_4Fe(CN)_6$ * $3H_2O$	0.5 ml	Sigma
X-Gal Stock (40x)	0.5 ml	Peqlab
	20 ml	

Table 11: Composition of X-Gal staining solution. X-Gal Stock: 40 mg/ml in NN Dimethylformamide, stored at -20 °C in the dark.

2.12 Western Blot analyzing expression of SCD/ NP/ Vinculin

Antibody target	Host	Dilution	Source
SCD	rat	1:1000 in Roti-Block	Kind gift from Transgene S.A., Illkirch-Graffenstaden, France
MeV N-protein	rabbit	1:6000 in TBS Tween	Abcam, Cambridge, UK
Vinculin	mouse	1:5000 in TBS-Tween with 5% powdered milk	Sigma -Aldrich

Table 12: Primary antibodies used for western blot analysis of SCD/NP/Vinculin expression in NET/NEC cell lines.

Antibody target	Host	Dilution	Source
Rabbit IgG	HRP-coupled, goat	1:8000 in TBS Tween	Bio-Rad
Rat IgG	HRP-coupled, goat	1:4000 in TBS Tween	Bio-Rad
Mouse IgG	HRP-coupled, goat	1:8000 in TBS-Tween	Bio-Rad

Table 13: Secondary antibodies used for western blot analysis of SCD/NP/Vinculin expression in NET/NEC cell lines.

Cell line	Cell count per well	MOI MeV-SCD
BON1	$5*10^5$	0.075
H727	$4*10^5$	0.75
UMC-11	$4*10^5$	0.5
QGP-1	$4*10^5$	1
HROC57	$4*10^5$	0.075

Table 14: Cell count and MOI used for western blot in the respective NET/NEC cell lines.

NET/NEC cells were seeded in a six-well plate and infected with MeV-SCD at MOIs adjusted to the respective cell line-dependent sensitivity to virus infection as can be seen in the table 14 above. At 3 hpi, the inoculum was replaced by standard growth medium. At 96 hpi cells were washed with PBS and lysed in lysis buffer (50 mM Tris (pH 7.6), 150 mM NaCl, 1 % Nonidet P-40). In order to release proteins samples were snap frozen in liquid nitrogen and

then thawed at 37 °C in a heating block. This was repeated three times. Samples were centrifuged for 10 min at 14 000 rpm, 4 °C in an Eppendorf centrifuge. Supernatants were transferred into new tubes. Afterwards, protein concentrations in cell lysates were determined by Bradford protein assay (Bio-Rad, Hercules, CA, USA). First published in 1976 [91], it is a photometric method for determining protein concentrations. If proteins bind to the used Coomassie Brilliant Blue G-250 dye, it causes an absorption shift from initially 465 nm to 595 nm, making it possible to measure protein concentration with reference to a calibration curve.

A total of 50 µg protein was diluted in 6-fold Roti Load Buffer (Carl Roth, Karlsruhe, Germany) and denatured for 5 minutes at 95 ˚C.

The Sodium-dodecylsulfate- (SDS) polyacrylamide gel electrophoresis (PAGE) is a method used for separating proteins according to their molecular weight. In this assay, β-mercaptoethanol reduces disulfide bridges, thereby unfolding proteins, helping SDS attach to the exposed proteins, charging them according to their mass.

The required resolving (table 15) and stacking gels (table 16) were prepared as described below. Importantly, the polyacrylamide concentration used in this assay determines both the pore size of the gels as well as the duration of the electrophoresis.

The resolving gel consisting of H_2O_{dd}, 30 % acrylamide, Tris pH 8.8 and 10 % SDS was mixed. To start the polymerization process, ammonium persulfate (APS) and tetramethylethylendiamine (TEMED) were added last. Immediately afterwards, the resolving gel was filled into the gel cassette. Next, it was covered by 70 % isopropanol, creating a flat surface on which the resolving gel was filled after the resolving gel had polymerized. After the polymerization process took about 30 minutes, the isopropanol was removed and the surface of the gel was rinsed once with H_2O_{dd}. Now the polymerization of the stacking gel was started by the addition of APS and TEMED as well and the solution was filled on top of the resolving gel and a ten-finger-comb, which created ten slots, was inserted. After 15 minutes in which polymerization took place the gel cassette was transferred into the buffer tank containing running buffer 1:5 H_2O_{dd} diluted running buffer (15.1 g/l Trizma Base, 72 g/l Glycine, 5 g/l SDS, filled up to 1 l with H_2O_{dd} with the pH adjusted to 8.3).

After the comb was removed, the calculated volumes of cell lysates corresponding to 50 µg of protein were mixed with a fifth of 6 x SDS loading buffer and boiled for ten minutes at 95 °C. Then samples were filled into the slots. A positive control and a molecular weight marker (Full range rainbow protein marker, Amersham Biosciences) were loaded in addition to identify the assessed band of protein and control the progress of the electrophoresis.

After the proteins were separated by SDS-PAGE, they were transferred to a hydrophobic polyvinylidene difluoride (PVDF) membrane (Hybond-P, GE Healthcare, Waukesha, WI, USA).

The western blot aimed to prove successful oncolytic measles virus infection by the detection of the measles N protein as well as the SCD-protein, which is encoded by a transgene.

The PVDF-membrane was activated with methanol and then embedded between gel, Whatman papers and sponges as displayed in figure 10. All layers were transferred in a box with 1 x transfer buffer and were compressed to keep close contact between acrylamide gel and PVDF-membrane, avoiding air bubbles between the different components.

After blocking for one hour with 5 % powdered milk (Carl Roth) in Tris-buffered saline containing 0.02 % Tween-20 (TBS-T) to avoid non-specific binding of antibodies, membranes were incubated with primary antibodies overnight at 4 ˚C as displayed in table 12 above. Membranes were washed three times with TBS-T, secondary antibodies as described above were added

for one hour while gently shaking and membranes were washed again three times with TBS-T.

Proteins were detected using enhanced chemiluminescence (ECL). Therefore, 1 ml of ECL solution was applied for one minute. Next, membranes were fixed in a plastic foil in a photo cassette (Dr. GOOS Suprema GmbH). Finally, membranes were exposed to the chemiluminescence film Amersham Hyperfilm ECL (GE Healthcare). A Fuji developer (Fuji Photo Film Ltd) developed the films.

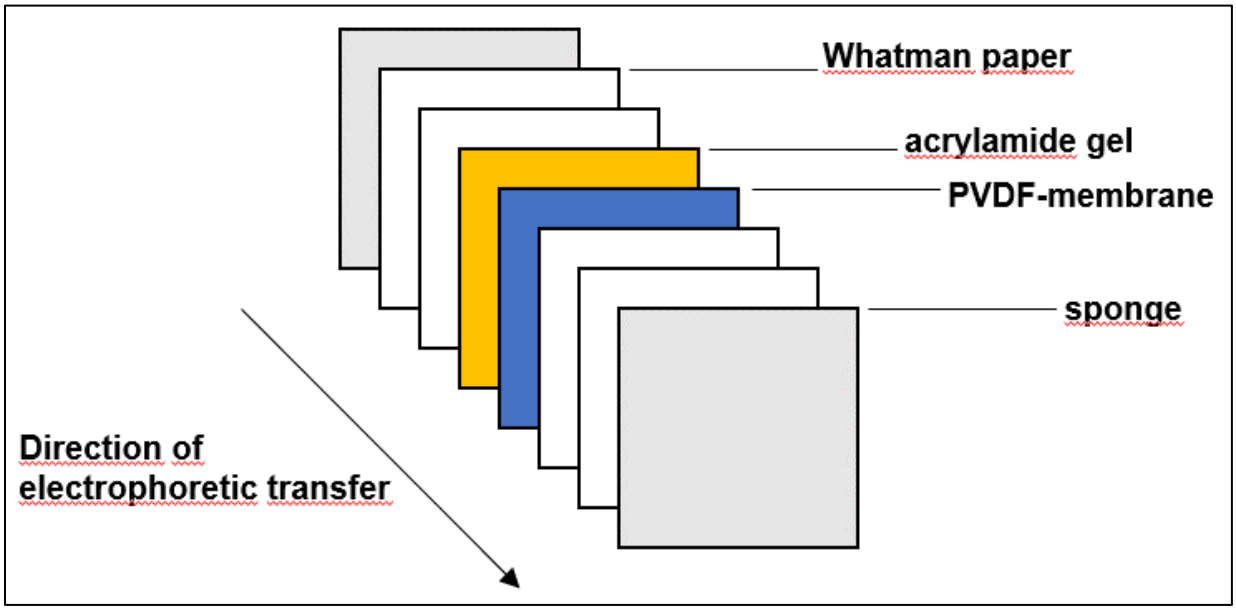

Figure 10: Correct arrangement of blotting membranes. From back to front the demonstrated setup was used: sponge – two Whatman papers – acrylamide gel – PVDF-membrane – two Whatman papers – sponge. All layers were compressed to keep close contact between acrylamide gel and PCDF-membrane, avoiding air bubbles between the different components.

20 ml resolving gel (8 % acrylamide)	
H_2O_{dd}	9.3 ml
30 % acrylamide mix	5.3 ml
1.5 M Tris (pH 8.8)	5.0 ml
10 % SDS	0.2 ml
10 % APS	0.2 ml
TEMED	0.016 ml

Table 15: Composition of resolving gel used for SDS-Page. Sodium dodecyl sulfate (SDS), ammonium persulfate (APS), tetramethylethylendiamine (TEMED).

8 ml stacking gel (5 % acrylamide)	
H_2O_{dd}	5.5 ml
30 % acrylamide mix	1.3 ml
1.5 M Tris (pH 6.8)	1.0 ml
10 % SDS	0.08 ml
10 % APS	0.08 ml
TEMED	0.008 ml

Table 16: Composition of stacking gel used for SDS-Page. Sodium dodecyl sulfate (SDS), ammonium persulfate (APS), tetramethylethylendiamine (TEMED).

2.13 Crystal Violet staining after treating cells with CX 5461

2.5* 10^3 Cells of each NET/NEC cell line were seeded in an individual six-well plate in 2 ml of their respective growth medium. The next day, medium was removed and replaced by CX 5461 diluted in normal growth medium in the following concentrations: 50 nM, 100 nM, 200

nM, 300 nM, 500 nM, mock; afterwards plates were stored in the incubator. After 24 hours, the medium containing CX-5461 was replaced by normal growth medium again.

On the day of staining, the medium was removed and cells were once washed with 2 ml of PBS followed by fixing the cells with 3 ml of methanol for 5 minutes. Afterwards, methanol was discarded and cells were stained for 10 minutes using 3 ml of 1 % crystal violet diluted in H_2O_{dd}. The staining solution was removed and cells were washed with H_2O several times before plates were dried upside down. The next day, pictures were taken on white paper as a background.

3. Results

3.1 Basic experiments

3.1.1 Determination of CD46 receptor molecule expression on NET/NEC cell surfaces

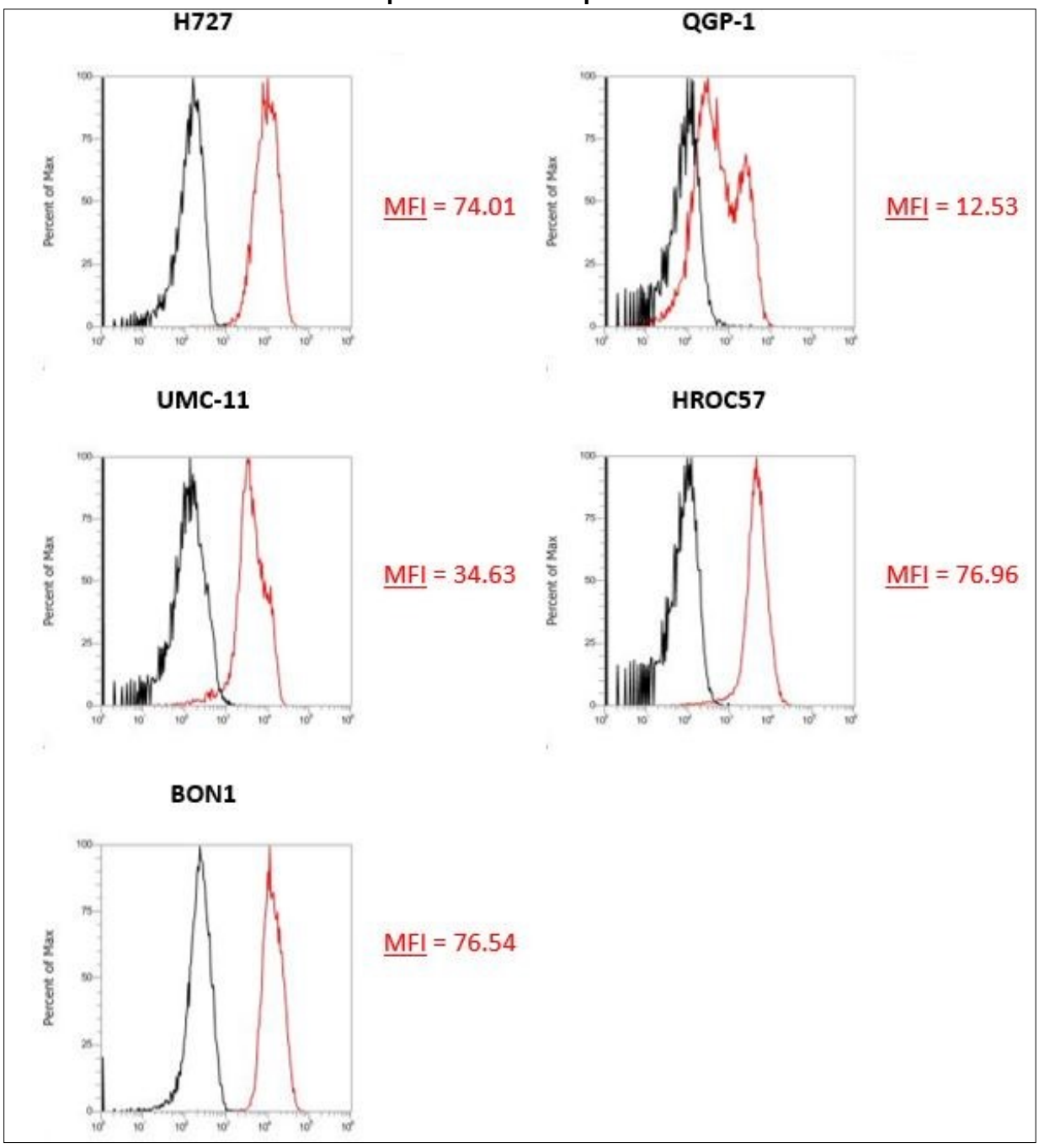

Figure 11: Determination of CD46 receptor expression on human NET/NEC cell lines by flow cytometry. Tumor cells were stained with CD46 antibody (red histograms) or isotype control (black histograms). Mean fluorescence index (MFI) is the arithmetic mean of CD46 receptor divided by the arithmetic mean of the isotype control. Sufficiently high levels of CD46 are required for syncytia formation.

The expression of CD46 on cell surfaces is essential for sufficient measles virus entry and cell fusion. Of note, CD46 is often found to be overexpressed on various tumor cells. Thus, all five NET/NEC cell lines were examined using flow cytometry for the expression and density of CD46 receptor molecules in order to evaluate a potential infection with oncolytic measles viruses.

It is commonly accepted that viral entry correlates progressively with CD46 receptor density, while there is a certain threshold for cell-to-cell fusion, ultimately leading to syncytia formation and cell death [19].

The CD46 receptor molecule was found to be expressed on every cell line examined (see figure 11), although the density varied as expressed in the mean fluorescence index (MFI), which refers to the index of the arithmetic mean of CD46 receptor divided by the arithmetic mean of the isotype control.

HROC57, BON1 and H727 were found to have the highest CD46-receptor density, all three of them with an MFI around 75, followed by UMC-11 with an MFI of about 35. Interestingly, QGP-1 showed an MFI of under 20, which was the lowest of all examined cell lines.

In conclusion, at least four out of five examined cell lines showed a promising and sufficient CD46 receptor quantity for measles virus infection and potential cell fusion, leading to syncytia formation.

3.1.2 Examination of the infection efficiency of MeV-GFP

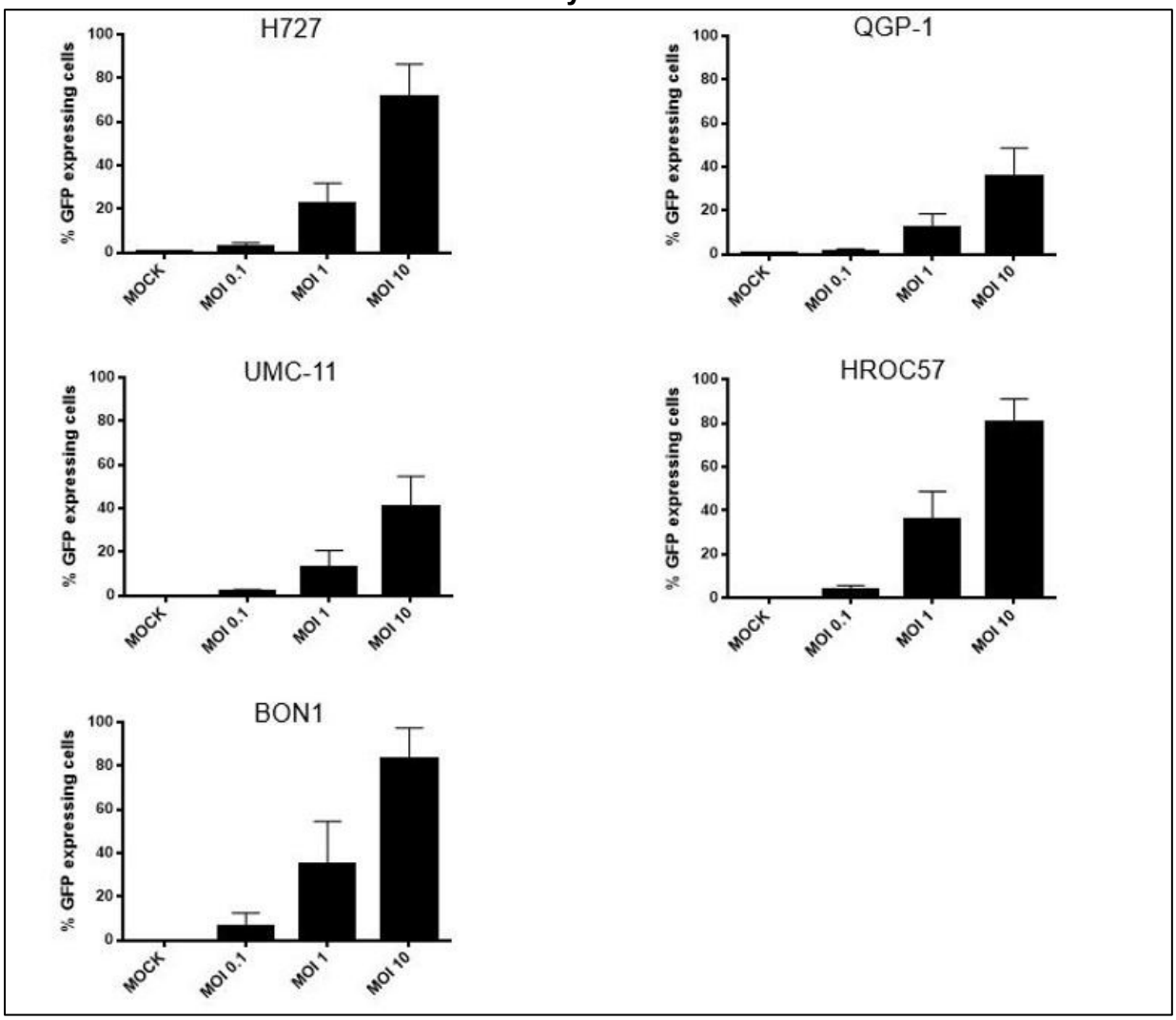

Figure 12: Quantification of infection rates of MeV-GFP in five human NET/NEC cell lines. Cells were infected at the indicated MOIs. At 24 hpi the percentage of GFP-expressing cells was determined by flow cytometry. Mean and SD of at least three independent experiments are shown.

Primary infection rates refer to the percentage of infected cells in relation to all cells at a certain point of time. Based on the observation that all NET/NEC cell lines express the CD46 entry receptor in a sufficient amount (3.1.1), the primary infection rates of measles vaccine virus in the selected cell lines were analyzed to further emphasize the potential of MeV to infect tumor cells of neuroendocrine origin. Therefore, cells were infected using a genetically modified measles vaccine virus expressing green fluorescent protein (MeV-GFP), allowing already at 24 hpi visualization of the successful infection of the NET/NEC cell lines by flow cytometry.

As can be seen in figure 12 above, MeV-GFP at the MOI of 10 resulted in about 80 % infected cells in the first 24 hours for HROC57, BON1 and H727, while causing about 40-50 % infected cells in the UMC-11 and QGP-1 cell lines, thus showing varying kinds of susceptibility towards primary infection with MeV-GFP. Interestingly, the cell lines with the highest MFI (BON1, H727, HROC57) also displayed the highest primary infection rates at 24 hpi while the two ones with a lower MFI also were less likely to be infected by MeV-GFP at 24 hpi.

3.1.3 Fluorescence monitoring revealed successful infection with MeV-GFP

After showing that NET/NEC cells (over)express CD46 and relatively high primary infection rates can be achieved using MeV-GFP, another experiment was conducted to illustrate successful infection of tumor cell lines using fluorescence microscopy. Therefore, tumor cells were again infected with MeV-GFP encoding green fluorescent protein, which can be detected by fluorescence microscopy, at increasing MOIs ranging from 0.001 to 10. Representative images of all cell lines successfully infected with the virus are shown below (figure 13). Green dots indicate successful infection displayed by syncytia formation which was visible in every cell line. The corresponding phase contrast pictures can be seen on the left-hand side of the fluorescence microscopy pictures.

As a result, green fluorescent protein was clearly detectable both at 72 and 96 hpi in all examined cell lines, supporting the possibility to successfully infect those cell lines with oncolytic measles virus. Moreover, the pictures reveal syncytia formation in all cell lines, as well as reduced cell density in the phase contrast pictures as a sign of reduced cell masses caused by the oncolytic effect of MeV-GFP.

NCI-H727

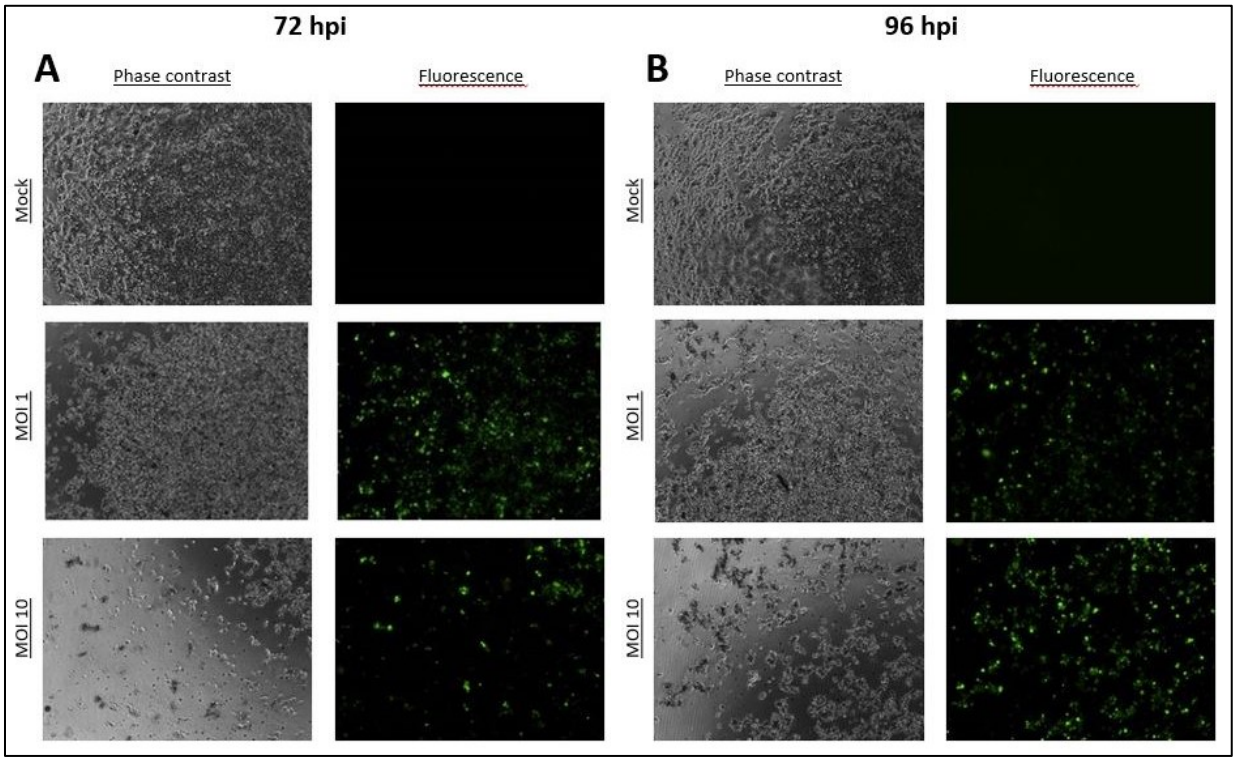

UMC-11

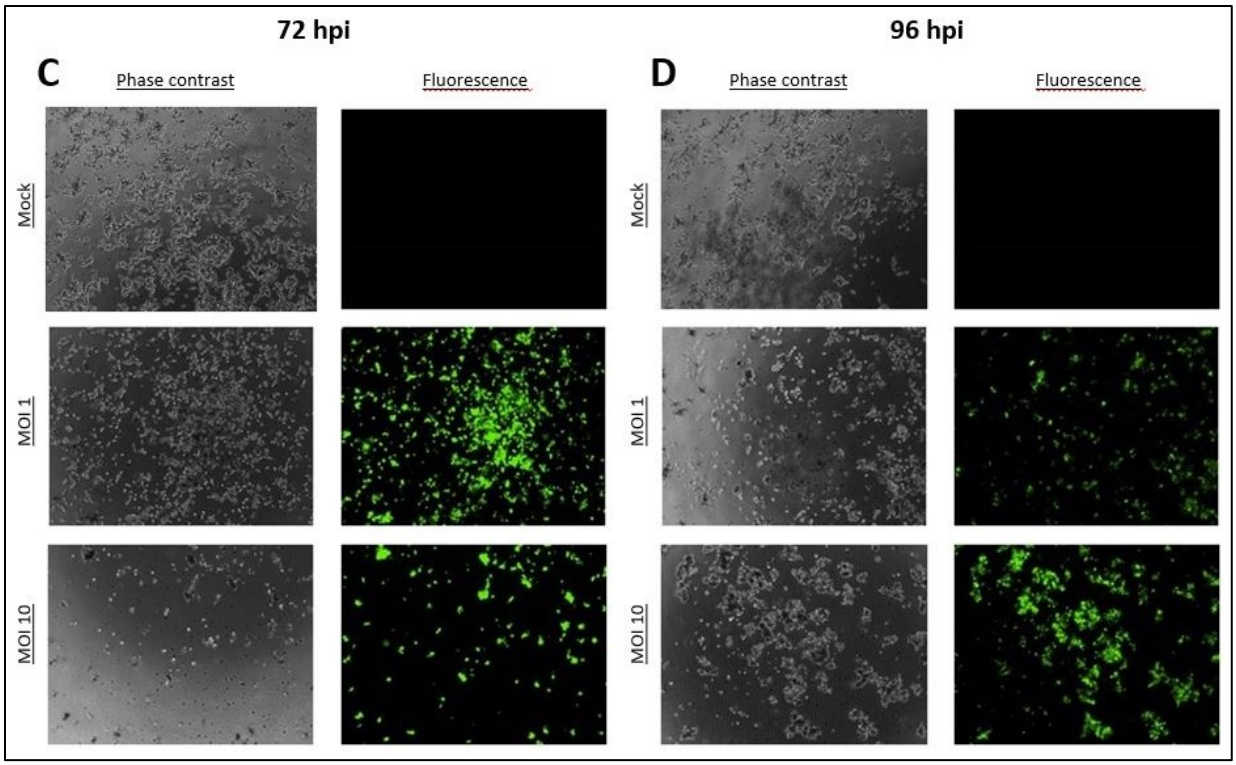

BON1

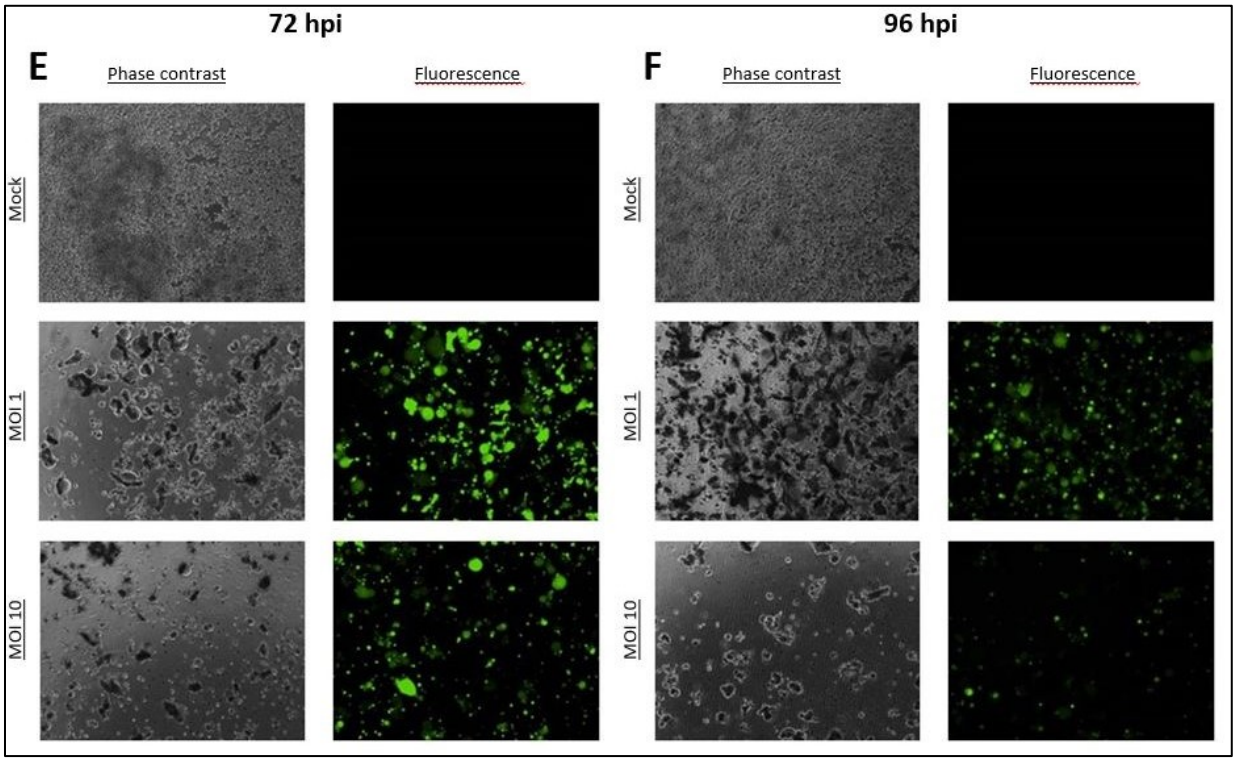
72 hpi
96 hpi
E
Phase contrast
Fluorescence
F
Phase contrast
Fluorescence
Mock
MOI 1
MOI 10
Mock
MOI 1
MOI 10

QGP-1

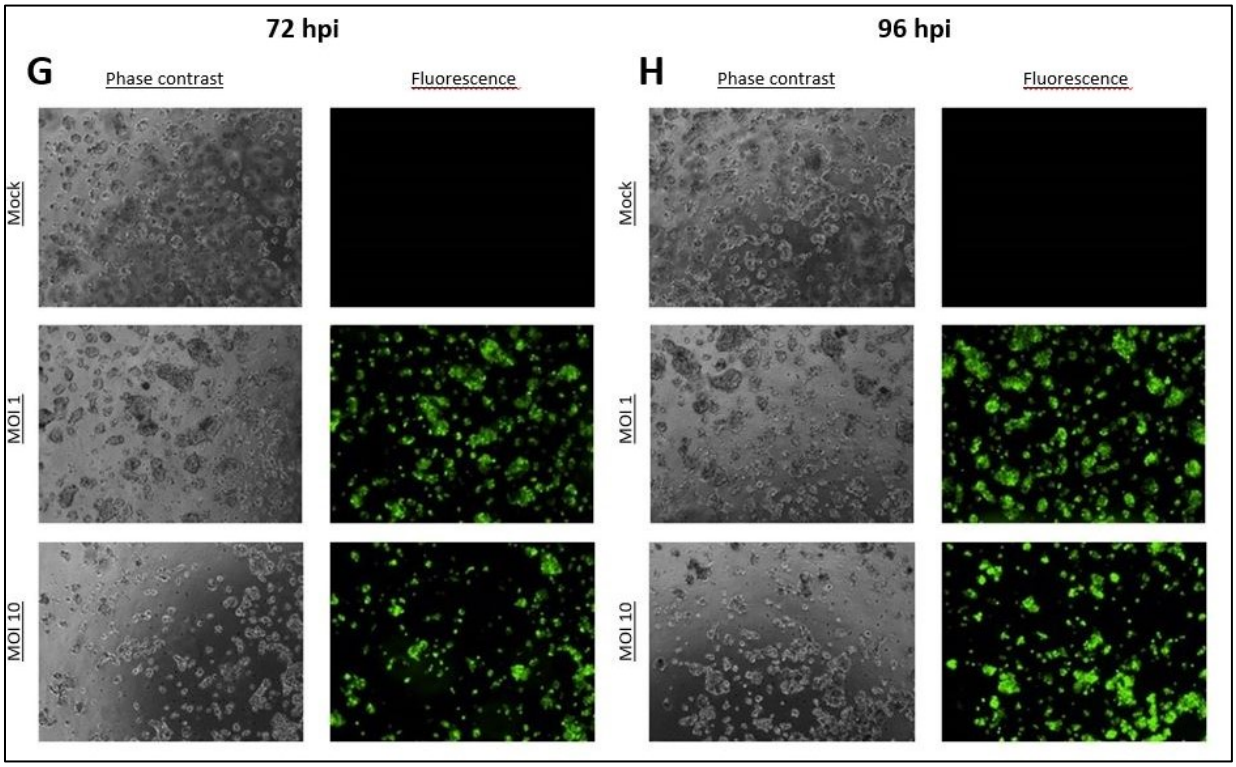
72 hpi
96 hpi
G
Phase contrast
Fluorescence
H
Phase contrast
Fluorescence
Mock
MOI 1
MOI 10
Mock
MOI 1
MOI 10

HROC57

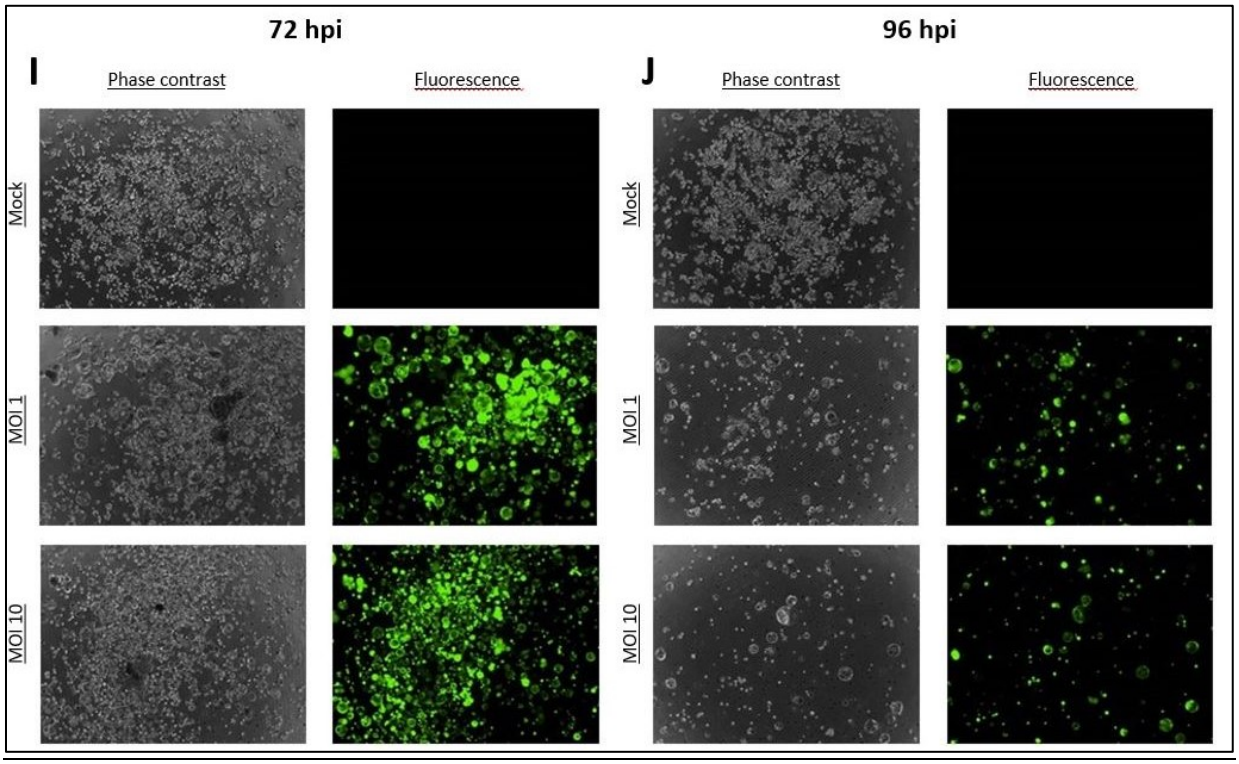

Figure 13: Fluorescence monitoring revealed successful infection with MeV-GFP. H727 (A, B), UMC-11 (C, D), BON1 (E, F), QGP-1 (G, H) and HROC 57 (I, J) were infected at MOIs 1 and 10 or were mock infected (untreated control). Fluorescence and corresponding serial phase contrast pictures were taken 72 and 96 hpi at the same magnification. While mock infected cells showed no green fluorescence, it was clearly detected in all infected cells, revealing syncytia formation as well.

3.1.4 Cytotoxic effect of MeV-SCD monotherapy

To investigate the susceptibility of the five NET/NEC cell lines to MeV-SCD-mediated oncolytic activity, cells were infected with MeV-SCD at MOIs ranging from 0.001 to 10. The remaining cell masses were determined at 96 hpi by SRB viability assay. A remaining tumor cell mass of more than 50 % at a MOI of 1 relative to the mock infected control was defined as partially resistant. Four out of five cell lines proved to be susceptible to MeV-SCD-mediated oncolysis with tumor cell masses below 50 % at a MOI of 1 (figure 14). The only exception was the pancreatic cell line QGP-1, which showed a partial resistance (remaining tumor cell mass of about 60 %) to MeV-SCD-infection according to the chosen criteria (partial resistance = remaining tumor cell mass of 50 – 75% at a MOI of 1).

On the contrary, MeV-SCD`s oncolytic capability seemed to be very strong in BON1 and HROC57 cells where a reduction of up to 90 % of the tumor cell mass was reached at a MOI of 1 in comparison to mock treated cells. Of note, increasing the MOI up to 10 resulted in less than 25 % of remaining tumor cell mass compared to mock treated cells in every cell line, punctuating the possibility to overcome partial resistance by increasing the MOI.

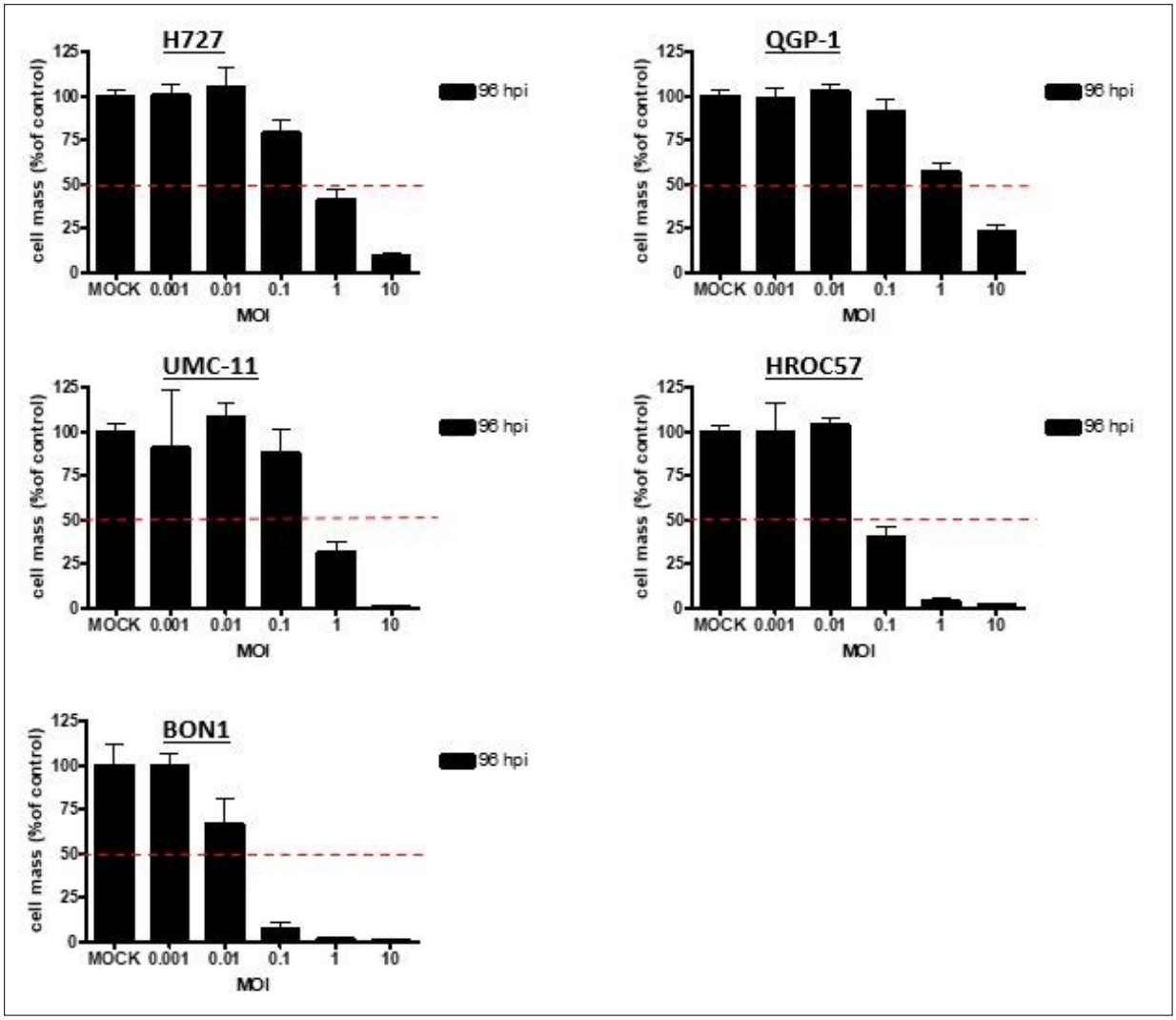

Figure 14: Remaining tumor cell masses after single (monotherapeutic) treatment with oncolytic measles vaccine virus MeV-SCD. Five human NET/NEC cell lines were infected with the suicide-gene armed measles vaccine virus MeV-SCD at the indicated MOIs. At 96 hpi, the remaining tumor cell masses were determined by SRB viability assay. Each MOI was tested in quadruplicates. Displayed are mean and standard deviation of one experiment. Dotted red lines indicate the 50 % threshold for remnant tumor cell masses at 96 hpi. MOCK: untreated control.

3.1.5 Expression of MeV N and SCD protein

In the next experiment the expression of the MeV N and of the virus-encoded SCD protein was examined by western blot analysis. For this purpose, the five NET/NEC cell lines were infected at MOIs adjusted to the respective cell line-dependent sensitivity to virus infection (3.1.4). MOIs were chosen which resulted in around 80 % remaining tumor cell mass at 96 hpi when cell lysates were prepared. In every cell line tested, both viral proteins (N and SCD) were expressed only in MeV-SCD infected cells while in uninfected control cells (MOCK) no viral proteins could be detected (figure 15). The intensity of the protein bands and therefore the amount of viral proteins differed markedly between the cell lines. Interestingly, HROC57, QGP-1 and BON1 showed the highest intensity of N protein and SCD protein band, while it was a lot less intense in both UMC-11 and H727 cells. Nevertheless, the respective proteins were detected in every analyzed cell line as shown below displaying both a successful infection and a functional transcription of the encoded genes, thus making it possible to exploit MeV-SCD's suicide gene function in the following experiments (3.2).

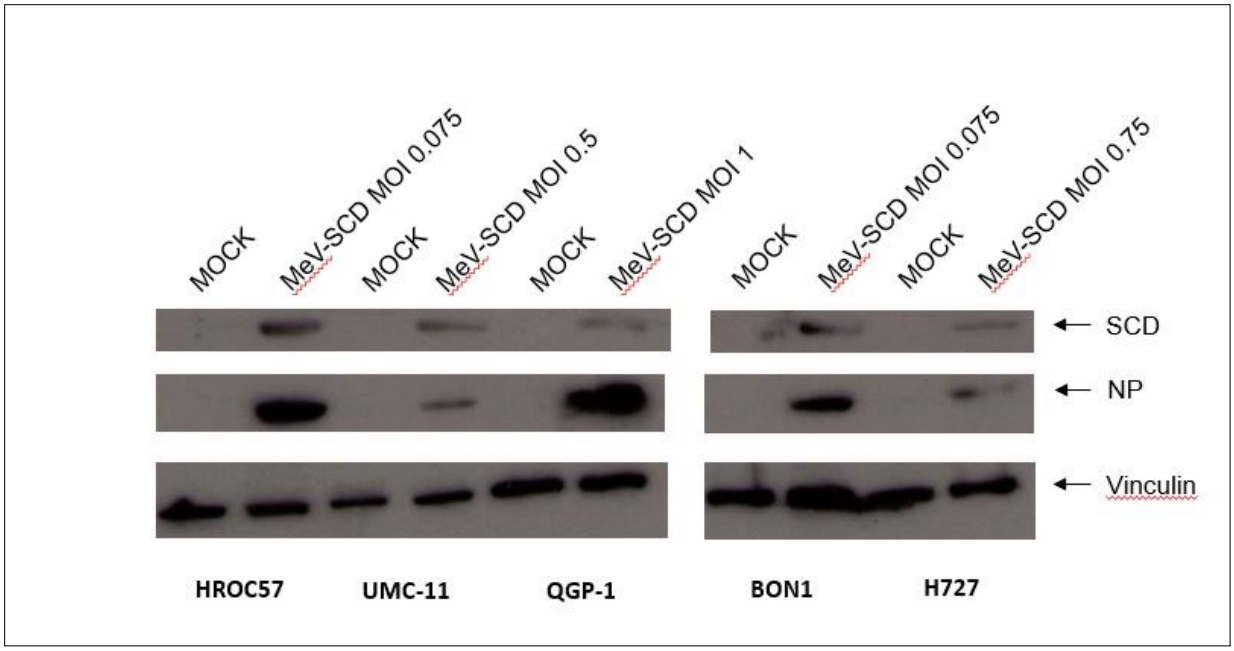

Figure 15: Western Blot analysis of MeV N protein and MeV encoded SCD protein expression in five human NET/NEC cell lines. Tumor cells were infected with MeV-SCD at the indicated MOIs or MOCK infected. Whole cellular protein extraction was performed at 96 hpi. Vinculin was used as a loading control.

3.1.6 Cytotoxic effect of 5-Fluorouracil (5-FU) monotreatment

In a next step, the susceptibility of the five cell lines towards the chemotherapeutic compound 5-FU, which is commonly used in the treatment of NENs, was evaluated. Therefore, cells were treated with concentrations of 5-FU ranging from 1 nm to 1 mM and remaining tumor cell masses were determined at 96 hours post treatment (hpt) by SRB assay (figure 16). Cell masses of all five cell lines started to decrease significantly at a concentration of 10 µM 5-FU. The strongest effect in tumor cell mass reduction was obtained at the highest used dose of 1 mM, when tumor cell masses declined over 80 % in every NET/NEC cell line tested in comparison to mock treated controls. Thus, all cell lines proved to be sensitive towards 5-FU in a dose-dependent manner with UMC-11 and BON1 being the most susceptible cell lines tested.

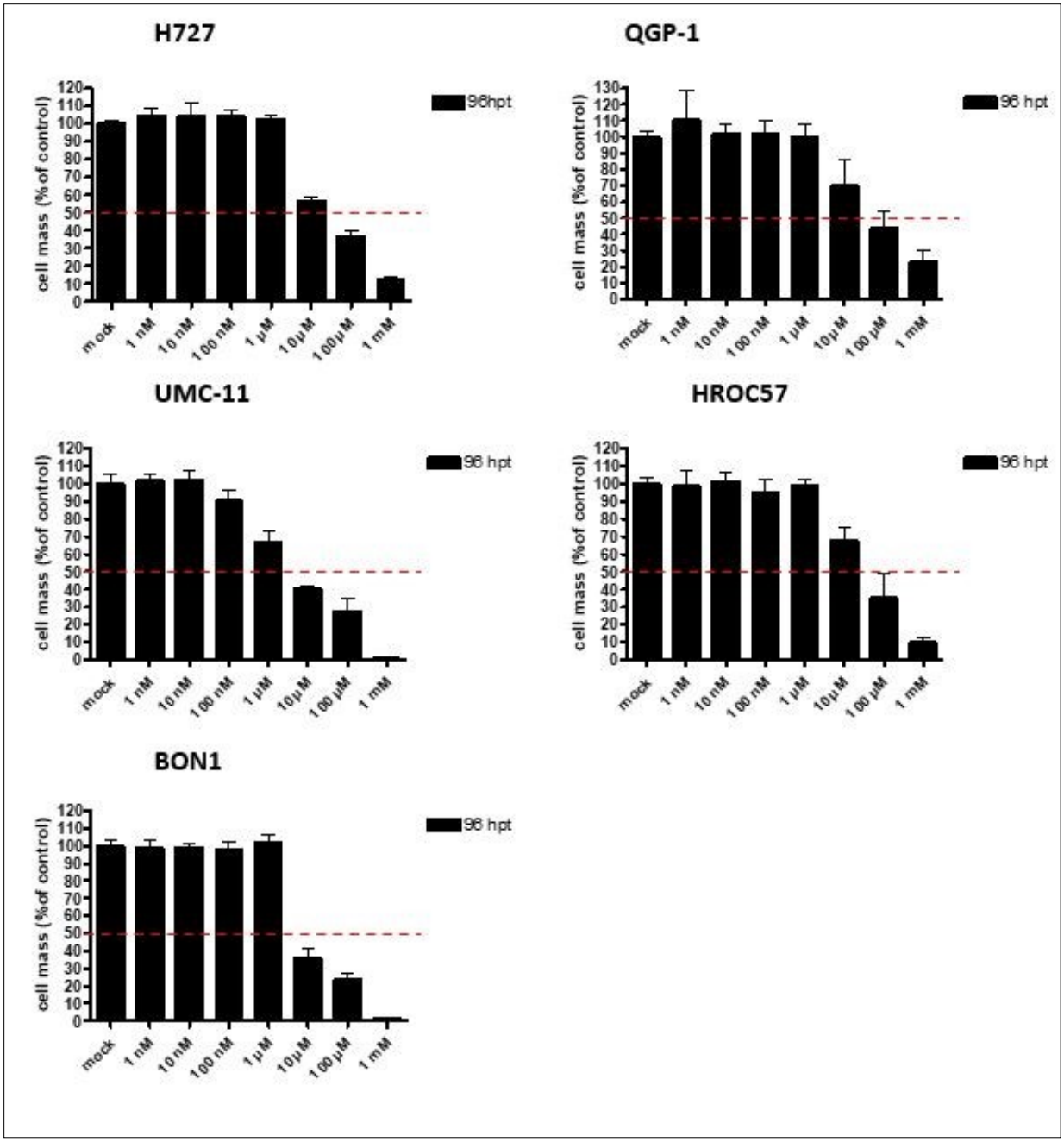

Figure 16: Susceptibility of human NET/NEC cells to the chemotherapeutic compound 5-FU. Tumor cells were treated with increasing concentrations of 5-FU and tumor cell masses in % of control were measured at 96 hpt by SRB viability assay. Displayed are means and standard deviation of two independent experiments with each concentration of 5-FU tested out in triplicates. Dotted red lines indicate the 50 % threshold of remnant tumor cell masses at 96 hpt. Mock: untreated control.

3.1.7 Cytotoxic effect of everolimus monotreatment

In another experiment the cytotoxic effect of the mTOR-inhibitor everolimus, which is clinically approved and used for the treatment of metastatic NENs, was evaluated. The different cell lines were treated with concentrations of everolimus ranging from 0.01 nM up to 10 µM. Although the susceptibility varied from cell line to cell line with UMC-11 again being the most susceptible one and H727 the most unaffected one, all cell lines were found to be sensitive to everolimus monotreatment in a dose-dependent manner with tumor cell masses starting to decrease significantly at a concentration of 1 nM everolimus (Figure 17). While everolimus was able to reduce cell masses of BON1 and UMC-11 cells by more than 50 % when treated with

a concentration of 10 µM, this was not the case for H727, QGP-1 and HROC57, where about 50 % of the tumor cells remained.

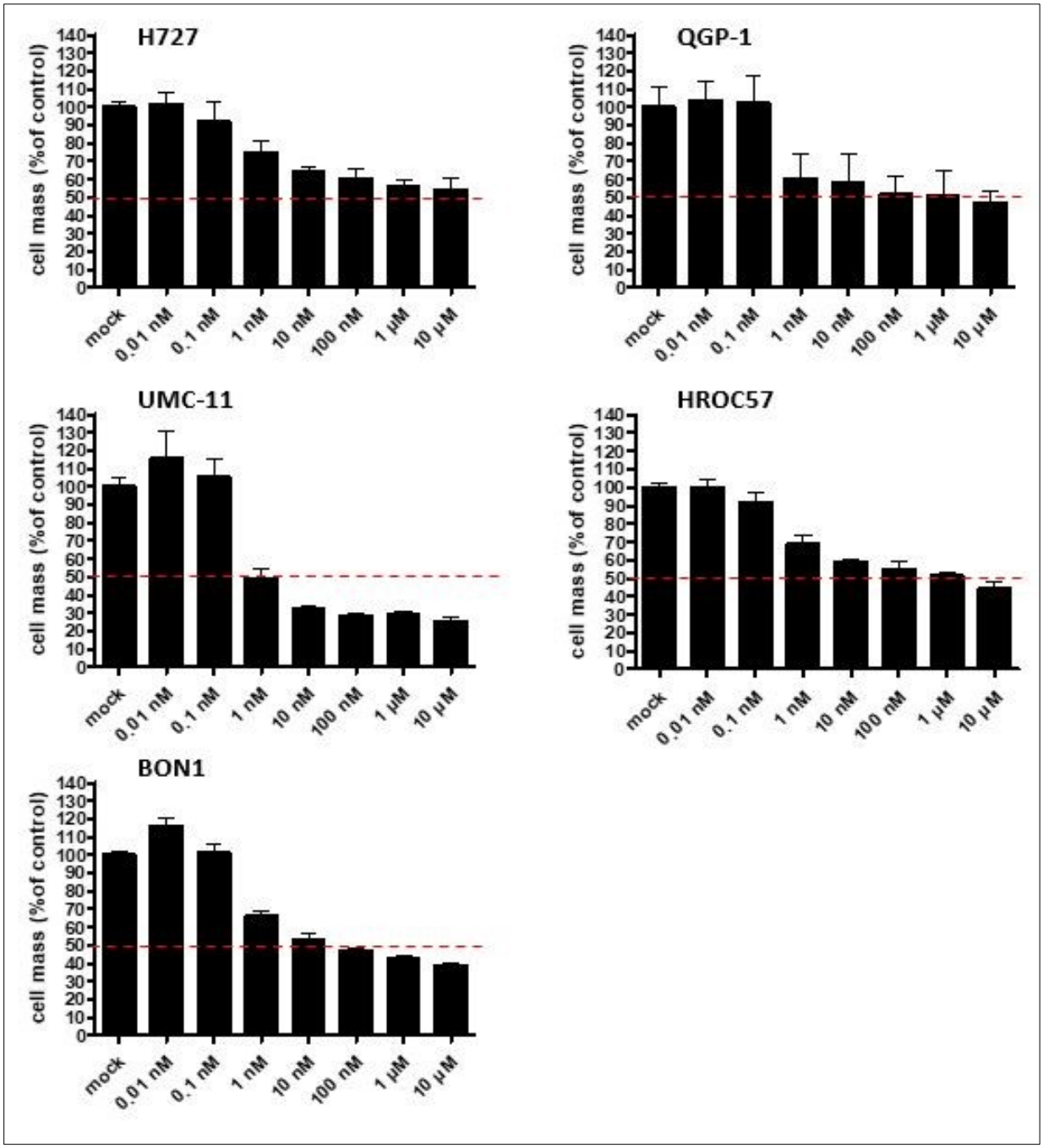

Figure 17: Susceptibility of human NET/NEC cells to the mTOR-inhibitor everolimus. Tumor cells were treated with increasing concentrations of everolimus and tumor cell masses in % of control were measured at 96 hpt by SRB viability assay. Displayed are means and standard deviation of two independent experiments with each concentration of everolimus tested out in triplicates. Dotted red lines indicate the 50 % threshold of remnant tumor cell masses at 96 hpt. Mock: untreated control.

3.2 MeV-SCD based combination treatment settings

3.2.1 Addition of the prodrug 5-fluorocytosine (5-FC) enhances the oncolytic effect of MeV-SCD on human NET/NEC cell lines

Since all cell lines proved to be sensitive to both MeV-SCD and 5-fluorouracil monotreatment in a dose-dependent manner, the exploitation of MeV-SCD's suicide gene, the supercytosine deaminase, was consequently evaluated in a next step (figure 18).

Therefore, cells were infected with MeV-SCD, followed by the addition of the prodrug 5-FC, which is converted locally into the chemotherapeutic compound 5-FU. Importantly, cell lines were infected with MeV-SCD at MOIs adjusted to the respective cell line-dependent sensitivity to virus infection (compare 3.1.4), leaving enough range for a potential boost resulting of the prodrug activation.

As a result, the prodrug-converting system was able to further enhance the oncolytic effect of MeV-SCD in all five cell lines with a reduction of more than 50 % of cell mass, even if very low MOIs were used.

In HROC57 cells, infection with MeV-SCD alone at a MOI of 0.05 led to a remaining cell mass of about 70 %, however, addition of 1 mM 5-FC further reduced cell mass to about 50 %. The lung carcinoid cell line H727 had a good benefit of the exploitation of the suicide gene (further tumor cell mass reduction of around 30 %), while it had the lowest impact on the pancreas cell line BON1 with only about 10 % additional tumor cell mass reduction, bearing in mind a very low MOI of 0.05 was used due to BON1's high sensitivity to MeV-SCD monotreatment.

The strongest effect was observed in UMC-11 cells, where MeV-SCD monotreatment with a MOI of 0.25 led to about 60 % remaining tumor cell mass. By exploiting the suicide gene function MeV-SCD was able to kill more than 75 % of the tumor cells in comparison to untreated controls.

Importantly, QGP-1 cells, which showed a partial resistance to MeV-SCD monotreatment according to our chosen criteria (see 3.1.4) showed promising results when exploiting the suicide gene function resulting in only about 20 % remaining tumor cells at a MOI of 1.

To sum it up, the addition of 5-FC and thus the exploitation of MeV-SCD's suicide gene function led to enhanced oncolytic activity compared to the monotherapy with MeV-SCD alone.

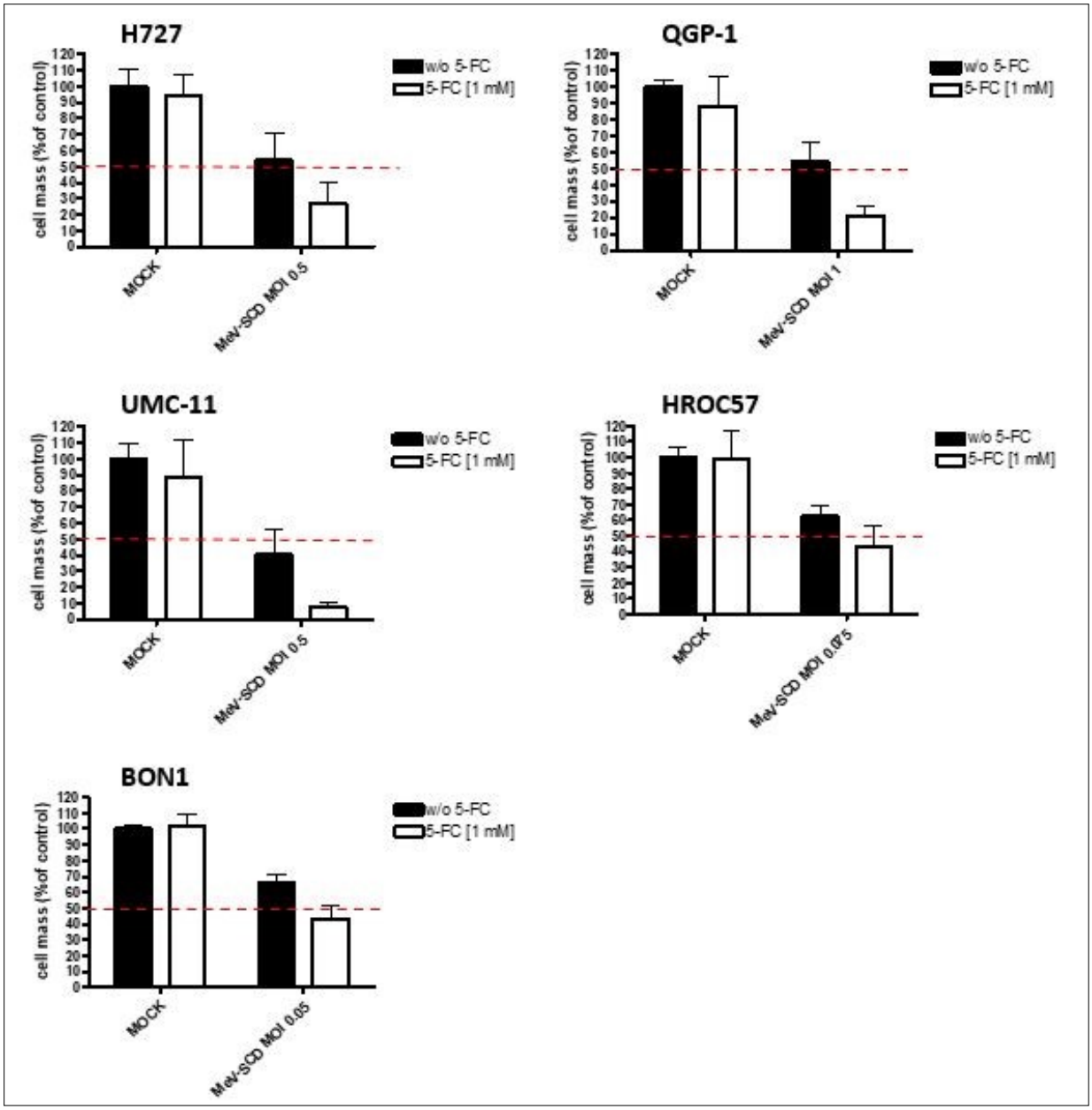

Figure 18: Remaining NET/NEC tumor cell masses after treatment with MeV-SCD and the prodrug 5-FC. Human NET/NEC cell lines were infected with the suicide gene-armed measles vaccine virus MeV-SCD at MOIs which were adjusted to the respective tumor cell line dependent sensitivity to MeV-SCD. At 3 hpi the prodrug 5-FC was added. At 96 hpi the remaining tumor cell masses were determined by SRB viability assay. Displayed are means and standard deviation of two independent experiments with each MOI tested out in quadruplicates. Dotted red lines indicate the 50 % threshold of remnant tumor cell masses at 96 hpi. MOCK: untreated control.

3.3 Replication characteristics of MeV-SCD

3.3.1 Examination of measles virus growth kinetics with and without everolimus in human NET/NEC cell lines

Since MeV-SCD showed an oncolytic effect on NET/NEC cell lines, the kinetics of viral infection, replication and spreading were further observed using virus growth curves. As everolimus also showed a cytotoxic effect on the different tumor cell lines and is clinically among other things used as an immunosuppressive drug, viral replication was also evaluated in the presence and absence of everolimus.

Therefore, tumor cells were infected with MeV-SCD. At 3 hpi, the mTOR-inhibitor everolimus was added or not. Both tumor cells and supernatants were harvested at the indicated points of time. Titration was performed on Vero cells.

MeV-SCD proved to replicate in all examined cell lines reaching at least 10^3 PFU/ml in every cell line. Replication reached its climax at 48-72 hpi in all tested cell lines, the maximum of PFU/ml varied from cell line to cell line, reaching a maximum of more than 10^5 PFU/ml e.g. in BON1 cells. The addition of the mTOR-inhibitor did neither impair nor enhance replication, resulting in unaltered growth curves (figure 19).

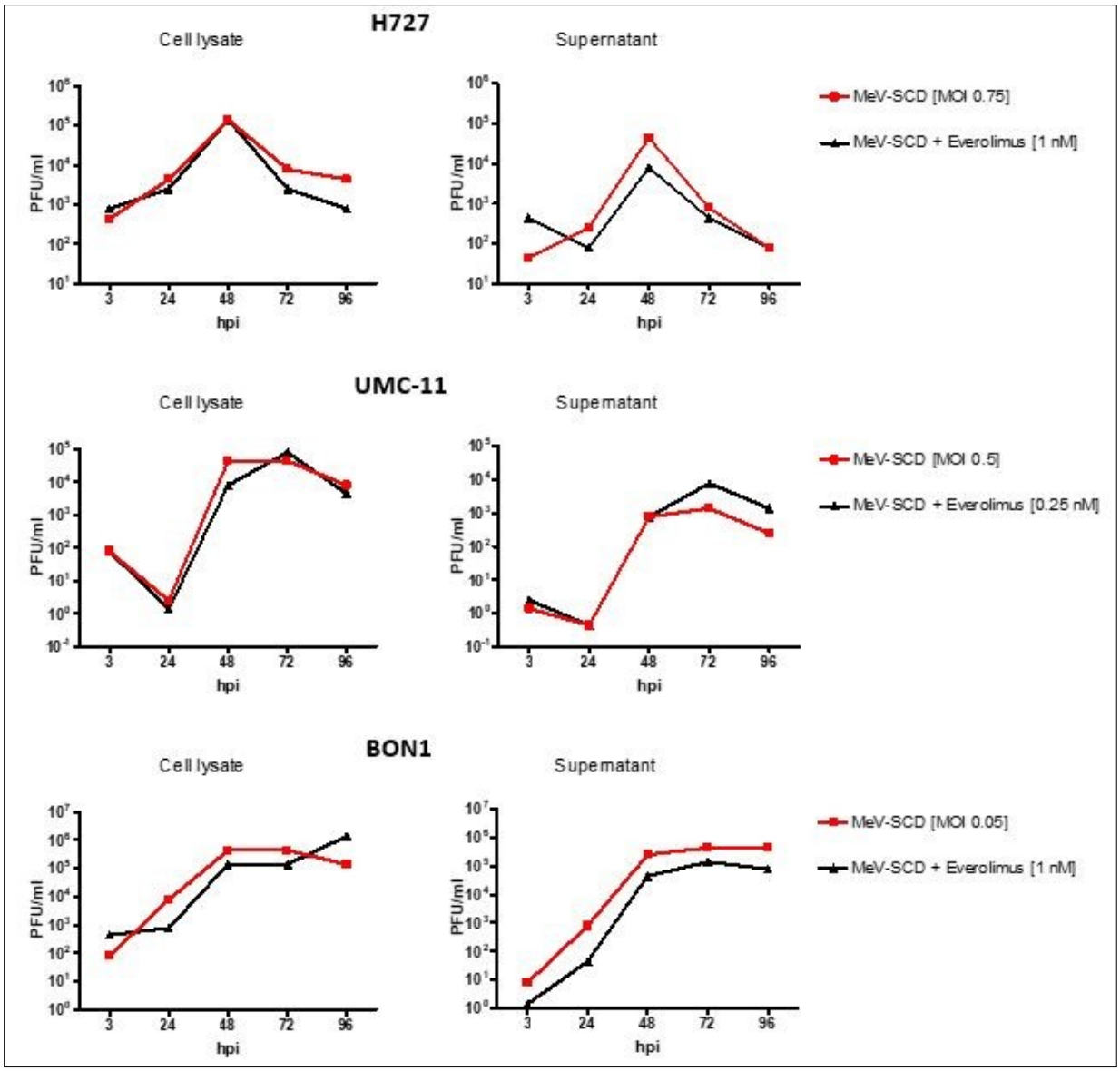

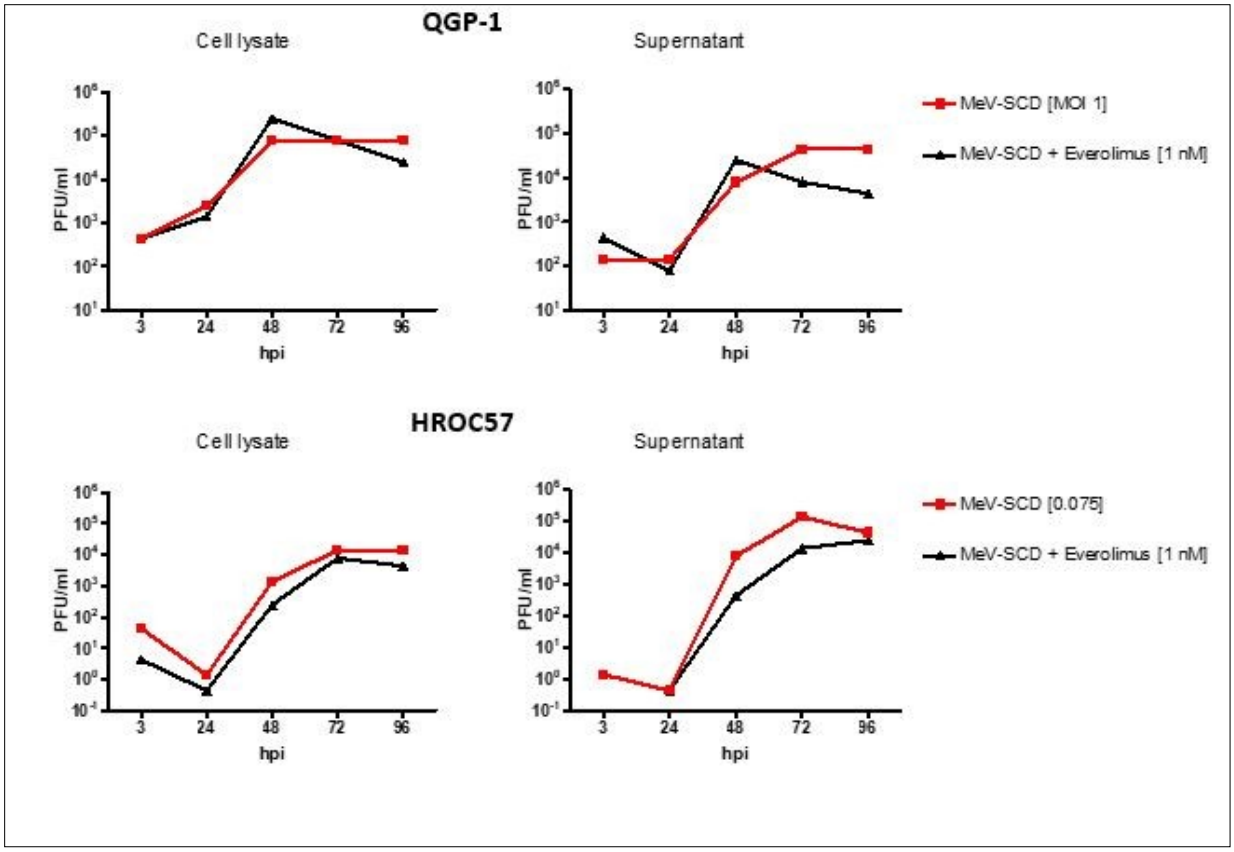

Figure 19: Quantification of the replication of virotherapeutic vector MeV-SCD in five human NET/NEC cell lines. Tumor cell lines were infected with the suicide gene-armed measles vaccine virus based virotherapeutic MeV-SCD at the indicated MOIs which were adjusted to respective tumor cell line dependent sensitivity to MeV-SCD. At 3 hpi, the mTOR-inhibitor everolimus was added (black graph); red graph w/o everolimus. Tumor cells and supernatants were harvested at the indicated time points. Titration was performed on Vero cells.

3.4 Senescence

3.4.1 β-Gal Assays of two human NET cell lines after senescence inducing treatment

Since it was shown that oncolytic measles viruses exhibit an enhanced killing of therapy-induced senescent tumor cells [64], these experiments aimed to analyze a potential benefit of the combination of the senescence inducing compound CX-5461 and the oncolytic measles vaccine virus MeV-GFP. CX-5461 is an inhibitor of RNA-polymerase I transcription of ribosomal RNA genes, resulting in the induction of replication stress and activation of the DNA damage response.

β-Gal assays were performed on H727 and BON1 cells to examine whether the compound CX-5461, which showed senescence inducing activity in other cell lines, could be used to successfully induce senescence in human NET cell lines. In this experiment, the common chemotherapeutic drug Doxorubicin, which is known to induce senescence, was used as a positive control. Cells were treated for 24 hours with CX-5461, afterwards the medium was exchanged. Exemplary pictures of H727 cells after β-Gal staining were taken 4 and 5 days after treatment and are shown below. Blue stained cells indicate senescent cells in this assay.

As a result, CX-5461 was capable of inducing senescence in NET cell lines both 4 and 5 days after treatment as can be seen in the detected blue stained cells, although the effect was neither strictly dose dependent nor very strong (figure 20).

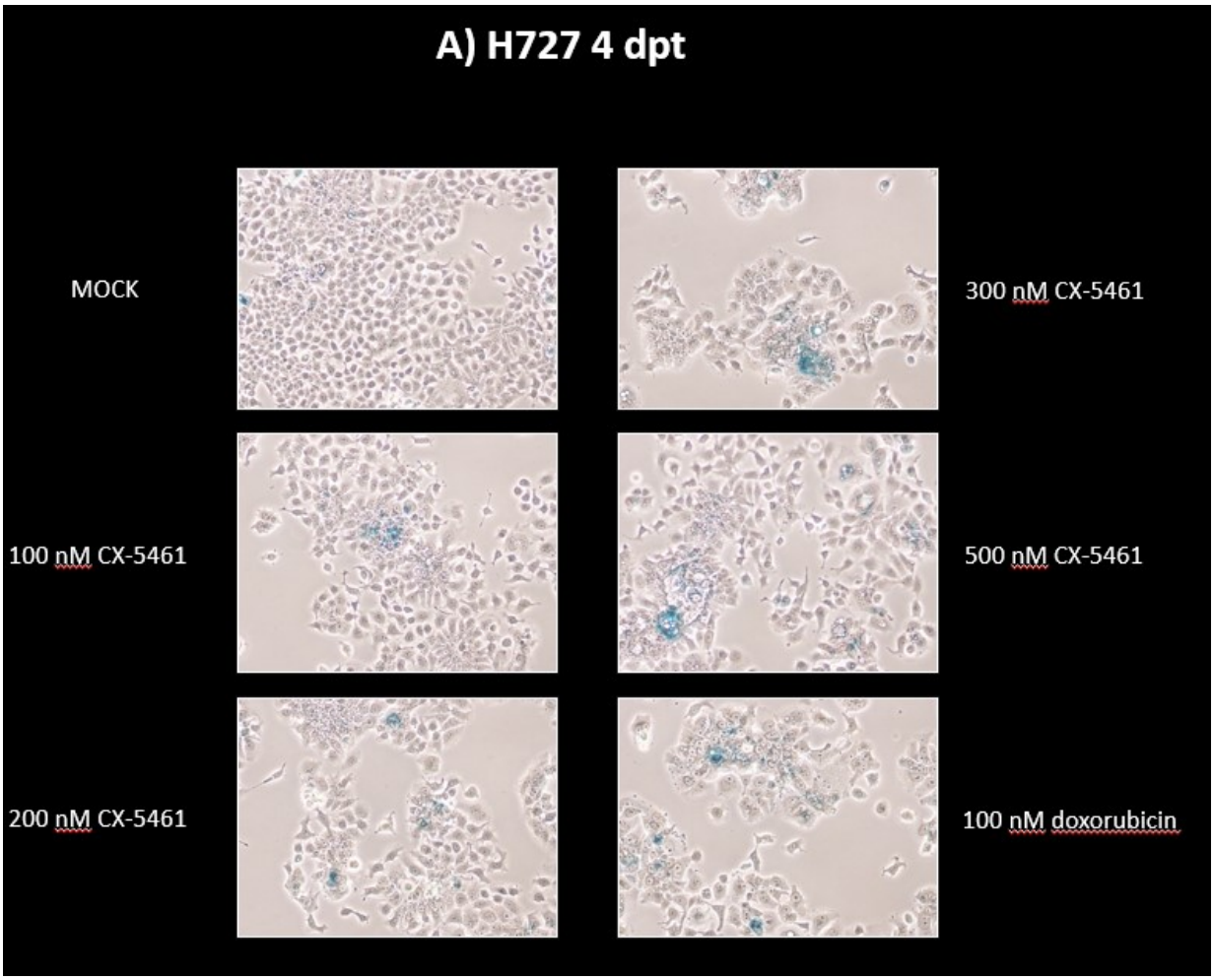
A) H727 4 dpt
MOCK
300 nM CX-5461
100 nM CX-5461
500 nM CX-5461
200 nM CX-5461
100 nM doxorubicin

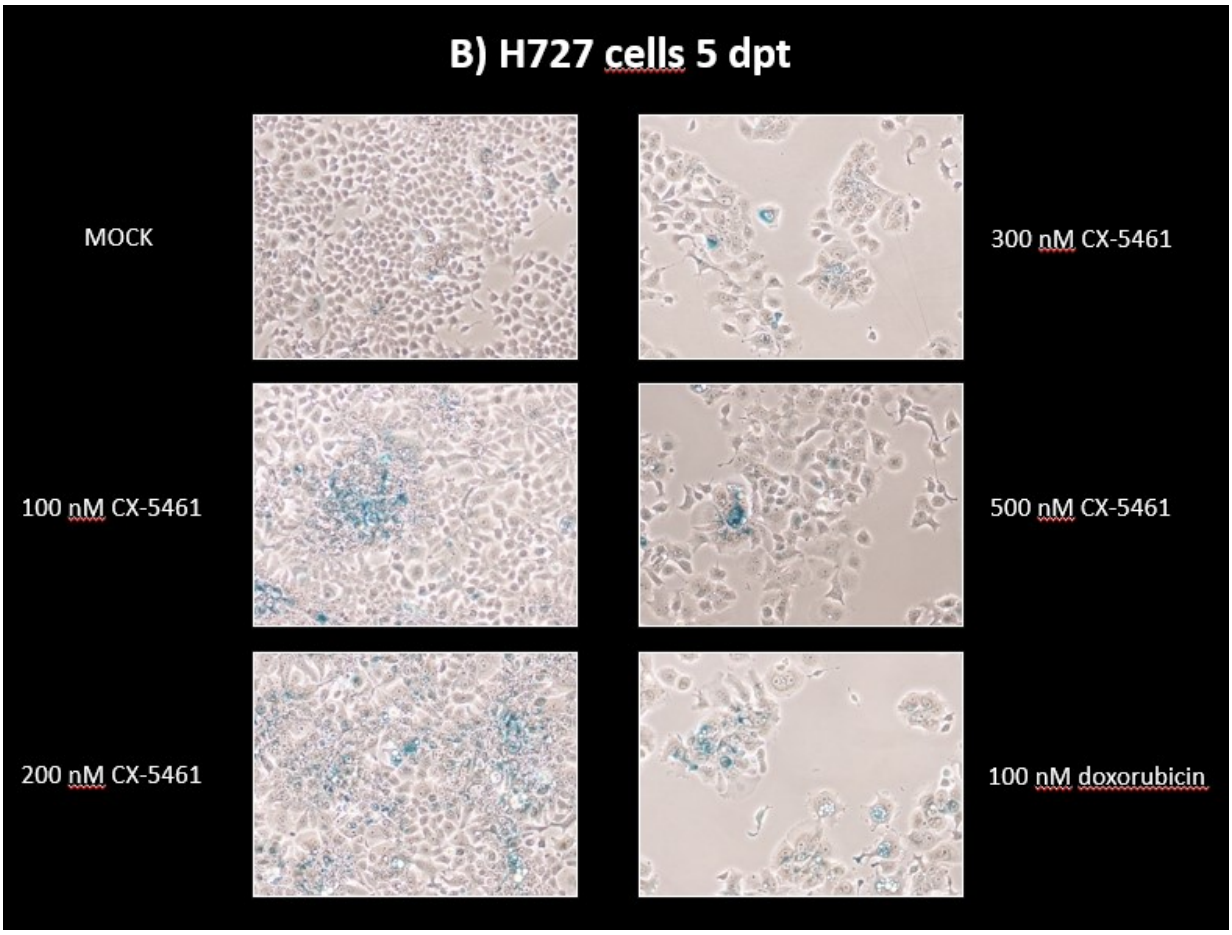

Figure 20: β-Gal assay of H727 cells after senescence inducing treatment 4 (A) and 5 (B) dpt. H727 cells were treated with increasing concentrations of the senescence inducing compound CX-5461. Plates were fixated and stained and pictures taken 4 and 5 days post treatment, respectively. Doxorubicin served as a positive control. MOCK: untreated cells. Blue stained cells indicate senescence.

3.4.2 Crystal violet staining of NET cell lines reveals senescence inducing concentration of CX-5461

In order to identify a senescence-inducing concentration of CX-5461 in the various NET/NEC cell lines, crystal violet staining was performed after treating the cells with CX-5461 for 24 hours in concentrations ranging from 50 nM to 500 nM. Afterwards, the medium was exchanged. Inhibition of clonal tumor cell growth was achieved in every tested cell line, although the necessary concentration of CX-5461 varied as can be seen in table 17 below with H727 being the most sensitive cell line towards CX-5461, requiring the lowest concentration in order to restrain clonal tumor cell growth. Furthermore, an exemplary picture of the result of BON1 cells is shown below in figure 21.

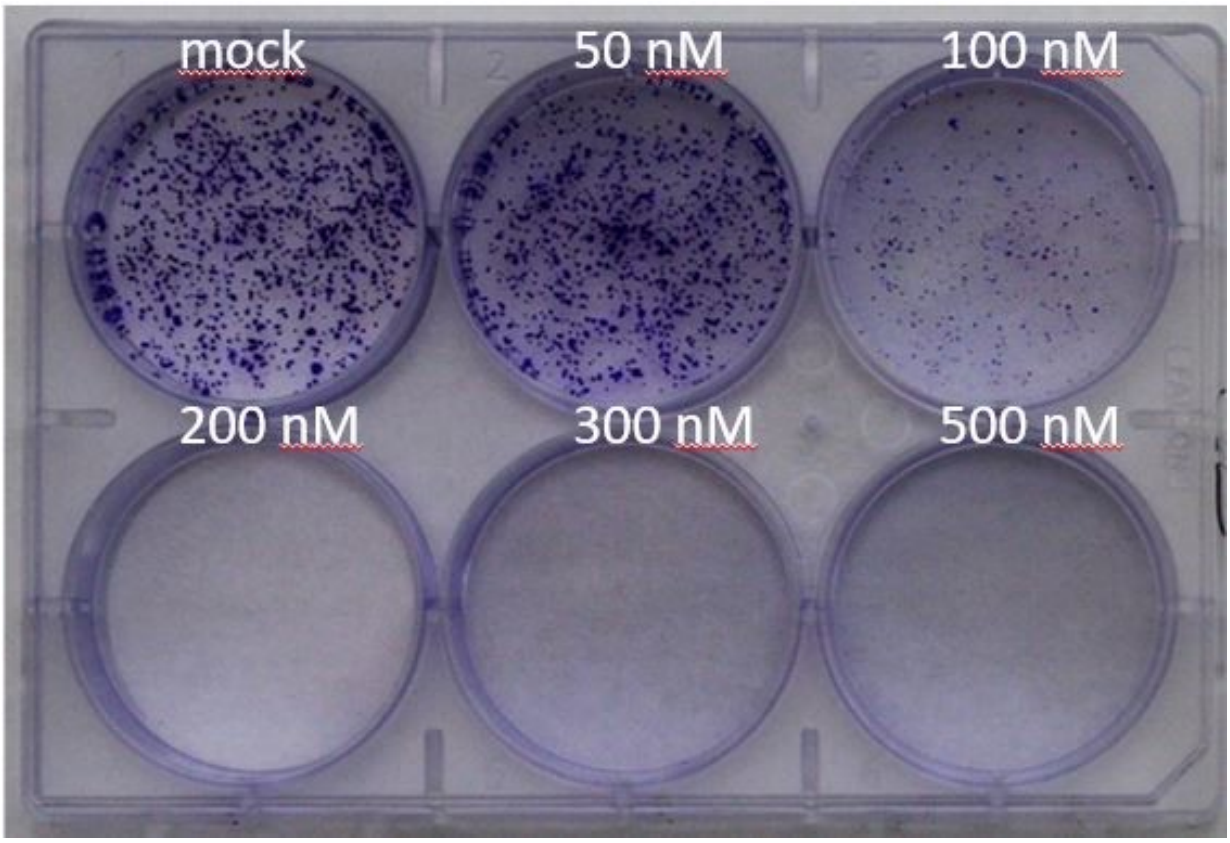

Figure 21: Crystal violet staining of BON1 cells reveals sufficient concentration of the senescence inducing compound CX-5461. BON1 cells were treated for 24 h with increasing concentrations of CX-5461 ranging from 50 nM to 500 nM. Mock: untreated control. Inhibition of clonal tumor cell growth was achieved when using a concentration of 200 nM CX-5461.

Cell line	Required concentration of CX-5461
BON1	200 nM
H727	50 nM
UMC-11	200 nM
QGP-1	200 nM
HROC57	100 nM

Table 17: Required concentration of the senescence inducing compound CX-5461 to inhibit clonal tumor cell growth. Necessary concentrations for the five NET/NEC cell lines tested are displayed in nM.

3.4.3 CX-5461 and MeV-GFP based combination treatment settings on two human NET cell lines

First, the impact of CX-5461 alone on BON1 cells was analyzed. Therefore, the concentration of CX-5461 was used that was found to be sufficiently inhibiting clonal tumor cell growth in 3.4.2 (200 nM). As expected, cell masses of treated cells remained significantly lower, more precisely only 40 % of mock treated cells as can be seen in figure 22.

In a next step, both H727 and BON1 cells were evaluated in the setting shown below in figure 23. To sum it up, cells were first treated with CX-5461 and three or four days later infected with MeV-GFP. SRB assays were then performed at 72 and 96 hpi. As displayed in the graph below, CX-5461 treated cells showed a strongly reduced proliferation resulting in a decreased

cell number in comparison to mock treated cells before infection (table 18), especially in BON1 cells.

While MeV-GFP successfully reduced cell masses 72 and 96 hpi in mock treated cells as shown in various experiments before, there was hardly any effect on CX-5461 pretreated cells. This effect seemed slightly stronger in H727 than in BON1 cells and was visible in both 3- and 4-days post treatment infected cells (figure 24 and 25). The effect can be seen best in H727 96 hpi (figure 24A and 25) both for the 3 and 4 dpt setting, likely due to the fact that in the other settings, especially when using BON1 cell, the treatment with CX-5461 alone already resulted in a strongly reduced cell number, making a further reduction caused by the infection and oncolysis of MeV-GFP harder to observe.

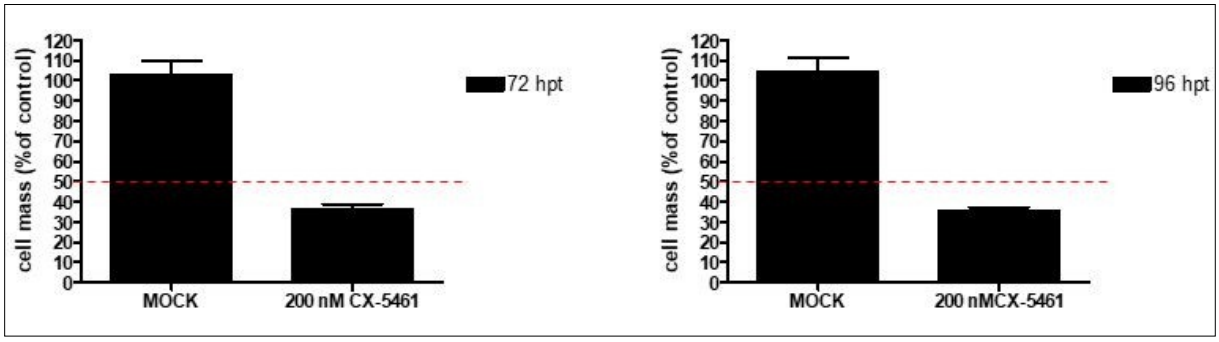

Figure 22: Monotherapeutic treatment of BON1 cells with 200 nM of the senescence inducing compound CX-5461. BON1 cells were treated with 200 nM of CX-5461 for 24 hours and tumor cell masses in % of control were measured at 72/96 hpt by SRB viability assay. Both mock and 200 nM CX-5461 were tested three times. Displayed are mean and standard deviation. Mock: untreated control.

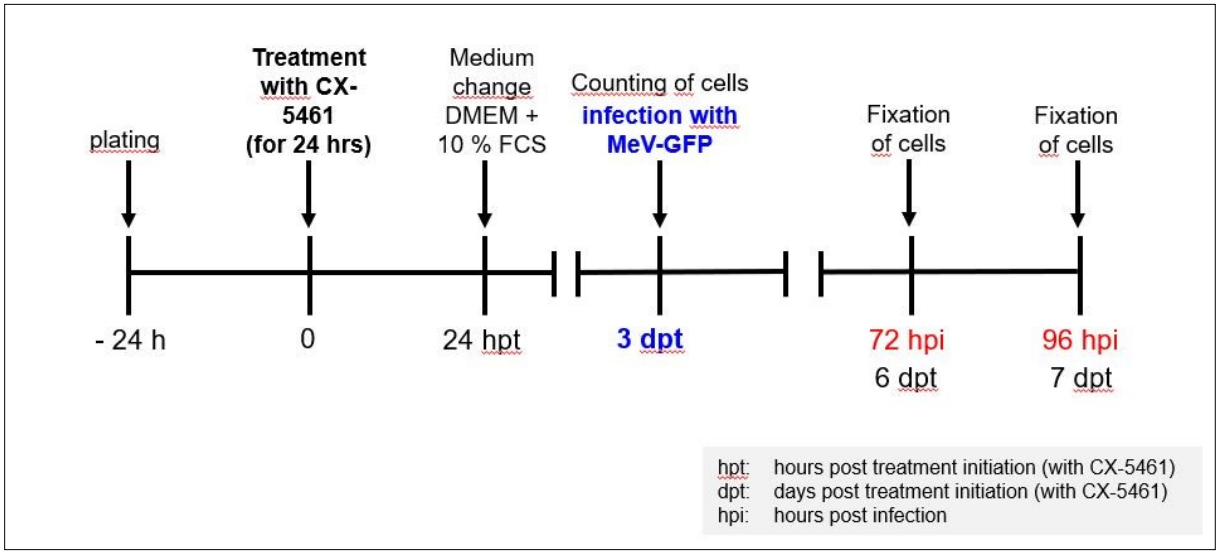

Figure 23: Setting of the combination therapy experiments using CX-5461 and MeV-GFP. 24 hours after plating, cells were treated with 200 nM CX-5461. 24 hpt, medium was exchanged. 3 dpt, cells were counted and infected with MeV-GFP. 72 hpi (= 6 dpt) and 96 hpi (=7 dpt), respectively, cells were fixated.

Cell line	Cell number seeded	Treatment (start 24 h after seeding)	Duration of treatment	Cell number before infection
H727	2 x 10^4	MOCK	3 d	6.375 x 10^4
H727	2 x 10^4	CX-5461 200 nM	3 d	5 x 10^4
BON1	2 x 10^4	MOCK	3 d	22 x 10^4
BON1	2 x 10^4	CX-5461 200 nM	3 d	4.4375 x 10^4

Table 18: Cell number three days after treatment with CX-5461 before infection with MeV-GFP.

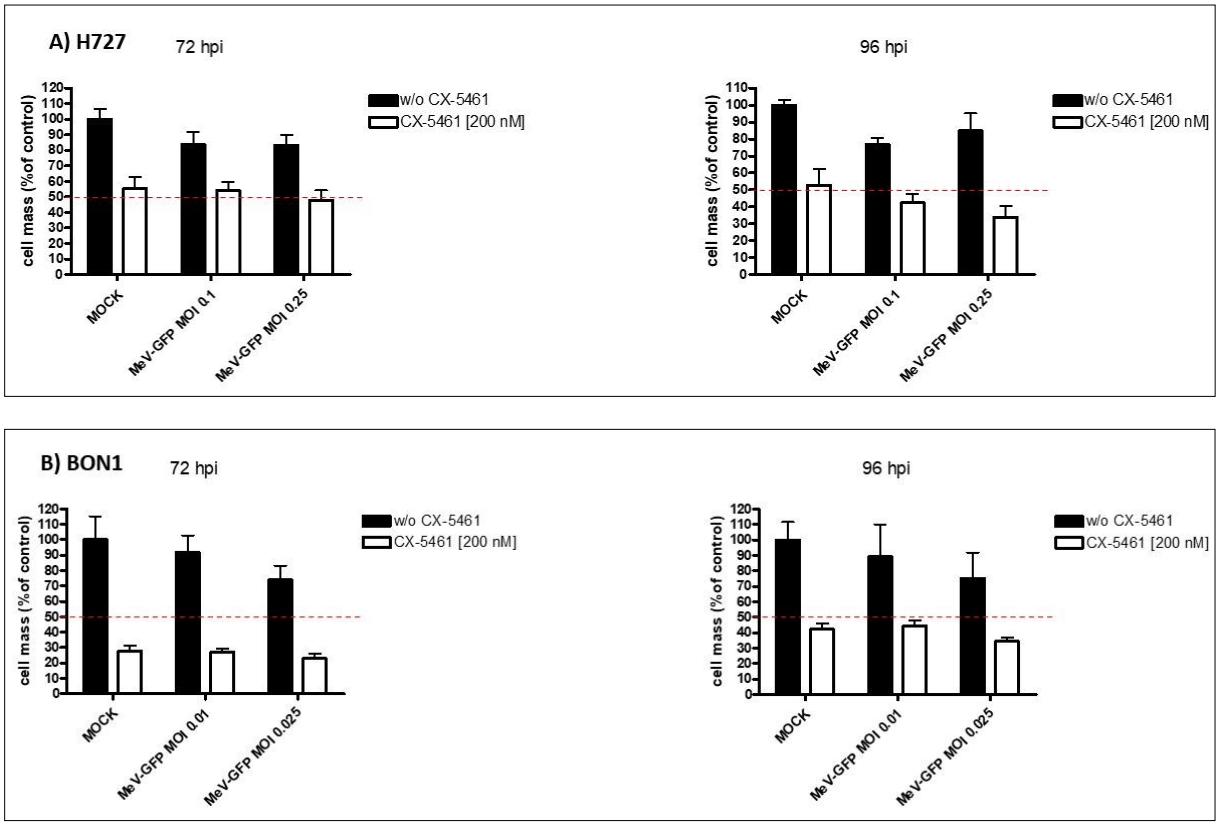

Figure 24: Combination therapy experiments using the senescence inducing compound CX-5461 and MeV-GFP on H727 (A) and BON1 (B) cells. 24 hours after plating, cells were treated with 200 nM CX-5461. 24 hpt, the medium was exchanged. 3 dpt, cells were counted and infected with MeV-GFP. 72 hpi (= 6 dpt) and 96 hpi (=7 dpt), respectively, cells were fixated. Tumor cell masses in % of control were measured 72/96 hpi by SRB viability assay. Mean values and standard deviation of one experiment are shown. Red dotted lines indicate threshold of 50 % remaining tumor cells.

The same experiment was conducted again with H727 cells, the only change in setup was that cells were infected 4 days post treatment with CX-5461 instead of 3 days, thus 72 hpi equal 7 dpt and 96 hpi 8 dpt in this setting. Results are shown in figure 25 below. As can be seen, there was a slightly additive effect regarding tumor lysis at best, which can be seen best in the 96 hpi graph.

Cell line	Cell number seeded	Treatment (start 24 h after seeding)	Duration of treatment	Cell number before infection
H727	4 x 10^4	MOCK	4 d	14.125 x 10^4
	4 x 10^4	CX-5461 200 nM	4 d	6.5 x 10^4

Table 19: Cell number 4 days after treatment with CX-5461 before infection with MeV-GFP. Treatment with CX-5461 resulted in a strongly reduced proliferation when compared to mock treated control cells.

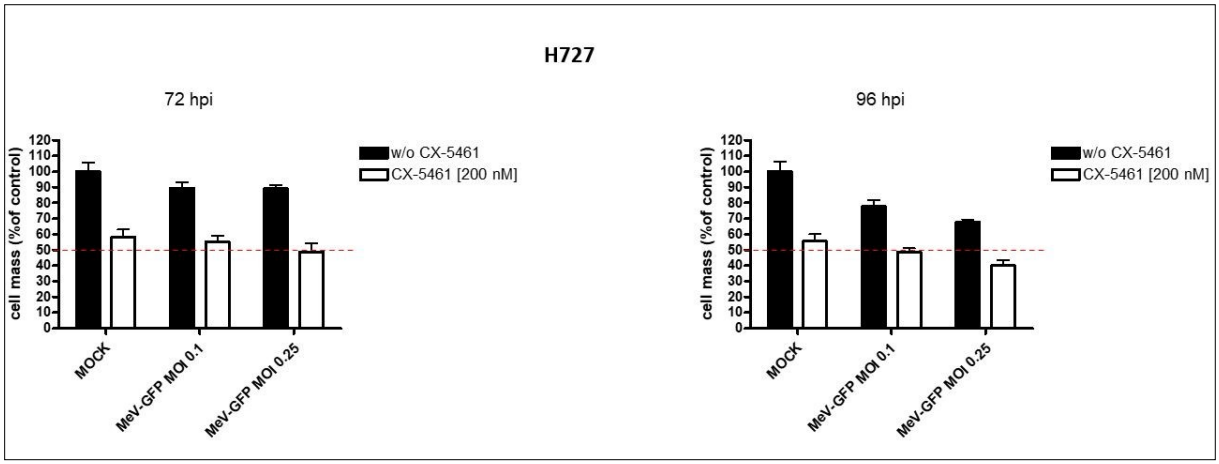

Figure 25: Combination therapy experiments using the senescence inducing compound CX-5461 and MeV-GFP on H727 cells. 24 hours after plating, cells were treated with 200 nM CX-5461. 24 hpt, medium was exchanged. 4 dpt, H727 cells were counted and infected with MeV-GFP. 72 hpi (= 7 dpt) and 96 hpi (= 8 dpt), respectively, cells were fixated. Tumor cell masses in % of control were measured at 72/96 hpi by SRB viability assay. Mean values and standard deviation of one experiment are shown. Red dotted lines indicate threshold of 50 % remaining tumor cells.

4. Discussion

Neuroendocrine neoplasm (NEN) is a rare malignant disease; however, the rising incidence and the poor prognosis in advanced stages provide an urgent need for new and effective therapies.

Immunotherapy has revolutionized the treatment of cancers in the 21st century, with oncolytic viruses being a promising new treatment approach. Oncolytic viruses therefore ideally (i) selectively infect, (ii) replicate in and finally (iii) oncolyse tumor cells, sparing healthy tissue and thereby minimizing side effects.

Several oncolytic viruses for a variety of different tumors are nowadays tested in clinical trials [92]. There has been some promising research for the treatment of NENs with oncolytic viruses, too, which ultimately led to clinical trials [65]. The virus that is currently tested in a phase I/II clinical trial is a triple-modified adenovirus called AdVince developed by a research group in Uppsala, Sweden, which is administered either into the hepatic artery to directly target liver metastases or guided by ultrasound via fine needle puncture also directly into liver metastases.

However, there are several more viruses that showed promising pre-clinical data for the treatment of NENs, among them the recombinant herpes simplex virus type 1 derived virotherapeutic vector T-VEC [71] and oncolytic vaccinia virus GLV-1h68 [70].

Measles vaccine virus (MeV) is one of several oncolytic viruses that possesses a natural tumor tropism, making it an interesting candidate for oncolytic virotherapy also for NEN.

While there are some tumors that show resistance phenomena, a genetically modified oncolytic measles virus encoding the suicide gene SCD, a fusion protein of cytosine deaminase and uracil phosphoribosyltransferase (MeV-SCD), has shown to be able to overcome primary resistances and enhance the oncolytic effect when exploiting the suicide gene function by the addition of the prodrug 5-FC which is locally converted into the chemotherapeutic compound 5-fluorocytosin (5-FU) [59].

To the best of my knowledge MeV vectors have not been tested yet for potential oncolytic effects on NENs.

Therefore, this thesis set out to evaluate the oncolytic effects of MeV-SCD on NENs. Furthermore, combination therapy with different agents in oncology often is more effective than monotherapy. Therefore, MeV-SCD was tested also in combination with a well-established drug for the treatment of NENs, everolimus, which is classified as a mTOR-inhibitor. Additionally, a combination with a senescence inducing compound called CX-5461 was evaluated as well.

MeV is able to infect all tested NEN-cell lines

CD46 has been identified as a receptor on cell surfaces for MeV Edmonston vaccine strains and is often found to be overexpressed on tumor cells.

CD46 was detected on all five tested cell lines of the chosen NEN cell line panel including cell lines from various anatomic origins with different densities expressed in the MFI. Only the pancreatic NET cell line QGP-1 showed a MFI < 20, which is commonly considered the threshold required for cell-to-cell fusion, ultimately leading to syncytia formation and cell death [19], while all other tested cell lines exhibited MFIs above 20.

Next, the primary infection rates in the different cell lines were evaluated.

A MOI of 10 caused infection rates of at least 40 % in all five NEN cell lines 24 hpi with infection rates of up to 80 %.

Of note, the pancreatic cell line QGP-1 and the lung cell line UMC-11, which showed the lowest CD46 density, also had the lowest primary infection rates.

As a proof of concept, the five NEN cell lines were infected with MeV-GFP and GFP expression was monitored by fluorescence microscopy at 72 and 96 hpi. In all five tested cell lines, GFP could be observed inside the cells, visualizing the successful infection of the respective cell line.

In a final step the expression of measles N protein and the inserted transgene SCD in the respective tumor cells was investigated on a protein level. Western blot analysis showed that both proteins were expressed in every tested cell line, although the quantity differed remarkably between the different cell lines.

Taken together, these experiments showed that all tested NEN cell lines can be successfully infected with MeV-SCD, which then replicates in the NEN cell lines, translating encoded genes into proteins. The infectability differed among the cell lines with QGP-1 being the “most resistant” one, which might be due to its low CD46 expression.

Cytotoxic effects of different monotherapeutic strategies

In a next step, the cytotoxic effects of monotherapy with the different agents used in this dissertation, MeV-SCD, everolimus and 5-FU, were to be evaluated.

Therefore, a well-established viability assay, the SRB assay, was used to evaluate the cytotoxic effects on the panel of five different NEN cell lines.

5-FU, a common chemotherapeutic drug, which is used in the treatment of NENs as well, proved to reduce cell mass in all five tested cell-lines in a dose dependent manner.

In the next monotherapeutic experiment, everolimus, which is also an FDA approved drug for the treatment of NENs, was shown to reduce tumor cell mass in a dose dependent manner, too. Cell mass started to decline significantly when using 10 nM of everolimus, while the highest tested dose of 10 µM led to a reduction of more than 50 % in two tested cell lines, and around 50 % in the other 3 cell lines. Those findings correlate well with data published about the effectiveness of everolimus monotreatment on various NEN cell lines [93], [71].

However, the authors of the study detected a limit of the treatment effect when using a dose of approximately 100 nM everolimus, a further increase of the dosage did not result in further reduced tumor cell mass. This was contributed to everolimus rather being a growth-inhibitory than a cytotoxic drug [71].

The effect of everolimus on NENs was not only tested in vitro, but in vivo in a murine NEN model as well, where it was also found to be effective [93].

Moreover, it was shown that performing a positron emission tomography (PET) using ^{18}F-fluorothymidine (^{18}F-FLT), a tumor-specific PET-tracer which accumulates in proliferating cells, can be used early after treatment initiation with everolimus in order to identify responders and non-responders to everolimus therapy, helping to tailor an effective therapy for patients suffering from NENs [93].

Finally, all cell lines were tested for their susceptibility towards MeV-SCD monotreatment without exploiting MeV-SCD’s suicide function yet.

MeV-SCD proved to reduce tumor cell mass in a MOI dependent manner as well, although the susceptibility varied between the different cell lines.

According to the chosen criteria (partial resistance = 50 – 75 % remaining tumor cell mass at a MOI of 1 at 96 hpi), only the pancreatic QGP-1 cells showed a partial resistance, while the other cell lines were found to be highly susceptible.

Again, the partial resistance of QGP-1 cells might be due to the reduced CD46 receptor density on the cell surface resulting in reduced primary infection rates.

Comparing the effectiveness of the different monotreatment strategies, 5-FU and MeV-SCD proved to reduce tumor cell mass further than everolimus. This is likely due to the fact that everolimus only exhibits antiproliferative effects while both 5-FU and MeV-SCD also have cytoreductive effects.

How do those results compare with other tumor cell lines screened for their susceptibility towards oncolytic measles vaccine virus?

For solid tumors, MeV-SCD has been extensively screened with the National Cancer Institute-60 tumor cell panel (NCI-60), which comprises 60 human cancer cell lines, 54 of them representing solid tumors. These 54 tumor cell lines have been analyzed in this thesis work with the same resistance criteria as mentioned above [59].

As a result, 50 % of the screened cell lines of the NCI-60 panel proved to be susceptible to MeV-SCD according to the chosen criteria, while 39 % showed a partial resistance with 50 – 75 % remaining tumor cell mass at 96 hpi with a MOI of 1 and 11% showed a high grade resistance with more than 75 % tumor cell mass remaining.

The average remaining tumor cell mass in the susceptible cell lines was 31 %.

Similar results were found in another study in which the susceptibility of 8 sarcoma cell lines towards MeV-SCD had been evaluated [94]. In this study, 5 of the sarcoma cell lines were found to be susceptible to MeV-SCD mediated oncolysis, while 3 of the sarcoma cell lines exhibited primary resistance.

Although the sample size of NEN cell lines is obviously way smaller, 4 out of 5 cell lines being susceptible with only one partially resistant cell line highlights that NENs are indeed a promising tumor entity for the treatment with MeV-SCD.

Furthermore, with almost none to 45 % remaining tumor cell mass in the susceptible NEN cell lines (see 3.1.4), the tumor mass reduction was on average stronger than in the susceptible tumor cell lines of the NCI-60 panel, further encouraging the research on MeV-SCD used for the treatment of NENs.

Exploitation of MeV-SCD`s suicide gene function can overcome partial resistance

As described above, NEN cells showed high susceptibility towards both 5-FU and MeV-SCD, making them an interesting target for combining both by the addition of the prodrug 5-FC thus exploiting the suicide gene function of MeV-SCD.

All tested NEN cell lines showed a further significant tumor cell reduction by the exploitation of the suicide gene function compared to MeV-SCD monotherapy.

Most importantly, the partially resistant pancreatic cell line QGP-1 now showed only 20 % remaining tumor cell masses at a MOI of 1, thereby showcasing that MeV-SCD in combination with 5-FC can successfully overcome partial resistance phenomena towards MeV-SCD in NEN cell lines as it has been demonstrated for other resistant tumor cell lines, too [59].

Moreover, from a clinical point of view, administering chemotherapeutic drugs systemically as a prodrug, which only have the desired local effect on tumor cells, thereby achieving high local concentrations and minimizing common side effects displays a lot of potential benefits for the patient in comparison to systemic chemotherapy.

Everolimus does not impair replication of MeV-SCD in monolayer cell culture

In a next step, the kinetics of replication of MeV-SCD in NEN cells were evaluated using viral growth curves.

MeV-SCD proved to replicate well in all tested cell lines.

The same experiments were conducted in the presence of everolimus in order to investigate a potential effect of the antiproliferative and immunosuppressive drug on the replication behavior of MeV-SCD in NEN cells. It was found that everolimus neither impaired nor enhanced replication in vitro.

The effect of everolimus on the replication of other viruses tested for the treatment of NENs has been studied, too.

In these studies, everolimus did not change the replication pattern of the oncolytic vaccinia virus GLV-1h68 [70] or the oncolytic herpes simplex virus Talimogene Laherparepvec either [71]. Nevertheless, these experiments were conducted in monolayer cell culture and the pleiotropic effects of everolimus in vivo e.g. on the immune system in combination with MeV-SCD have yet to be investigated, especially since there is some evidence that mTOR-inhibitors can potentially enhance oncolytic virotherapy in vivo [95, 96].

It was shown that the efficacy of a systemically administered oncolytic vaccinia virus for the treatment of malignant gliomas in vitro and in vivo can be enhanced by combining it with rapamycin, which is a first generation mTOR inhibitor, too. The combination enhanced viral replication and prolonged survival of the animals bearing tumors compared to those only treated with virotherapy [95].

The same group proved that combining a recombinant vaccinia virus with rapamycin in two immunocompetent animal models of glioma resulted in enhanced replication of the virotherapeutic drug and led to prolonged survival of the mice compared to virotherapeutic monotreatment. Some of the animals were even considered “cured” according to the authors’ chosen criteria of terminating the experiments after 120 days [96].

Despite the evidence of potential benefits from a combinatorial therapeutic regimen, in our laboratory combination therapy using different oncolytic viruses and everolimus only was slightly superior to monotherapy in the treatment of NENs at best. Unlike in the studies mentioned above, no enhanced viral replication was observed when combining oncolytic virus with everolimus in vitro.

However, effects of the combination might be stronger in vivo when everolimus can potentially suppress an antiviral immune response.

Comparison of different oncolytic viruses for the treatment of NENs

As described in detail in the introduction, several oncolytic viruses have already been tested for the treatment of NENs.

Which one seems to be the most promising candidate?

One of the viruses studied in our lab is the recombinant herpes simplex virus type 1 derived virotherapeutic vector T-VEC, also known as Talimogene Laherparepvec, the first FDA and EMA approved oncolytic virus.

Infection of NEN cell lines with T-VEC resulted in a dose-dependent reduction of tumor cell mass in all tested cell lines [71].

While T-VEC reduced tumor cell masses in all lung NEN cell lines (H727, UMC-11) as well as in one pNEN cell line (BON1) and one NEC cell line (HROC57) at strikingly low MOIs (0.01), the pNEN cell line QGP-1 required a tenfold higher MOI in order to reach the same tumor cell mass reduction.

Moreover, with NEC-DUE1, there was one NEC cell line that showed partial resistance towards T-VEC treatment, with more than 60 % tumor cell mass remaining even at relatively high MOIs. An explanation for this partial resistance might be the slower viral replication kinetics observed in NEC-DUE1 cells.

The antitumoral impact of T-VEC in vivo could be even stronger since its encoded transgene GM-CSF could potentially trigger a strong inflammatory antitumoral response in the presence of immune cells. This effect could not be studied in vitro; however, strong transgene expression in NEN cells provides an indicator for its use in vivo.

Ultimately, there are several virostatic drugs which can inhibit the replication of herpes viruses, among them ganciclovir (GCV). It has been shown that GCV can efficiently prevent viral cytotoxicity caused by T-VEC, making it a useful tool as a safety compound for virotherapy in comparison to other oncolytic viruses such as MeV-SCD or GLV-1h68.

Another virus studied in our lab for the treatment of NENs is the oncolytic vaccinia virus GLV-1h68. GLV-1h68 was also found to be capable of reducing tumor cell masses in all tested NEN cell lines in a MOI dependent manner [70].

According to the author's chosen criteria for resistance, three cell lines (BON1, H727 and HROC-57) were classified as highly permissive, while three cell lines (UMC-11, NEC-DUE1, QGP-1) were classified as permissive. No resistant cell line was found.

The OV for NENs that is currently tested in a clinical trial (NCT02749331) is called AdVince and is a triple modified adenovirus (see introduction).

It has been tested in different cell lines than the other viruses mentioned above, more precisely primary cells derived from metastatic small intestinal NETs, and required MOIs of 1 to 10 to achieve sufficient tumor mass reduction in vitro [26].

Taken together, all four viruses discussed have been shown to exhibit profound antitumoral activity in NEN cell lines in vitro.

Pancreatic QGP-1 cells were less susceptible for all tested viruses; however, sufficient cell mass reduction could be achieved by either increasing the MOI of the respective virus or exploiting a suicide gene function (MeV-SCD).

T-VEC required the lowest MOIs of all viruses for sufficient tumor cell reduction and bears the advantage of a possible antiviral drug with GCV if required.

While the NEC cell line NEC-DUE1 showed a partial resistance to T-VEC, it was permissive towards GLV-1h68 and therefore GLV-1h68 might be the favorable antitumoral agent for NECs.

MeV-SCD meanwhile has the advantage of its suicide gene, which can decrease the required MOI for sufficient tumor cell reduction because of its enhanced killing.

For a clinical perspective, in the times of individualized medicine, a patient's tumor cells could be screened for the optimal virotherapeutic drug for his/her tumor. Therefore, a so called "virogram", which evaluates the preferential oncolytic virus with extensive in vitro tests for each patient individually, should be performed in the future analogously to the well-known antibiogram helping to find the best suited antibiotic/antimycotic drug for the respective bacteria/fungus.

This seems especially important in NENs because of the broad variance of anatomical origin and biological behavior.

CX-5461 can successfully induce senescence in NEN cell lines

Another combinatorial approach of MeV-SCD involves senescence-inducing drugs, since it was shown that measles vaccine virus exhibits enhanced oncolytic effects in therapy-induced senescent tumor cells [64].

Therefore, it was first investigated whether a known senescence-inducing compound, CX-5461, can successfully induce senescence in our NEN cell panel.

β-gal assays revealed that CX-5461 can indeed induce senescence in NEN cell lines. Further, minimal required concentration of CX-5461 in order to achieve inhibition of clonal tumor cell growth was evaluated.

The required concentration varied from cell line to cell line, nevertheless, inhibition of clonal tumor cell growth was accomplished in all tested cell lines, showing as a proof of concept that senescence can be successfully induced in NEN cells.

Enhanced killing of therapy-induced senescent tumor cells by oncolytic measles virus has been described in the literature [64], however, in this dissertation only minor synergistic effects were observed for the combination of CX-5461 with MeV-SCD. This might be because CX-5461 already reduced the cell number in comparison to mock treated cells that strongly especially in BON1-cells, that there was only very little room left for further reduction by MeV-SCD. The duration of the pre-treatment with CX-5461 did not alter the results, the effect remained slightly additive at best.

Limitations

The major limitation of this study is that monolayer cell culture only provides tumor cells in a two-dimensional model, lacking the tumor microenvironment as well as the host's immune cells which play a crucial role in the second step of antitumoral response caused by the activation of the immune system by the oncolytic release of both viral and tumoral antigens. Since this effect is thought to be even more important than direct oncolysis caused by the virus itself, experiments in vivo should be the next step.

Furthermore, the possible interactions of everolimus, which has pleiotropic effects on various cells, and among other influences the immune system, thereby potentially influencing the infectability of tumor cells on the one hand and altering the systemic immune response to the presentation of viral and tumor antigens in a highly inflammatory environment on the other hand, require further investigation in vivo.

Therefore, further research employing three-dimensional tumor models such as organoids or in vivo animal models is needed.

Conclusions and prospects

This thesis aimed to evaluate whether MeV can be used as a virotherapeutic drug for the treatment of NENs. Furthermore, potential combinatorial settings with everolimus and CX-5461 were to be evaluated.

MeV has been shown to be able to (i) infect, (ii) replicate in and finally (iii) oncolyse various NET and one NEC cell line from different anatomic sites in an in vitro model and therefore holds an immense potential for patients suffering from NENs.

Moreover, the exploitation of MeV-SCD's suicide gene function by the addition of the prodrug 5-FC was shown to further enhance the oncolytic efficiency and even overcome partial resistance towards MeV-SCD monotherapy.

Combining MeV-SCD application with everolimus did not impair the replication of MeV-SCD.

As another result, the use of senescence inducing drugs such as CX-5461 before treatment with oncolytic measles vaccine virus might enhance the oncolytic effect to a greater extent.

In order to further investigate the use of MeV-SCD in the treatment of NEN, in vivo experiments in for example murine models are needed now that it proved to be a potential treatment option in vitro. Comparing the efficiency of MeV-SCD with other oncolytic viruses used in our laboratory for the treatment of NENs such as vaccinia vaccine virus and herpes simplex virus type 1 in a NEN organoid or murine model and thus determining the best suited candidate for further evaluation will be the next step.

Furthermore, optimizing MeV-SCD's use with the best suited combinatorial drug might eventually lead to new clinical treatment options for patients suffering from NENs.

5. Summary / Zusammenfassung

5.1 Summary

Neuroendocrine neoplasms (NENs) comprise a heterogenous group of various malignancies and metastatic disease remains a challenge to treat, leading to a poor prognosis in advanced disease. Therefore, new therapeutic options are desperately needed.

Oncolytic viruses are emerging as a new class of anticancer agents, which are successfully used in the treatment of various malignancies, amongst others for NENs.

Measles vaccine virus (MeV) has a natural tropism towards tumor cells and has demonstrated strong tumoricidal effects on various tumors.

Its efficiency can be further enhanced by the insertion of transgenes.

In this thesis, a state-of-the-art suicide-gene (SCD) armed oncolytic measles vaccine virus (MeV-SCD) was tested in five well characterized NEN cell lines of different anatomic origin.

First, it was shown that all tested NEN cell lines express the CD46-receptor which is necessary for cell entry of measles vaccine virus.

Next, it was proved that measles vaccine virus can successfully infect NEN cell lines by examining primary infection rates by flow cytometry and fluorescence microscopy.

Western blot analysis of measles vaccine virus N protein as well as SCD protein expression revealed effective replication of the virus and expression of its transgene in vitro.

The kinetics of measles vaccine virus replication within NEN tumor cells was further analyzed by viral growth curves.

Finally, by measuring cell viability via SRB assay, MeV was shown to be able to successfully oncolyse the NEN cell lines in a MOI-dependent manner.

This oncolytic virus based tumoricidal effect could be further enhanced by the addition of the prodrug 5-FC, which is enzymatically converted into the common chemotherapeutic drug 5-FU within infected tumor cells only, thereby sparing healthy tissue and reducing potential side effects, thus exploiting MeV-SCD's suicide-gene. Since 5-FU is used in clinical practice for NENs and showed high dose-dependent efficiency as a monotherapy in this thesis as well, applying it locally via virotherapy might be a huge benefit for patients suffering from NENs.

Additionally, combinatorial regimens using the mTOR-inhibitor everolimus and the senescence-inducing compound CX-5461 were employed.

In summary, this thesis showed that MeV-SCD can successfully (i) infect, (ii) replicate in and (iii) finally oncolyse tumor cells of neuroendocrine origin in a MOI dependent manner, making it a promising treatment option for NEN patients in the future.

However, further preclinical and clinical experiments are needed in order to evaluate its efficiency in vivo and to optimize potential combinatorial therapeutic regimens.

5.2 Zusammenfassung

Neuroendokrine Neoplasien (NEN) bestehen aus einer heterogenen Gruppe verschiedener bösartiger Tumore, bei denen die Behandlung metastasierter Formen nach wie vor eine große Herausforderung darstellt, was zur schlechten Prognose bei fortgeschrittener Erkrankung führt.

Deshalb werden neue Behandlungsmethoden dringend benötigt.

Onkolytische Viren sind eine neue Behandlungsmodalität im Spektrum der onkologischen Behandlungsansätze, die bereits erfolgreich in der Therapie verschiedener Tumore benutzt werden, darunter NEN.

Das Masern-Impfvirus besitzt einen natürlichen Tropismus für Tumorzellen und seine onkolytische Wirkung wurde bereits bei einer Vielzahl von Tumoren demonstriert. Dabei kann die Effizienz der Onkolyse durch das Einfügen von Fremdgenen in das Masern-Impfvirus deutlich gesteigert werden.

In dieser Doktorarbeit wurde ein mit einem sogenannten „Suizidgen“ ausgestattetes Masern-Impfvirus an fünf bekannten und gut erforschten Zelllinien neuroendokrinen Ursprungs aus verschiedenen anatomischen Regionen getestet.

Zunächst konnte gezeigt werden, dass alle getesteten NEN-Zelllinien den CD46-Rezeptor exprimieren, welcher für den Zelleintritt des Masern-Impfvirus benötigt wird.

Als nächstes wurde mittels Fluoreszenzmikroskopie und Durchflusszytometrie gezeigt, dass Masern-Impfviren NEN-Zelllinien erfolgreich infizieren können.

Mittels Western Blot konnte in den infizierten Zelllinien sowohl das Masern-Impfvirus N-Protein als auch das SCD-Protein, ein Fusionsprotein aus Cytosindesaminase und Phosphoribosyltransferase, nachgewiesen werden, sodass auch auf der Proteinebene die erfolgreiche Replikation des Masern-Impfvirus nachgewiesen werden konnte.

Die genaue Kinetik der Virusreplikation wurde mit Wachstumskurven detailliert analysiert.

Schlussendlich konnte mittels eines bekannten Viabilitätsassays, dem sogenannten SRB-Assay, gezeigt werden, dass Masern-Impfviren NEN-Zelllinien in einer dosisabhängigen Weise lysieren können.

Dieser durch das onkolytische Masernvirus ausgelöste Effekt konnte durch die Ausnutzung des auf dem Vektor MeV-SCD integrierten SCD Suizidgenes verstärkt werden. Durch die Zugabe der Prodrug 5-FC, das nur in infizierten Tumorzellen enzymatisch in das bekannte Chemotherapeutikum 5-FU umgewandelt wird, können systemische unerwünschte Arzneimittelwirkungen reduziert werden.

Dadurch dass 5-FU in der Klinik routinemäßig bei NEN-Patienten eingesetzt wird und auch als Monotherapie in dieser Doktorarbeit starke dosisabhängige Effekte auf NEN-Zelllinien hatte, könnte diese Art der Applikation in Kombination mit dem zusätzlichen onkolytischen Effekt durch Masern-Impfviren einen großen Vorteil für NEN-Patienten in der Zukunft haben.

Darüber hinaus wurden mögliche Kombinationstherapien mit dem mTOR-Inhibitor Everolimus sowie der Seneszenz-induzierenden Verbindung CX-5461 erforscht.

Zusammenfassend konnte in dieser Doktorarbeit gezeigt werden, dass Masern-Impfviren Tumorzellen neuroendokrinen Ursprungs (i) erfolgreich infizieren, (ii) in ihnen replizieren und sie letztendlich in einer dosisabhängigen Weise (iii) lysieren können, was sie in der Zukunft zu

einer vielversprechenden potenziellen Therapieoption für Patienten mit neuroendokrinen Neoplasien macht.

Nichtsdestotrotz werden weitere präklinische und klinische Experimente benötigt, um die Effizienz in vivo zu demonstrieren und Kombinationsstrategien mit anderen Medikamenten zu optimieren.

List of abbreviations

5-FC: 5-fluorocytosine

5-FU: 5-fluorouracil

5-FUMP: 5-fluorouridine monophosphate

5-FdUMP: 5-fluorodeoxyuridine monophosphate

5-FUTP: 5-fluorouridine triphosphate

5-FβAL: 5-fluoro-β-alanine

^{18}F-FLT: ^{18}F-fluorothymidine

ADV: Adenovirus

AML: Acute myeloid leukemia

APS: Ammonium persulfate

ATCC: American Type Culture Collection

ATRX: ATRX Chromatin Remodeler

CD: Cluster of differentiation

CEA: Carcinoembryonic antigen

CgA: Chromogranin A

DMEM: Dulbecco's modified eagle's medium

DMSO: Dimethyl sulfoxide

DNA: Deoxyribonucleic acid

DPD: Dihydropyrimidine dehydrogenase

Dpt: Days post treatment

dTTP: Deoxythymidine triphosphate

E1A: Adenovirus early region 1 A

ECL: Enhanced chemiluminescence

Elisa: Enzyme-linked immunosorbent assay

EMA: European Medicines Agency

EGFRvIII: Epidermal growth factor receptor variant three

FCS: Fetal calf serum

FDA: Food and Drug Administration

Fig.: Figure

GCV: Ganciclovir

GEP-NET: Gastroenteropancreatic neuroendocrine tumor

GFP: Green fluorescent protein

GI-tract: Gastrointestinal tract

GM-CSF: Granulocyte-macrophage colony-stimulating factor

gNET: Gastric neuroendocrine tumor

h: Hours

HP-NAP: Helicobacter pylori neutrophil-activating protein

hpi: Hours post infection

hpt: Hours post treatment

HSV-1: Herpes simplex virus type 1

i.v.: Intravenous

IFN: Interferon

IL: Interleukin

ITGβ1: Integrin β1

JAK: Janus-associated kinase

JCRB: Japanese Collection of Research Bioresources Cell Bank

Ki-67: Kiel Protein 67

MEN1: Menin 1

MeV: Measles virus

MeV-SCD: Suicide gene-armed oncolytic measles vaccine virus

MFI: Mean fluorescence index

mLST8: Mammalian lethal with SEC13 protein 8

MOI: Multiplicity of infection

MTC: Medullary thyroid carcinoma

mTOR: Mechanistic target of rapamycin

mTORC 1/2: Mechanistic target of rapamycin complex 1/2

NCI: National Cancer Institute

NCT: National clinical trial

NEC: Neuroendocrine carcinoma

NEN: Neuroendocrine neoplasia

NET: Neuroendocrine tumor

NIS: Human thyroidal iodide symporter

NRSE: Neuron-restrictive silencer gene

OV: Oncolytic virus

Parag: Paraganglioma

PBS: Phosphate buffered saline

PE: Phycoerythrin

PET-CT: Positron emission tomography-computed tomography

PFU: Plaque forming units

Pheo: Pheochromocytoma

PI3K: Phosphatidylinositol-3-kinase

PIP_2: Phosphatidylinositol-4,5-bisphosphate

PIP_3: Phosphatidylinositol-3,4,5-trisphosphate

pNET: Pancreatic neuroendocrine tumor

PRAS 40: Proline-rich Akt substrate of 40 kDa

PTD: Protein transduction domain

PTEN: Phosphatase and tensin homolog

PVDF: Polyvinylidene difluoride

RB1: Retinoblastoma transcriptional corepressor 1

Rheb: Ras homolog enriched in brain

RNA: Ribonucleic acid

RPM: Revolutions per minute

RPMI: Cell culture medium developed at the Roswell Park Memorial Institute

RT: Room temperature

SA: Senescence-associated

SCLC: Small cell lung cancer

SCD: Super Cytosine Deaminase

SD: Standard deviation

SDS-PAGE: Sodium-dodecylsulfate polyacrylamide gel electrophoresis

SLAMF1: Signaling lymphocyte activation molecule family member 1

siNET: Small intestinal neuroendocrine tumor

SRB: Sulforhodamine B

SSA: Somatostatin analogue

SSPE: Subacute sclerosing panencephalitis

SVV-001: Seneca Valley Virus 1

SFV: Semliki forest virus

Syn: Synaptophysin

TCA: Trichloroacetic acid

$TCID_{50}$: Tissue culture infectious dose 50

TEMED: Tetramethylethylendiamine

TNF: Tumor necrosis factor

TP53: Tumor protein 53

TP53wt: Tumor protein 53 wildtype

TRIS: Tris(hydroxymethyl)-amino-methane

TS: Thymidylate synthase

TSC1/2: Tuberous sclerosis proteins 1 and 2

T-VEC: Talimogene Laherparepvec

UPRT: Yeast uracil phosphoribosyl-transferase

USA: United States of America

VACV: Vaccina virus

VSV: Vesicular Stomatitis Virus

WHO: World health organization

List of figures

List of tables

References

1. Taal, B.G. and O. Visser, *Epidemiology of neuroendocrine tumours.* Neuroendocrinology, 2004. **80 Suppl 1**: p. 3-7.
2. Modlin, I.M., M.D. Shapiro, and M. Kidd, *Siegfried Oberndorfer: origins and perspectives of carcinoid tumors.* Hum Pathol, 2004. **35**(12): p. 1440-51.
3. Nagtegaal, I.D., et al., *The 2019 WHO classification of tumours of the digestive system.* Histopathology, 2020. **76**(2): p. 182-188.
4. Kımıloğlu Şahan, E., et al., *P53, KI-67, CD117 expression in gastrointestinal and pancreatic neuroendocrine tumours and evaluation of their correlation with clinicopathological and prognostic parameters.* Turk J Gastroenterol, 2015. **26**(2): p. 104-11.
5. Hitchcock, C.L., *Ki-67 staining as a means to simplify analysis of tumor cell proliferation.* Am J Clin Pathol, 1991. **96**(4): p. 444-6.
6. Williams, E.D. and M. Sandler, *The classification of carcinoid tum ours.* Lancet, 1963. **1**(7275): p. 238-9.
7. Gosain, R., et al., *Geographic and demographic features of neuroendocrine tumors in the United States of America: A population-based study.* Cancer, 2019.
8. Alwan, H., et al., *Incidence trends of lung and gastroenteropancreatic neuroendocrine neoplasms in Switzerland.* Cancer Med, 2020. **9**(24): p. 9454-9461.
9. Riihimäki, M., et al., *The epidemiology of metastases in neuroendocrine tumors.* Int J Cancer, 2016. **139**(12): p. 2679-2686.
10. Pavel, M., et al., *ENETS Consensus Guidelines Update for the Management of Distant Metastatic Disease of Intestinal, Pancreatic, Bronchial Neuroendocrine Neoplasms (NEN) and NEN of Unknown Primary Site.* Neuroendocrinology, 2016. **103**(2): p. 172-85.
11. Garcia-Carbonero, R., et al., *ENETS Consensus Guidelines for High-Grade Gastroenteropancreatic Neuroendocrine Tumors and Neuroendocrine Carcinomas.* Neuroendocrinology, 2016. **103**(2): p. 186-94.
12. Lawler, S.E., et al., *Oncolytic Viruses in Cancer Treatment: A Review.* JAMA Oncol, 2017. **3**(6): p. 841-849.
13. Raja, J., et al., *Oncolytic virus immunotherapy: future prospects for oncology.* J Immunother Cancer, 2018. **6**(1): p. 140.
14. zur Hausen, H., *Papillomaviruses in the causation of human cancers - a brief historical account.* Virology, 2009. **384**(2): p. 260-5.
15. Bluming, A.Z. and J.L. Ziegler, *Regression of Burkitt's lymphoma in association with measles infection.* Lancet, 1971. **2**(7715): p. 105-6.
16. Kelly, E. and S.J. Russell, *History of oncolytic viruses: genesis to genetic engineering.* Mol Ther, 2007. **15**(4): p. 651-9.
17. Engeland, C.E. and G. Ungerechts, *Measles Virus as an Oncolytic Immunotherapy.* Cancers (Basel), 2021. **13**(3).
18. Mastrangelo, M.J., et al., *Intratumoral recombinant GM-CSF-encoding virus as gene therapy in patients with cutaneous melanoma.* Cancer Gene Ther, 1999. **6**(5): p. 409-22.
19. Anderson, B.D., et al., *High CD46 receptor density determines preferential killing of tumor cells by oncolytic measles virus.* Cancer Res, 2004. **64**(14): p. 4919-26.

20. Yu, Z., et al., *Enhanced nectin-1 expression and herpes oncolytic sensitivity in highly migratory and invasive carcinoma.* Clin Cancer Res, 2005. **11**(13): p. 4889-97.

21. Martuza, R.L., et al., *Experimental therapy of human glioma by means of a genetically engineered virus mutant.* Science, 1991. **252**(5007): p. 854-6.

22. Hammond, A.L., et al., *Single-chain antibody displayed on a recombinant measles virus confers entry through the tumor-associated carcinoembryonic antigen.* J Virol, 2001. **75**(5): p. 2087-96.

23. Lange, S., et al., *A novel armed oncolytic measles vaccine virus for the treatment of cholangiocarcinoma.* Hum Gene Ther, 2013. **24**(5): p. 554-64.

24. Ramachandran, M., et al., *An infection-enhanced oncolytic adenovirus secreting H. pylori neutrophil-activating protein with therapeutic effects on neuroendocrine tumors.* Mol Ther, 2013. **21**(11): p. 2008-18.

25. Maurer, S., et al., *Suicide genearmed measles vaccine virus for the treatment of AML.* Int J Oncol, 2019. **55**(2): p. 347-358.

26. Yu, D., et al., *Preclinical Evaluation of AdVince, an Oncolytic Adenovirus Adapted for Treatment of Liver Metastases from Neuroendocrine Cancer.* Neuroendocrinology, 2017. **105**(1): p. 54-66.

27. Veinalde, R., et al., *Oncolytic measles virus encoding interleukin-12 mediates potent antitumor effects through T cell activation.* Oncoimmunology, 2017. **6**(4): p. e1285992.

28. Russell, S.J. and K.W. Peng, *Measles virus for cancer therapy.* Curr Top Microbiol Immunol, 2009. **330**: p. 213-41.

29. Ong, H.T., et al., *Systemically delivered measles virus-infected mesenchymal stem cells can evade host immunity to inhibit liver cancer growth.* J Hepatol, 2013. **59**(5): p. 999-1006.

30. Nosaki, K., et al., *A novel, polymer-coated oncolytic measles virus overcomes immune suppression and induces robust antitumor activity.* Mol Ther Oncolytics, 2016. **3**: p. 16022.

31. Miest, T.S., et al., *Envelope-chimeric entry-targeted measles virus escapes neutralization and achieves oncolysis.* Mol Ther, 2011. **19**(10): p. 1813-20.

32. Johnson, D.B., I. Puzanov, and M.C. Kelley, *Talimogene laherparepvec (T-VEC) for the treatment of advanced melanoma.* Immunotherapy, 2015. **7**(6): p. 611-9.

33. Andtbacka, R.H., et al., *Talimogene Laherparepvec Improves Durable Response Rate in Patients With Advanced Melanoma.* J Clin Oncol, 2015. **33**(25): p. 2780-8.

34. Ressler, J.M., et al., *Real-life use of talimogene laherparepvec (T-VEC) in melanoma patients in centers in Austria, Switzerland and Germany.* J Immunother Cancer, 2021. **9**(2).

35. Dummer, R., et al., *Combining talimogene laherparepvec with immunotherapies in melanoma and other solid tumors.* Cancer Immunol Immunother, 2017. **66**(6): p. 683-695.

36. Yu, X., et al., *Measles Virus Matrix Protein Inhibits Host Cell Transcription.* PLoS One, 2016. **11**(8): p. e0161360.

37. Di Pietrantonj, C., et al., *Vaccines for measles, mumps, rubella, and varicella in children.* Cochrane Database Syst Rev, 2020. **4**(4): p. Cd004407.

38. Buchanan, R. and D.J. Bonthius, *Measles virus and associated central nervous system sequelae.* Semin Pediatr Neurol, 2012. **19**(3): p. 107-14.

39. Patel, M.K., et al., *Progress Toward Regional Measles Elimination - Worldwide, 2000-2019.* MMWR Morb Mortal Wkly Rep, 2020. **69**(45): p. 1700-1705.

40. Laksono, B.M., et al., *Measles Virus Host Invasion and Pathogenesis.* Viruses, 2016. **8**(8).

41. Ni Choileain, S. and A.L. Astier, *CD46 processing: a means of expression.* Immunobiology, 2012. **217**(2): p. 169-75.

42. Elvington, M., M.K. Liszewski, and J.P. Atkinson, *CD46 and Oncologic Interactions: Friendly Fire against Cancer.* Antibodies (Basel), 2020. **9**(4).

43. Enders, J.F. and T.C. Peebles, *Propagation in tissue cultures of cytopathogenic agents from patients with measles.* Proc Soc Exp Biol Med, 1954. **86**(2): p. 277-86.

44. Mühlebach, M.D., *Measles virus in cancer therapy.* Curr Opin Virol, 2020. **41**: p. 85-97.

45. Msaouel, P., et al., *Clinical Trials with Oncolytic Measles Virus: Current Status and Future Prospects.* Curr Cancer Drug Targets, 2018. **18**(2): p. 177-187.

46. Dispenzieri, A., et al., *Phase I trial of systemic administration of Edmonston strain of measles virus genetically engineered to express the sodium iodide symporter in patients with recurrent or refractory multiple myeloma.* Leukemia, 2017. **31**(12): p. 2791-2798.

47. Ong, H.T., et al., *Oncolytic measles virus targets high CD46 expression on multiple myeloma cells.* Exp Hematol, 2006. **34**(6): p. 713-20.

48. Lok, A., et al., *p53 regulates CD46 expression and measles virus infection in myeloma cells.* Blood Adv, 2018. **2**(23): p. 3492-3505.

49. Leber, M.F., et al., *Engineering and combining oncolytic measles virus for cancer therapy.* Cytokine Growth Factor Rev, 2020. **56**: p. 39-48.

50. Peng, K.W., et al., *Intraperitoneal therapy of ovarian cancer using an engineered measles virus.* Cancer Res, 2002. **62**(16): p. 4656-62.

51. Dingli, D., et al., *Image-guided radiovirotherapy for multiple myeloma using a recombinant measles virus expressing the thyroidal sodium iodide symporter.* Blood, 2004. **103**(5): p. 1641-6.

52. Bucheit, A.D., et al., *An oncolytic measles virus engineered to enter cells through the CD20 antigen.* Mol Ther, 2003. **7**(1): p. 62-72.

53. Allen, C., et al., *Retargeted oncolytic measles strains entering via the EGFRvIII receptor maintain significant antitumor activity against gliomas with increased tumor specificity.* Cancer Res, 2006. **66**(24): p. 11840-50.

54. Leber, M.F., et al., *MicroRNA-sensitive oncolytic measles viruses for cancer-specific vector tropism.* Mol Ther, 2011. **19**(6): p. 1097-106.

55. Grote, D., R. Cattaneo, and A.K. Fielding, *Neutrophils contribute to the measles virus-induced antitumor effect: enhancement by granulocyte macrophage colony-stimulating factor expression.* Cancer Res, 2003. **63**(19): p. 6463-8.

56. Kanai, F., et al., *Adenovirus-mediated transduction of Escherichia coli uracil phosphoribosyltransferase gene sensitizes cancer cells to low concentrations of 5-fluorouracil.* Cancer Res, 1998. **58**(9): p. 1946-51.

57. Chung-Faye, G.A., et al., *In vivo gene therapy for colon cancer using adenovirus-mediated, transfer of the fusion gene cytosine deaminase and uracil phosphoribosyltransferase.* Gene Ther, 2001. **8**(20): p. 1547-54.

58. Heidelberger, C., et al., *Fluorinated pyrimidines, a new class of tumour-inhibitory compounds.* Nature, 1957. **179**(4561): p. 663-6.

59. Noll, M., et al., *Primary resistance phenomena to oncolytic measles vaccine viruses.* Int J Oncol, 2013. **43**(1): p. 103-12.

60. Kuriyama, S., et al., *Bystander effect caused by cytosine deaminase gene and 5-fluorocytosine in vitro is substantially mediated by generated 5-fluorouracil.* Anticancer Res, 1998. **18**(5a): p. 3399-406.

61. May, V., et al., *Chemovirotherapy for pancreatic cancer: Gemcitabine plus oncolytic measles vaccine virus.* Oncol Lett, 2019. **18**(5): p. 5534-5542.

62. Liu, C., et al., *Combination of measles virus virotherapy and radiation therapy has synergistic activity in the treatment of glioblastoma multiforme.* Clin Cancer Res, 2007. **13**(23): p. 7155-65.

63. Stewart, C.E., R.E. Randall, and C.S. Adamson, *Inhibitors of the interferon response enhance virus replication in vitro.* PLoS One, 2014. **9**(11): p. e112014.

64. Weiland, T., et al., *Enhanced killing of therapy-induced senescent tumor cells by oncolytic measles vaccine viruses.* Int J Cancer, 2014. **134**(1): p. 235-43.

65. Essand, M., *Virotherapy of neuroendocrine tumors.* Neuroendocrinology, 2013. **97**(1): p. 26-34.

66. Burke, M.J., *Oncolytic Seneca Valley Virus: past perspectives and future directions.* Oncolytic Virother, 2016. **5**: p. 81-9.

67. Leja, J., et al., *Oncolytic adenovirus modified with somatostatin motifs for selective infection of neuroendocrine tumor cells.* Gene Ther, 2011. **18**(11): p. 1052-62.

68. Tseng, A.W., et al., *Tumor-specific promoter-driven adenoviral therapy for insulinoma.* Cell Oncol (Dordr), 2016. **39**(3): p. 279-86.

69. Smith, T.L., et al., *AAVP displaying octreotide for ligand-directed therapeutic transgene delivery in neuroendocrine tumors of the pancreas.* Proc Natl Acad Sci U S A, 2016. **113**(9): p. 2466-71.

70. Kloker, L.D., et al., *Oncolytic vaccinia virus GLV-1h68 exhibits profound antitumoral activities in cell lines originating from neuroendocrine neoplasms.* BMC Cancer, 2020. **20**(1): p. 628.

71. Kloker, L.D., et al., *The Oncolytic Herpes Simplex Virus Talimogene Laherparepvec Shows Promising Efficacy in Neuroendocrine Cancer Cell Lines.* Neuroendocrinology, 2019. **109**(4): p. 346-361.

72. Matsushima, H., et al., *Efficacy of a third-generation oncolytic herpes simplex virus in neuroendocrine tumor xenograft models.* Oncotarget, 2019. **10**(67): p. 7132-7141.

73. Reddy, P.S., et al., *Seneca Valley virus, a systemically deliverable oncolytic picornavirus, and the treatment of neuroendocrine cancers.* J Natl Cancer Inst, 2007. **99**(21): p. 1623-33.

74. Rudin, C.M., et al., *Phase I clinical study of Seneca Valley Virus (SVV-001), a replication-competent picornavirus, in advanced solid tumors with neuroendocrine features.* Clin Cancer Res, 2011. **17**(4): p. 888-95.

75. Leja, J., et al., *A novel chromogranin-A promoter-driven oncolytic adenovirus for midgut carcinoid therapy.* Clin Cancer Res, 2007. **13**(8): p. 2455-62.

76. Leja, J., et al., *Double-detargeted oncolytic adenovirus shows replication arrest in liver cells and retains neuroendocrine cell killing ability.* PLoS One, 2010. **5**(1): p. e8916.

77. Gentschev, I., et al., *Efficient colonization and therapy of human hepatocellular carcinoma (HCC) using the oncolytic vaccinia virus strain GLV-1h68.* PLoS One, 2011. **6**(7): p. e22069.

78. Binz, E., et al., *Chemovirotherapy of Pancreatic Adenocarcinoma by Combining Oncolytic Vaccinia Virus GLV-1h68 with nab-Paclitaxel Plus Gemcitabine.* Mol Ther Oncolytics, 2017. **6**: p. 10-21.

79. Motzer, R.J., et al., *Phase 3 trial of everolimus for metastatic renal cell carcinoma : final results and analysis of prognostic factors.* Cancer, 2010. **116**(18): p. 4256-65.

80. Pusceddu, S., et al., *How do the results of the RADIANT trials impact on the management of NET patients? A systematic review of published studies.* Oncotarget, 2016. **7**(28): p. 44841-44847.

81. Laplante, M. and D.M. Sabatini, *mTOR signaling in growth control and disease.* Cell, 2012. **149**(2): p. 274-93.

82. Wolin, E.M., *PI3K/Akt/mTOR pathway inhibitors in the therapy of pancreatic neuroendocrine tumors.* Cancer Lett, 2013. **335**(1): p. 1-8.

83. Le Sage, V., et al., *Adapting the Stress Response: Viral Subversion of the mTOR Signaling Pathway.* Viruses, 2016. **8**(6).

84. Avota, E., et al., *Disruption of Akt kinase activation is important for immunosuppression induced by measles virus.* Nat Med, 2001. **7**(6): p. 725-31.

85. Sankhala K, Mita A, Kelly K, Mahalingam D, Giles F and Mita M. *The emerging safety profile of mTOR inhibitors, a novel class of anticancer agents.* Target Oncol, 2009. **4**(2): p. 135-42.

86. Vandamme, T., et al., *Whole-exome characterization of pancreatic neuroendocrine tumor cell lines BON-1 and QGP-1.* J Mol Endocrinol, 2015. **54**(2): p. 137-47.

87. Gock, M., et al., *Establishment, functional and genetic characterization of a colon derived large cell neuroendocrine carcinoma cell line.* World J Gastroenterol, 2018. **24**(33): p. 3749-3759.

88. Giaccone, G., et al., *Neuromedin B is present in lung cancer cell lines.* Cancer Res, 1992. **52**(9 Suppl): p. 2732s-2736s.

89. Olszewski, U., et al., *Genome-wide gene expression analysis of chemoresistant pulmonary carcinoid cells.* Lung Cancer (Auckl), 2010. **1**: p. 107-117.

90. Skehan, P., et al., *New colorimetric cytotoxicity assay for anticancer-drug screening.* J Natl Cancer Inst, 1990. **82**(13): p. 1107-12.

91. Bradford, M.M., *A rapid and sensitive method for the quantitation of microgram quantities of protein utilizing the principle of protein-dye binding.* Anal Biochem, 1976. **72**: p. 248-54.

92. Lauer, U.M. and J. Beil, *Oncolytic viruses: challenges and considerations in an evolving clinical landscape*. Future Oncol, 2022.

93. Johnbeck, C.B., et al., *18F-FDG and 18F-FLT-PET imaging for monitoring everolimus effect on tumor-growth in neuroendocrine tumors: studies in human tumor xenografts in mice.* PLoS One, 2014. **9**(3): p. e91387.

94. Berchtold, S., et al., *Innate immune defense defines susceptibility of sarcoma cells to measles vaccine virus-based oncolysis.* J Virol, 2013. **87**(6): p. 3484-501.

95. Lun, X.Q., et al., *Efficacy of systemically administered oncolytic vaccinia virotherapy for malignant gliomas is enhanced by combination therapy with rapamycin or cyclophosphamide.* Clin Cancer Res, 2009. **15**(8): p. 2777-88.

96. Lun, X., et al., *Efficacy and safety/toxicity study of recombinant vaccinia virus JX-594 in two immunocompetent animal models of glioma.* Mol Ther, 2010. **18**(11): p. 1927-36.

97. The Nobel Prize in Physiology or Medicine 2018. NobelPrize.org. Nobel Prize Outreach AB 2023. Sun. 9 Apr 2023.

X1. O'Dorisio TM VA, Ruggle T. What is neuroendocrine cancer? Uihc.org. University of Iowa [Web]

[cited 2022, 29 March]; Available from: https://uihc.org/health-topics/what-neuroendocrine-cancer.

Posterpräsentationen

- Forschungkolloquium der Medizinischen Fakultät der Universität Tübingen: *Scheicher NV, Berchtold S, Lauer UM. Virotherapy of Neuroendocrine Tumors (NETs).* Januar 2018.

- 20th International AEK Cancer Congress, Heidelberg: *Scheicher NV, Berchtold S, Lauer UM. Virotherapy of Neuoendocrine Tumors (NETs) using oncolytic measles vaccine virus.* Februar 2019.

Erklärung zum Eigenanteil

Die Arbeit wurde in der Medizinischen Universitätsklinik Tübingen in der Abteilung VIII für Medizinische Onkologie und Pneumologie (Ärztlicher Direktor: Prof. Dr. med. Lars Zender) in der Arbeitsgruppe Virotherapie unter Betreuung von Herrn Prof. Dr. med. Ulrich M. Lauer durchgeführt.

Die Konzeption der Studie erfolgte in Zusammenarbeit mit Prof. Dr. med. Ulrich M. Lauer (Leiter der Arbeitsgruppe Virotherapie) und Dr. med. Susanne Berchtold (Laborleiterin und wissenschaftliche Mitarbeiterin).

Sämtliche Versuche wurden nach Einarbeitung durch Irina Smirnow (MTA), Dr. med. Susanne Berchtold und Andrea Schenk (MTA) vollständig eigenständig von mir durchgeführt.

Ausnahmen hiervon sind die Versuche zur Primärinfektion (3.1.2) sowie den Western Blots (3.1.5), bei denen einige Versuchsdurchläufe auch von Irina Smirnow und Dr. med. Susanne Berchtold durchgeführt wurden.

Die Datenanalyse und statistische Auswertung erfolgten durch mich.

Ich versichere, das Manuskript selbständig unter Anleitung und Korrektur durch Dr. med. Susanne Berchtold verfasst zu haben und keine weiteren als die von mir angegebenen Quellen verwendet zu haben.

Rottenburg, den 14.09.2023

Danksagung

Ich möchte mich an dieser Stelle bei allen bedanken, die zum Gelingen dieser Arbeit beigetragen haben.

Zunächst möchte ich mich bei Herrn Prof. Dr. med. Ulrich M. Lauer bedanken, der mir diese Arbeit in seiner Arbeitsgruppe ermöglichte und mir immer mit Rat zur Seite stand. Insbesondere danke ich ihm für die große Unterstützung bei der Beantragung des IZKF Promotionskollegs sowie der Möglichkeit der Posterpräsentation.

Des Weiteren möchte ich den beiden MTAs Andrea Schenk und Irina Smirnow für die sehr gute Einarbeitung und praktische Unterstützung im Labor bedanken. Darüber hinaus danke ich Herrn Dr. rer. nat. Markus Burkhard, Christian Leischner sowie Prof. Dr. Dr. Venturelli für die sehr freundliche und unterstützende Atmosphäre im Labor.

Außerdem möchte ich mich für die großzügige Unterstützung durch das IZKF Promotionskolleg sowie das Deutschlandstipendium der Universität Tübingen bedanken.

Mein besonderer Dank gebührt Dr. med. Susanne Berchtold, die mich als direkte Betreuerin und Ansprechpartnerin bei allen Fragen und Herausforderungen die ganze Zeit hervorragend unterstützt hat.